Plenary 1: Calcium in the heart in health and disease

Eisner, D.A.

Unit of Cardiac Physiology, Institute of Cardiovascular Sciences, The University of Manchester.

Calcium is the master controller of cardiac function. It needs to increase on each beat to trigger the heart to contract to pump blood. It must fall to low enough levels between beats so that the heart can relax to fill again with blood. Heart disease, the major killer world-wide, is associated with abnormal calcium signaling.

It is more than 130 years since Sydney Ringer found that calcium is required for cardiac contraction. Enormous progress has been made recently in unraveling the regulation of calcium but there is much left to do.

In this lecture I will present an overview of cardiac calcium signaling, showing how imaging, electrophysiology, molecular tools and animal models have contributed to our understanding of the physiology. The first half of the talk will concentrate on the simple, yet elegant mechanisms that regulate calcium. The remainder will focus on abnormal calcium regulation and how this can lead to some of the changes seen in heart failure as well as contributing to the origins of cardiac arrhythmias.

1A.1: Interrogation of arcuate nucleus GABAergic NPY neural circuitry in prenatally androgenized female mice

Marshall, C.J.[1], Campbell, R.E.[1]

[1]Department of Physiology and Centre for Neuroendocrinology, University of Otago, Dunedin, NZ.

Fertility is governed by gonadotropin-releasing hormone (GnRH) neurons that reside in the hypothalamus. GnRH neurons are ultimately regulated by circulating steroid hormones that act via an upstream neural network, essential for orchestrating reproductive function. A recently defined neural circuit between steroid hormone-sensitive GABAergic neurons in the arcuate nucleus (ARN) and GnRH neurons is enhanced in prenatally androgenized (PNA) mice that model polycystic ovarian syndrome (PCOS)[1], implicating them in the steroid hormone mediated regulation of fertility. Recent evidence has revealed that a large subset of ARN GABA neurons co-express neuropeptide Y (NPY)[2], a signalling molecule that is known regulate GnRH neurons. The aim of these experiments was therefore to assess whether this NPYergic subset of ARN GABA neurons is similarly impaired in PCOS.

AgRP-Cre;τGFP-reporter mice were treated with sesame oil (VEH) alone or with dihydrotestosterone (250μg, PNA) in late pregnancy. GFP expression in ARN NPY/GABA somata and fibre processes was coupled with immunofluorescent detection of progesterone receptor (PR) to assess ARN NPY/GABA progesterone sensitivity, or GnRH to assess their innervation of GnRH neurons. Fewer PR-positive cells were detected in the ARN of PNA female mice (108.4 ± 6.2 cells/section, n=10) compared with VEH females (137.2 ± 5.8 cells/section; n=8, $p < 0.01$). However, in ARN NPY neurons, there was a near complete lack of PR immunoreactivity overall (< 0.5%). ARN NPY neurons appear to heavily innervate GnRH neuron somata and proximal dendrites, however, the density of innveration is not different between VEH (n=5) and PNA (n=8) mice. These data suggest that NPY/GABA composes a significant subpopulation of progesterone-insensitive ARN GABA neurons, which project heavily to GnRH neurons irrespective of PNA treatment. This subset of neurons is therefore likely not to be the same population of ARN GABA neurons previously shown to be perturbed in PCOS model mice.

1. Moore, A.M., Prescott, M., **Marshall, C.J.**, Yip, S.H., Campbell, R.E. (2015). *Enhancement of a robust arcuate GABAergic input to gonadotropin-releasing hormone neurons in a model of polycystic ovarian syndrome*. Proc Natl Acad Sci USA. 112(2): 596-601.
2. **Marshall, C.J**., Desrosziers, E., McLennan, T., Campbell, R.E. (Neuroendocrinology, in review). *Defining subpopulations of arcuate nucleus GABA neurons in male, female and prenatally androgenized female mice.*

1A.2: Patient-specific computational model to optimise mechanical ventilation

Win, Z.[1], Clark, A.[1], Chase, G.[2], Tawhai, M.[1]

[1]Auckland Bioengineering Institute, University of Auckland, Auckland, NZ, [2]University of Canterbury, Christchurch, NZ.

Mechanical ventilation (MV) is important in supporting patients in intensive care units. However, it is associated with high mortality due to ventilator-induced lung injury (VILI). First-generation computational models have been developed to support clinical decision making for MV, however they cannot speculate patient outcome from different MV strategies as patient physiology is not considered. I aim to develop a patient-specific computational model to predict patient response to MV without requiring invasive procedures.

A computational model of positive-pressure ventilation was parameterised using upper-airway pressures from eight MV patients. The characteristic pressure waveform for a breath was calculated by fitting to data over 5 breaths. Key model parameters (which determine lung compliance (C_{lung}) and airway resistance (R_{aw})) were optimised such that the model gave the best match to clinical data for airflow rate at the mouth. Literature data on C_{lung} and R_{aw} for MV patients with different conditions were collated, to define the expected relationship between C_{lung} and R_{aw} for typical conditions that require MV. R_{aw} and C_{lung} from the model were compared with these data, to determine whether a simple optimisation can provide meaningful parameters for the patient group.

The predicted airflow fell within the 95% confidence intervals of the clinical data. Literature data suggests that C_{lung} and R_{aw} are 0.02-0.13L/cmH_2O and 1-32cmH_2O/L/s in Acute Respiratory Distress Syndrome (ARDS) and 0.015-0.15L/cmH_2O and 1-5cmH_2O/L/s in Acute Respiratory Failure (ARF) respectively. The model predicted that seven patients fell in the range of ARDS and one in ARF.

Our model has shown potential for continuous monitoring of respiratory parameters, to predict the patient condition, to optimise the ventilator setting with patient physiology and pathophysiology accounted for, and to avoid VILI.

1A.3: The role of the cytoskeleton and myosin-Vc in the trafficking of KCa3.1 to the basolateral membrane of polarised epithelial cells

Farquhar, R.[1], Rodrigues, E.[2], Hamilton, K.L.[1]

[1]Department of Physiology, Otago School of Medical Sciences, University of Otago, Dunedin, NZ, [2]Department of Medicine, Otago School of Medical Sciences, University of Otago, Dunedin, NZ.

Ca^{2+}-activated K^+ channel (KCa3.1), an intermediate conductance channel, is targeted to the basolateral membrane (BLM) in polarised epithelia. KCa3.1 is important in salt and fluid transport regulation, membrane potential, and the electrochemical gradient. We investigated the role of the microtubule (MT) cytoskeleton and actin motor protein Myosin-Vc in anterograde trafficking of KCa3.1 to BLM of polarised epithelial cells. Fischer Rat Thyroid (FRT) cells were stably transfected with a biotin-ligase-acceptor peptide (BLAP)-KCa3.1 sequence (FRT-KCa3.1-BLAP) and grown on permeable inserts to form a polarised epithelial monolayer. KCa3.1 was labelled at the BLM with streptavidin. Immunoblot and Ussing chamber techniques were used to study the functional membrane expression of KCa3.1 and changes in response to pharmacological inhibition of MTs. Myosin-Vc was selected as a target protein in the trafficking of KCa3.1 using broad spectrum inhibitors. To determine the role of MTs in the trafficking of KCa3.1, cells were treated with MT-inhibitor colchicine (10 µM) resulting in a reduced membrane expression of KCa3.1 by 63 ▯ 7% (P☒0.01, n=5), while KCa3.1 K^+ current was reduced by 54±19% (p≤0.05, n=5). FRT-KCa3.1-BLAP cells treated with ML9 (10☐M), an inhibitor of myosin light chain kinase, reduced expression of KCa3.1 by 83☐2% (p≤0.01, n=5) with KCa3.1 specific K^+ current reduced by 54±2% (P☒0.01, n=7). Cells treated with non-muscle Myosin-II and Myosin-V inhibitor BDM (10 mM) reduced expression and function of KCa3.1 by 58±5% (p≤0.05, n=5) and 51 ▯ 7% (p≤0.01, n=8), respectively. Knock-down of Myosin-Vc reduced KCa3.1 membrane expression by 45 ▯ 5% (n=6 p☒0.01) and KCa3.1 K^+ current by 1.04±0.14 µA (n=6 p≤0.01). These data suggest that the anterograde trafficking of KCa3.1 in a polarised epithelium is dependent on both the MT cytoskeleton and Myosin-Vc.

1A.4: Vasopressin secretion exacerbates the development of angiotensin II-dependent hypertension

Korpal, A.K.[1,2,3], Schwenke, D.O.[3], Brown, C.H.[1,2,3]

[1]Brain Health Research Centre, [2]Centre for Neuroendocrinology, and [3]Department of Physiology, Otago School of Medical Sciences, University of Otago, Dunedin, NZ.

Arginine vasopressin (AVP) magnocellular neurosecretory cells (MNCs) of the hypothalamic paraventricular nucleus (PVN) and supraoptic nucleus (SON) secrete AVP into the bloodstream, causing vasoconstriction and reabsorption of water from the kidneys. These actions increase arterial blood pressure (ABP). Normally, AVP MNC activity is tonically inhibited by peripheral arterial baroreceptors. Hence, low blood pressure decreases this baroreceptor inhibition of AVP MNCs, permitting AVP release to return blood pressure towards normal. Paradoxically, we have demonstrated that AVP MNC activity is increased at the onset of hypertension in Cyp1a1-Ren2 transgenic rats in which moderate ANG II-dependent hypertension can be induced through the addition of indole-3-carbinol (I3C) to the diet for 7 days. Because increased AVP MNC activity increases the secretion of AVP into the bloodstream, we hypothesised that the ANG II-induced increase in ABP is exacerbated by the vasoconstrictive actions of AVP at peripheral AVP V1a receptors. To determine whether increased AVP secretion contributes to the development of ANG II-dependent hypertension, a potent V1a receptor antagonist ((Phenylac^{1},D-Tyr(Et)^{2},Lys^{6},Arg^{8},des-Gly^{9})-vasopressin trifluoroacetate salt, 230 ng/h) was subcutaneously infused during the 7 day period of I3C-diet treatment. In vehicle-treated rats, I3C increased systolic blood pressure (SBP) from 139 ± 6 mmHg to 185 ± 4 mmHg (n = 7) after 7 days. However, in V1a receptor antagonist-treated rats, I3C increased SBP to a similar level to that in vehicle-treated rats until day 3, after which SBP did not increase further (from 137 ± 5 to 161 ± 3 mmHg on day 7; n = 7; P = 0.003, two-way repeated measures ANOVA, Bonferroni's *post-hoc* test). Hence, whilst ANG II drives the initial rise in blood pressure at the onset of ANG II-dependent hypertension, AVP is recruited by day 3 to further increase blood pressure via activation of peripheral V1a receptors.

1A.5: Three-dimensional quantification of collagen morphology in ventricular tissue

Hasaballa, A.I.[1], Sands, G.B.[1,2], Wilson, A.J.[1,2], Wang, V.Y.[1], LeGrice, I.J.[1,2], Nash, M.P.[1,3]

[1]Auckland Bioengineering Institute, [2]Department of Physiology, [3]Department of Engineering Science, University of Auckland, Auckland, NZ.

The progression of heart failure (HF) is associated with substantial changes in myocardial microstructure and organisation that lead to an alteration in the mechanical behaviour and, hence, the impairment of cardiac function. Given that the collagen network is the primary determinant of myocardial stiffness, a robust quantitative description of collagen morphology is essential for developing an understanding of the structure-function relationship in cardiac muscle during HF.

Extended-volume confocal microscopy was used to obtain high-resolution three-dimensional (3D) images of 12-month-old spontaneously hypertensive rats (SHR) and age-matched Wistar-Kyoto (WKY) rats as controls. A novel method, based on the use of eigenanalysis of the co-variance (inertia) matrix to derive 3D morphological parameters, has been developed to characterise the shape of the collagen distributions in the 3D confocal images. Analysis of the collagen morphology parameters revealed that the statistical distributions are different for WKY and SHR hearts. Specifically, collagen distributions in WKY mostly form elongated structures, whereas in SHR collagen is arranged predominantly in a sheet-like form. Incorporating these microstructural shape parameters into a micro-mechanical constitutive equation, which links the observed changes in cardiac microstructure and ventricular function during HF, could pave the way towards a better understanding of the pathophysiology of HF, and lead to more effective treatments that target the underlying mechanisms of HF.

1A.6: Compromised energy supply in right heart failure

Power, A.S.[1,2], Crossman, D.J.[1], Hickey, A.J[2], Ward, M-L[1]

[1]Department of Physiology, Faculty of Medical and Health Science, University of Auckland, Auckland, NZ, [2]School of Biology, University of Auckland, Auckland, NZ.

The heart is a highly aerobic organ with more than 90% of ATP supplied by oxidative phosphorylation in the mitochondria. Previous reports suggest that ATP supply is compromised in heart failure. However, the contribution of mitochondrial dysfunction to the contractile deficit is still debated. The aim of this study was to determine whether mitochondrial energy supply compromised contractile function in a rat model of right heart failure induced by a single injection of monocrotaline (MCT, 60 mg Kg^{-1}). Four weeks post injection, steady-state stress and intracellular Ca^{2+} transients (fura-2) were measured in isolated right ventricular (RV) trabeculae subjected to an energetic challenge (β-adrenergic stimulation, 1 µM isoproterenol). Trabeculae were then chemically permeabilised using saponin and contractures induced using buffered Ca^{2+} solutions, with, and without, exogenous ATP added. In separate experiments mitochondrial function was assesed in RV fibres using high-resolution respirometry (oxygraph, Oroboros™) to identify specific electron transport system deficits.

Intact MCT trabeculae produced similar stress to controls, despite smaller Ca^{2+} transients, and showed a decreased response to isoproterenol. Removal of exogenous ATP from permeabilised trabeculae showed no difference in Ca^{2+} activated stress for contols, whereas MCT trabeculae showed decreased stress, suggesting compromised endogenous mitochondrial ATP generation. Decreased mitochondrial function in RV tissue from MCT was confirmed by respirometry. In conclusion, our preliminary results suggest that in the MCT model of right heart failure, trabeculae were unable to generate sufficient ATP when challenged. Therefore, improving mitochondrial ATP production could be a beneficial treatment for restoring contractile function in right heart failure.

1A.7: CaMKII inhibition restores contractile performance in cardiac muscle from a rat model of type 2 diabetes

Daniels, L.J.[1], Lamberts R.R.[1], McDonald F.J.[1], Erickson J.R.[1]

[1]Department of Physiology, University of Otago, Dunedin School of Medicine, NZ.

Calmodulin-dependent protein kinase (CaMKII) is a multifunctional serine-threonine kinase shown to be up-regulated in human patients and animal models of diabetes. Excessive CaMKII activation in the myocardium promotes hypertrophy and apoptosis, ultimately leading to heart failure. Therefore we hypothesized that inhibition of CaMKII activity would preserve myocardial contractility in heart tissue from the Zucker diabetic fatty rat (ZDF), a model of type 2 diabetes. *Methods*- 20-week old type 2 diabetic ZDF (*n*=10) and control (CTRL) rats (*n*=10) underwent echocardiography to assess *in vivo* cardiac function. Cardiac muscles (trabeculae) were subsequently isolated from the right ventricle and myocardial force measurements were performed in the presence of an inhibitor of CaMKII activity (KN-93) or a peptide analogue with no CaMKII inhibitory effects (KN-92). Additional experiments were conducted using a peptide inhibitor of CaMKII (AIP) that blocks the catalytic domain and inhibits the autonomously active form of the kinase. Sections of heart tissue from the right ventricle were snap frozen for subsequent analysis of CaMKII expression in the diabetic heart. *Results*- After 20 weeks, fasted blood glucose was 25.8 ± 1.8 mmol/L for the ZDF diabetic rats and 8.2 ± 1.8 mmol/L for the CTRL rats. Echocardiography scans showed no signs of pathological remodeling or cardiac dysfunction in the ZDF diabetic rats at 20 weeks of age. Assessment of CaMKII expression and activation showed no change in expression (0.95 $\pm$ 0.08 vs 1.15 $\pm$ 0.10, CTRL vs type 2 diabetics) but CaMKII phosphorylation was significantly increased in the diabetic animals (0.77 $\pm$ 0.13 vs 1.40 $\pm$ 0.26, CTRL vs. type 2 diabetics). Trabeculae isolated from the diabetic ZDF rats had reduced contractile force (F_{dev} and dF/dt_{max}) across all stimulation frequencies, alongside impaired relaxation (dF/dt_{min}). Inhibition of CaMKII with KN93 & AIP in the diabetic trabeculae significantly improved contractile force, and relaxation kinetics. In addition, CaMKII inhibition with AIP altered the sensitivity contractility in response to isoproterenol, a non-selective beta-adrenergic agonist. *Conclusion*- The results indicate that CaMKII activity precedes advanced heart failure in the diabetic ZDF rat model, and that CaMKII contributes to the functional changes in the diabetic heart. Moreover they suggest a potential therapeutic role for CaMKII inhibitors in improving diabetic cardiac myocardial function.

1A.8: Developing and optimizing strategies to treat post-stroke hypertension in a rat model of ischemic stroke

Thakkar, P.C.[1], Barret, C.J.[1], Paton, J.F.R[2], McBryde, F.D.[1]

[1]Department of Physiology, University of Auckland, Auckland, NZ, [2]School of Physiology and Pharmacology, University of Bristol, Bristol, UK.

Stroke is the third largest killer in New Zealand, with ~24 new cases every day (1). After a stroke, almost all patients show a sudden and profound increase in blood pressure (BP). Because the reasons underlying this response remain uncertain, it is unclear whether post-stroke hypertension should be treated. Here, we determine a strategy to control BP in an animal model of ischemic stroke. The calcium channel blocker nifedipine preserves cerebral blood flow, and is clinically indicated for BP management after stroke (2). Male Wistar rats (439.2±11.1g, n=10) were instrumented to record BP via telemetry. First (n=4), intraperitoneal (i.p.) injections of nifendpine were given to determine dosage and time course. A single dose of 5 $mg.kg^{-1}$ reduced BP by 9.7±6 mmHg for ~4 hours. Next, ischemic stroke was induced via transient occlusion of the middle cerebral artery (MCAo). As nifedipine has a short *in vivo* half-life, repeated injections were necessary to control BP, especially in the first 24 hours. Repeated animal handling produced stress-related fluctuations in BP and heart rate. These considerations led us to investigate other options for drug delivery. Osmotic mini-pumps can be implanted chronically, and give a constant, fixed-duration infusion. To counteract the dynamic BP changes seen after stroke, we implanted a second group of rats (n=6) with two types of mini-pump (Alzet, USA: 2001D, 1003D) at the time of the stroke. This permitted us to give a higher dose for the first 24 hours (1.5 $mg.kg^{-1}.hr^{-1}$), and a lower dose for 24-72 hours after stroke (0.75 $mg.kg^{-1}.hr^{-1}$). Following stroke, our dosing strategy successfully restrained post-stroke hypertension to maximum of 11±6mmHg in treated rats, compared to 19±4mmHg in non-treated rats, and 5±3mmHg in sham MCAo animals. Future studies will examine the impact of preventing post-stroke hypertension on brain oxygenation, intracranial pressure, functional neurological outcomes and infarct volumes.

1. Stroke Foundation of New Zealand NCGSM. *NZ Clinical Guidelines Stroke Management* 2010.
2. Varon J, Marik PE. *Clinical review: the management of hypertensive crises.* Crit Care. 2003;7(5):374-84.

1B.1: Nancy Sirett Memorial Lecture: If I can stop one heart from breaking, I shall not live in vain

Cameron, V.A.[1]

[1]Christchurch Heart Institute, University of Otago, Christchurch, NZ.

The traditional view of a hormone is a chemical signal secreted by an endocrine gland that is transported through the circulation to communicate with a discrete set of cells within a target organ. This perception is changing, as it is increasingly recognised that there is considerable crosstalk between endocrine systems, that signaling molecules are secreted from a variety of non-endocrine tissues, and that many circulating signals are not classical hormones. Physiological, psychological or environmental stress activates a cascade of hormones, including the renin–angiotensin–aldosterone (RAAS) hormones, the CRH-ACTH-cortisol system, and the natriuretic peptide family of hormones. Each of these endocrine systems have both circulating and tissue components, within brain, kidneys, or heart tissue. There is abundant interplay between the hormone cascades to modify physiological responses in health and in the processes underlying disease, and this is pivotal in the pathogenesis of coronary heart disease and heart failure. Further, our understanding of cardiovascular diseases has accelerated since the release of the human genome sequence in 2000, leading to a new appreciation of non-coding DNA in susceptibility to complex diseases. Circulating non-coding RNAs (transcripts from non-coding DNA), such as microRNAs (miRNAs) and long non-coding RNAs (lncRNAs) are a new generation of chemical signals. Our increasing understanding of the range of chemicals that the body uses in communication is contributing to advances in biomarkers for detection and management of disease.

1B.2: Growth hormone receptor antagonism suppresses tumour regrowth after radiotherapy in an endometrial cancer model

Evans, A.[1], Jamieson, S.M.[2], Liu, D.X.[1], Wilson, W.R.[2], Perry, J.K.[1]

[1]Liggins Institute, University of Auckland, Auckland, NZ, [2]Auckland Cancer Society Research Centre, University of Auckland, Auckland, NZ.

Radiotherapy is used to treat approximately 50% of all cancer patients, with varying success. For many common cancers, adding novel molecularly targeted agents to radiotherapy can increase cure rates. Currently, however, the EGFR antagonist cetuximab is the only molecularly targeted agent approved as a radiosensitiser. Human GH expression is associated with poor survival outcomes for endometrial cancer patients, enhanced oncogenicity of endometrial cancer cells and reduced sensitivity to ionising radiation in vitro, suggesting that GH is a potential target for anticancer therapy. However, whether GH receptor inhibition sensitises to radiotherapy *in vivo* had not been tested.

In the current study, we evaluated whether the GH receptor antagonist, pegvisomant (Pfizer), sensitises to radiotherapy *in vivo* in an endometrial tumour xenograft model. Subcutaneous administration of pegvisomant (20 or 100 mg/kg/day, s.c.) reduced serum IGF1 levels by 23% ($p<0.05$; one-way ANOVA) and 68% ($p<0.001$; one-way ANOVA), respectively compared to vehicle treated controls. RL95-2 xenografts grown in immunodeficient NIH-III mice were treated with vehicle or pegvisomant (100 mg/kg/day), with or without fractionated gamma radiation (10×2.5 Gy over 5 days). When combined with radiation, pegvisomant significantly increased the median time tumours took to reach 3× the pre-radiation treatment volume (49 days versus 72 days; $p=0.001$). Immunohistochemistry studies demonstrated that 100 mg/kg pegvisomant every second day was sufficient to abrogate MAP Kinase signalling throughout the tumour. In addition, treatment with pegvisomant increased hypoxic regions in irradiated tumours, as determined by immunohistochemical detection of pimonidazole adducts, and decreased the area of CD31 labelling in unirradiated tumours, suggesting an anti-vascular effect. Pegvisomant did not affect intratumoral staining for HIF1, VEGF-A, CD11b, or phospho-EGFR. Our results suggest that blockade of the human GH receptor may improve the response of GH and/or IGF1-responsive endometrial tumours to radiation.

1. Evans A, Jamieson SJ, Liu DX, Wilson WR, Perry JK (2016) *Growth hormone receptor antagonism suppresses tumour regrowth after radiotherapy in an endometrial cancer xenograft model*. Cancer Letters, In Press.

1B.3: Changes in dendritic spine density of tuberoinfundibular dopaminergic neurons associated with estrous cyclicity in the rat

Yip. S.H.[1], York. J[1], Hyland B.[2], Grattan D.[1], Bunn SJ[1]

[1]Centre for Neuroendocrinology, Department of Anatomy, University of Otago, Dunedin School of Medicine, NZ, [2]Department of Physiology, University of Otago, Dunedin School of Medicine, NZ.

Prolactin secretion is tightly regulated by the hypothalamic tuberoinfundibular dopaminergic (TIDA) neurons in the arcuate nucleus (ARN). The activity of these neurons is influence by circulating steroidal hormones throughout the estrous cycle, resulting in fluctuating prolactin levels to meet physiological demand. Evidence showed that estradiol induces synaptic remodeling on TIDA neurons whereby inhibitory inputs are reduced[1]. However whether this is associated with an increase in excitatory inputs remains unknown. This study aimed to investigate the dynamic state of the dendritic spine density on TIDA neurons as an indication of excitatory inputs during proestrus, when estrogen is transiently elevated to drive the prolactin surge. Adult female tyrosine hydroxylase (TH)-promoter driven Cre-recombinase transgenic rats were stereotaxically injected with Cre-dependent adeno-associated virus expressing Brainbow into the ARN. Two weeks later, the brains were processed for immunohistochemistry. Approximately 95% of transfected neurons were TH-positive and transfection was limited to less than 50% of the TIDA neurons. This highly specificity and moderate efficiency of transfection, together with the multi-coloured Brainbow expression, allowed good resolution of the complex network of TIDA neuron processes within the ARN. Using confocal microscopy, 44 neurons from 3 proestrous and 49 from 3 estrous rats were randomly selected and scanned throughout the ARN. The number of spines around the cell soma and along the first 60 µm of its dendrites were evaluated. The density of spines was significantly higher in the proestrous compared to the estrous group at both the soma (0.09 ± 0.01 vs. 0.06 ± 0.01 spines per µm; $P < 0.01$) and dendrites (0.23 ± 0.02 vs. 0.18 ± 0.02 spines per µm; $P < 0.05$). This reorganization of excitatory inputs onto TIDA neurons associated with estrous cyclicity has opened an avenue to investigate the possible neurochemical nature of these inputs responsible for cyclical regulation of prolactin.

1. Csakvari, E. et al., (2008) *Estradiol-induced synaptic remodeling of tyrosine hydroxylase immunopositive Neurons in Rat Arcuate Nucleus*. Endocrinology. 149(8) 4137-41

1B.4: Conditional deletion of the prolactin receptor reveals functional subpopulations of dopamine neurons in the arcuate nucleus of the hypothalamus

Brown, R.S.E.[1,2], Kokay, I.C.[1,2], Phillipps, H.R.[1,2], Yip, S.H.[1,2], Gustafson, P.[1,2], Wyatt, A.[1,2], Larsen, C.M.[1,2], Knowles, P.[1,2], Ladyman, S.R.[1,2], LeTissier, P.[3], Grattan, D.R.[1,2,4]

[1]Centre for Neuroendocrinology, University of Otago, Dunedin, NZ, [2]Department of Anatomy, University of Otago, Dunedin, NZ, [3]Centre for Integrative Physiology, University of Edinburgh, United Kingdom, [4]Maurice Wilkins Centre for Molecular Biodiscovery, Auckland, NZ.

Tuberoinfundibular dopamine (TIDA) neurons, known as neuroendocrine regulators of prolactin secretion from the pituitary gland, also release GABA within the hypothalamic arcuate nucleus. As these neurons express prolactin receptors (Prlr), prolactin may regulate GABA secretion from TIDA neurons, potentially mediating actions of prolactin on hypothalamic function. To investigate whether GABA is involved in feedback regulation of TIDA neurons, we examined the physiological consequences of conditional deletion of Prlr in GABAergic neurons. For comparison, we also examined mice in which Prlr were deleted from most forebrain neurons. Both neuron-specific and GABA-specific recombination of the Prlr gene occurred throughout the hypothalamus and in some extra-hypothalamic regions, consistent with the known distribution of Prlr expression, indicative of knockout of Prlr. This was confirmed by a significant loss of prolactin-induced phosphorylation of STAT5, a marker of prolactin action. Several populations of GABAergic neurons that were not previously known to be prolactin-sensitive, noteably in the medial amygdala, were identified. Approximately 50% of dopamine neurons within the arcuate nucleus were labelled with a GABA-specific reporter, but Prlr deletion from these dopamine/GABA neurons had no effect on feedback regulation of prolactin secretion. In contrast, Prlr deletion from all dopamine neurons resulted in profound hyperprolactinemia. The absence of co-expression of tyrosine hydroxylase, a marker for dopamine production, in GABAergic nerve terminals in the median eminence suggested that rather than a functional redundancy within the TIDA population, the dopamine/GABA neurons in the arcuate nucleus represent a subpopulation with a functional role distinct from the regulation of prolactin secretion.

1B.5: Investigating the role of leptin receptor signalling on dopamine neurons in the control of feeding behaviour and body weight in male mice

Evans, M.C.[1], Anderson, G.M.[1]

[1]Centre for Neuroendocrinology and Department of Anatomy, University of Otago School of Medical Sciences, Dunedin, NZ.

Leptin's hunger-suppressing actions in the hypothalamus are well characterized, yet the mechanisms by which leptin modulates the midbrain dopamine (DA) system to suppress hedonic feeding remain less clear. A subset of midbrain DA neurons express leptin receptors (Lepr), and direct leptin administration to the midbrain reduced food intake and suppressed DA neuron firing in rats, suggesting leptin may directly modulate DA neurons. However, in contrast to global Lepr knockout mice ($Lepr^{NULL}$), the selective deletion of Lepr from DA neurons had no effect on body weight (BW), food intake or hedonic responses, either suggesting leptin acts via an indirect pathway, or demonstrating sufficient compensation took place to mask any direct leptin-DA actions. Therefore, to further explore whether direct leptin-DA signalling modulates appetitive behaviour, we generated transgenic mice in which Lepr were expressed exclusively in DA neurons ($Lepr^{DA}$). We then compared weekly BW, daily food intake (standard chow diet), hyperphagic feeding (1-hr access to a high-fat high-sugar diet), and leptin-induced suppression of feeding between these $Lepr^{DA}$ mice and their wild-type ($Lepr^{WT}$) and $Lepr^{NULL}$ littermates. As expected, both the $Lepr^{NULL}$ and $Lepr^{DA}$ mice exhibited significantly increased BW and food intake compared to the $Lepr^{WT}$ mice. Interestingly, the $Lepr^{DA}$ mice exhibited significantly increased post-weaning BW compared to the $Lepr^{NULL}$ mice (4-11 weeks), yet no differences in food intake were observed. Furthermore, neither the $Lepr^{NULL}$ nor $Lepr^{DA}$ mice exhibited a reduction in 4-hr food intake when treated with leptin (5 mg/kg, i.p.) vs. saline, whereas the $Lepr^{WT}$ mice exhibited a significant leptin-induced decrease in food intake. Lastly, $Lepr^{DA}$ mice appear to exhibit a blunted hyperphagic response compared to the $Lepr^{NULL}$ mice. While still preliminary, it appears direct leptin-DA signaling does indeed play a role in modulating appetitive behavior. Hedonic feeding assessments and further investigations using metabolic cages are currently underway.

2A.1: Recovery phase dynamics of gastric slow wave activity

Paskaranandavadivel, N.[1], Cheng, L.[1,2], Rogers, J.[3], Du, P.[1], O'Grady, G.[1]

[1]Auckland Bioengineering Institute, University of Auckland, NZ, [2]Department of Surgery, Vanderbilt University, Nashville, TN, USA, [3]Department of Biomedical Engineering, University of Alabama, Birmingham, AL, USA, [2]Department of Surgery, University of Auckland, NZ.

Slow waves play a central role in coordinating gastrointestinal contractions[1]. High-resolution (HR) extracellular mapping is used to record the spatiotemporal information of both normal and dysrhythmic slow waves[2]. However, all HR slow wave mapping studies to date have focused exclusively on the activation phase. The recovery (repolarization) phase has not been studied, but it likely conveys fundamental information on repolarization homogeneity, the excitable gap, and refractory tail interactions, all of which are vital to have an improved understanding of slow wave dysrhythmias. In this methodological study, we report novel techniques for defining and mapping the slow wave recovery phase, and demonstrate feasibility and applicability using HR mapping.

HR unipolar extracellular recordings was undertaken *in vivo* in an established pig model of gastric dysrhythmia[3], with ethical approval from the University of Auckland Ethics Committee. Spatially normal and dysrhythmic slow waves were mapped using HR electrode arrays (up to 256 electrodes covering 36cm^2). A wavelet transform technique was applied to detect the maximum positive deflection, by signal derivative estimation, to locate the recovery point. Activation-Recovery (ARi) and Recovery-Activation (RAi) intervals were then computed and mapped.

The ARi of normal slow wave activity was greater than dysrhythmic slow wave activity (4.9±0.35s vs 3.8±0.7s; $P<0.05$), while RAi was lower (8.4±0.5s vs 11.6±1.5s; $P<0.05$). A negative linear relationship was found between ARi and RAi across mapped cycles, being consistent between normal and dysrhythmic cycles. A positive relationship was identified between RAi and velocity during normal activity, but not dysrhythmic propagation. In summary, a novel method has been developed for spatiotemporal mapping of the slow wave recovery phase. Pilot studies revealed differences between normal and dysrhythmic slow waves, and further studies using these methods will contribute to an improved understanding of the initiation, maintenance and termination of slow wave dysrhythmias.

1. Huizinga J, Lammers W. *Gut peristalsis is governed by a multitude of cooperating mechanisms*. Am J Physiol Gastrointest Liver Physiol. 2009;296(1):G1-G8
2. O'Grady G, Du P, Paskaranandavadivel N, Angeli T, Lammers W, Asirvatham S, Windsor J, Farrugia G, Pullan A, Cheng L. *Rapid high-amplitude circumferential slow wave propagation during normal gastric pacemaking and dysrhythmias*. Neurogastroent Motil. 2012;24(7):e299-e312
3. Egbuji J, O'Grady G, Du P, Cheng L, Lammers W, Windsor J, Pullan A. *Origin, propagation and regional characteristics of porcine gastric slow wave activity determined by high-resolution mapping*. Neurogastroent Motil. 2010;22(10):e292-e300

2A.2: Myths and challenges of fetal life

Lear, C.A.[1], Davidson J.O.[1], Gunn, A.J.[1], Bennet, L.[1]

[1]Department of Physiology, University of Auckland, Auckland, NZ.

Severe asphyxia is a life-threatening problem that can occur at all gestational ages before or during labour. Survivors face high risks of neurodevelopmental disability. My goals were to find ways to better identify fetuses with failing adaptation to adverse events such as asphyxia before birth, and to better understand the unique events that contribute to preterm brain injury.

It is widely proposed that increased fetal heart rate variability (FHRV) in labour reflects a healthy sympathetic response, and that loss of variation reflects impaired sympathetic tone and fetal compromise. I tested this hypothesis directly in chronically instrumented fetal sheep at 0.85 of gestation by inducing repeated brief asphyxia with 2 min complete umbilical cord occlusions (UCO) repeated every 5 min for up to 4 h. I found that chemical sympathectomy did not reduce FHRV, and therefore that changes in FHRV do not reflect fetal sympathetic activity in this setting. This likely explains part of the poor predictive value of the current approach to fetal monitoring.

Maternal treatment with glucocorticoids before birth dramatically improves short term outcomes after preterm birth, but there is highly conflicting evidence for its effect on brain injury. We examined the impact of maternal dexamethasone (12mg i.m.) either 4h before or 15min after asphyxia induced by 25 min of UCO in 0.7 of gestation fetal sheep. Dexamethasone after asphyxia increased brain cell loss compared to saline ($p<0.05$) and impaired cerebral oxygenation ($p<0.05$) during recovery. Strikingly, dexamethasone given 4 h before asphyxia was associated with severe cystic white and grey matter lesions that never occurred with saline injections. We then showed that fetal hyperglycaemia similar to that induced with dexamethasone also exacerbated fetal brain injury. These findings raise the possibility that in the subgroup of preterm deliveries exposed to asphyxia, antenatal glucocorticoid treatment may not be desirable.

2A.3: Multi-scale cardiomyocyte organisation as a determinant of cardiac function

Munro, M.L.[1], Jayasinghe, I.D.[2], Shen, X.[1], Wang, W.[3], Ward, M.[1], Baddeley, D.[4], Crossman, D.[1], Wehrens, X.H.T.[3], Soeller, C.[1,2]

[1]Department of Physiology, University of Auckland, Auckland, NZ, [2]Biomedical Physics, University of Exeter, Exeter, UK, [3]Department of Molecular Physiology and Biophysics, Baylor College of Medicine, Houston, TX, USA, [4]Cell Biology, Yale University, New Haven, CT, USA.

Excitation-contraction (EC) coupling is the process underlying cardiac function, which requires precise organisation of key structures and proteins. This includes the transverse (t)-tubules, extensions of the cell membrane, which form a close association with the sarcoplasmic reticulum (SR) to create junctions. Many proteins essential to EC coupling are localised to junctions, including the SR calcium release channel – the ryanodine receptor (RyR). Heart failure (HF) is characterised by the loss of cardiac function, which is associated with impaired EC coupling and disruption of t-tubule organisation in human and animal models of HF. Currently, the link between cardiomyocyte reorganisation and cardiac function loss remains poorly understood. A protein implicated in maintenance of t-tubules and junction organisation is the lipophilic SR protein junctophilin-2 (JPH2). We have investigated several aspects of the relationship between cardiomyocyte structure and cardiac function using a combination of JPH2 transgenic mice and cardiac trabeculae from failing human hearts. Immunolabelling for t-tubules and junctional proteins was performed and imaged using super-resolution or confocal microscopy to investigate sub-cellular organisation. Superresolution imaging in JPH2 transgenic mice revealed an increase in RyR cluster size following JPH2 over-expression, despite these mice displaying smaller calcium sparks. This discrepancy was explained by examining the density of RyR and JPH2 within the junction. These results indicate that JPH2 expression directly influences RyR cluster organisation, providing a mechanism for modulating contractile function. In addition, trabeculae were obtained from explanted human hearts with end-stage failure, with force generation and tissue organisation assessed in each sample. Confocal microscopy revealed a high degree of variability in function, i.e. force development, which was strongly correlated with cardiomyocyte content. Our findings indicate a clear link between trabecula structure and function in the diseased human heart. This study provides novel mechanistic insights into the relationship between subcellular structure and contractile function on multiple scales.

2A.4: Regulation of oxytocin neurons by central kisspeptin in late-pregnant rats

Seymour, A.J.[1], Piet, R.[1], Campbell, R.E.[1], Brown, C.H.[1]

[1]Brain Health Research Centre, Centre for Neuroendocrinology and Department of Physiology, University of Otago, Dunedin, NZ

The hormone, oxytocin, is secreted from the posterior pituitary gland by magnocellular neurosecretory neurons in the hypothalamic supraoptic and paraventricular nuclei. Oxytocin causes contraction of the uterus to aid birth of the offspring during parturition. However, the mechanism by which oxytocin neurons are regulated at the onset of parturition is not completely understood. Recent work in our lab shows that the peptide, kisspeptin, might be involved in activation of oxytocin neurons in preparation for parturition, because central injection of kisspeptin excites oxytocin neurons in late-pregnant rats, but not in non-pregnant rats, or rats in early- or mid- pregnancy. Furthermore, density of kisspeptin fibres in the vicinity of the supraoptic nucleus is significantly higher in late-pregnant rats compared to non-pregnant rats.

To determine whether there are changes in the expression of kisspeptin in hypothalamic neuron populations in pregnancy, I conducted immunohistochemistry for kisspeptin. Kisspeptin expression in neurons of the periventricular nucleus was significantly higher, while expression in the arcuate nucleus was significantly lower, in late-pregnant rats compared to virgin rats. Retrograde tracing combined with immunohistochemistry was used to show that kisspeptin-positive fibres in the vicinity of the supraoptic nucleus originated from the periventricular nucleus. Patch-clamp electrophysiology was then used to show that kisspeptin does not act directly on supraoptic nucleus neurons. Furthermore, kisspeptin did not act indirectly on supraoptic nucleus neurons via local glutamatergic or GABAergic inputs. These results suggest that kisspeptin neurons of the periventricular nucleus increase synthesis in late pregnancy and that the peptide is transported to fibres in the vicinity of the supraoptic nucleus. Kisspeptin from these fibres might act to increase the activity of oxytocin neurons in preparation for parturition via a mechanism that is yet to be elucidated.

2B.1: Development of GABAergic altered wiring and plasticity in a mouse model of Polycystic Ovary Syndrome (PCOS)

Silva, M.S.B.[1], Prescott, M.[1], Campbell, R.E.[1]

[1]Centre for Neuroendocrinology, Department of Physiology, University of Otago, NZ.

Polycystic Ovary Syndrome (PCOS) is the most common neuroendocrine disorder resulting in female infertility and is typically associated with hyperandrogenism. Disruptions in brain circuits regulating Gonadotropin Releasing Hormone (GnRH) neurons are hypothesized to underlie some of the pathophysiological features of this disease. Specifically, increased GABAergic innervation of GnRH neurons has been identified in a prenatally androgenized (PNA) mouse model of PCOS. The present study aimed to determine when these circuit abnormalities develop and whether they can be modified by androgen blockade in adulthood. GABA inputs onto GnRH neurons were evaluated in brain sections collected from prepubertal [postnatal day (PND) 25], control and PNA GnRH-GFP female mice. Vesicular GABA transporter (VGAT) appositions to GnRH neurons (10-12 neurons/animal) were quantified using immunofluorescence and confocal microscopy. Prepubertal PNA mice (n=5), lacking any rise in plasma testosterone levels, presented significant enhanced GABAergic input to GnRH neurons compared to controls (n=4). Adult PNA and control females were treated with flutamide (25 mg/kg), an androgen receptor antagonist, or an oil vehicle for 20 days, from PND 40 to PND 60. As expected, VGAT appositions were significantly increased in PNA+oil (n=5) animals compared with control+oil (n=4) or control+flutamide (n=4) groups. In contrast, VGAT contact onto GnRH neurons in PNA+flutamide (n=7) females was restored to control levels and this was coincident with restored estrous cyclicity. These findings indicate that disruptions in the GABA-GnRH network in a PCOS-like condition are programed before the onset of puberty. However, blockade of androgen actions can ameliorate GABA-GnRH circuit abnormalities. These results provide important insights into the development and treatment of conditions such as PCOS that are evoked by prenatal androgen exposure

2B.2: Determining the role of RF-amide related peptide neurons in suppression of the preovulatory surge of luteinizing hormone during restraint stress

Stowe, S.M.[1], Timajo, D.A.[1], Anderson, G.M.[1]

[1]Centre for Neuroendocrinology and Department of Anatomy, University of Otago, Dunedin, NZ.

Ovulation in mammals is driven by a massive surge of luteinizing hormone (LH) from the pituitary gland, which itself is driven by a surge of gonadotrophin-releasing hormone (GnRH) from the hypothalamus. GnRH and LH release have recently been shown to be inhibited by the neuropeptide RF-amide related peptide-3 (RFRP-3), the production of which increases during stressful situations. The aim of this study was therefore to test whether stress inhibits the preovulatory GnRH/LH surge via the actions of RFRP neurons.

We first evaluated ovary-intact cycling (proestrus) mice as a model for preovulatory surge investigations. In unstressed mice, only 61% (8/13) of proestrus mice (identified by vaginal cytology) exhibited a preovulatory LH surge (> 2 ng/ml), indicating the difficulty of detecting proestrus in mice. Therefore, we instead used ovariectomized mice with estradiol-induced preovulatory-like surges as a more robust model. In this model, 78% (7/9) of unstressed mice exhibited a surge compared to 44% (4/9) of mice subjected to 1 h of restraint stress on the afternoon of surge induction. In mice subjected to 2 h of restraint stress, no surges were observed. Therefore, we are using the latter paradigm to evaluate the role of RFRP neurons in stress suppression of the preovulatory surge.

To accomplish this, we developed a technique to specifically ablate RFRP neurons in adult mice. A new transgenic mouse line in which the *Rfrp* gene also produces Cre recombinase was crossed with a line that enables Cre-dependant expression of the diphtheria toxin receptor. Consequently, injecting the offspring with diphtheria toxin resulted in apoptosis of cells expressing *Rfrp* (1.5±0.33 vs. 9.3±1.7 RFRP neurons/brain section in RFRP-Cre and control mice respectively at 4 weeks post injection; $P<0.05$). We will next use this RFRP-neuron-ablated mouse model to evaluate restraint stress-induced surge suppression. This experiment is currently in progress.

2B.3: Regulation of C-type natriuretic peptide (CNP) in brain tissues: generalised response to dexamethasone

Wilson, M.O.[1], McNeill, B.A.[2], Barrell, G.K.[1], Prickett, T.C.R.[3], Espiner, E.A.[3]

[1]Faculty of Agriculture and Life Sciences, Lincoln University, Christchurch, NZ, [2] Faculty of Health, School of Medicine, Deakin University, Geelong, Australia, [3]Department of Medicine, University of Otago, Christchurch, NZ

CNP has high abundance in brain tissues and cerebrospinal fluid (CSF). We have shown previously that plasma and CSF levels of CNP and aminoterminal proCNP (NTproCNP) are increased by dexamethasone. To determine the source of this increase, peptide concentration and CNP gene expression across a wide array of CNS tissues were studied in adult sheep given a single intravenous bolus of dexamethasone (0.25 mg/kg live weight) or saline solution (n = 7/group). Jugular venous blood and concurrent CSF samples were collected at 0 and 8 hours after which animals were killed and selected samples of brain, anterior and posterior pituitary gland, and spinal cord were excised and promptly stored for later analysis.

Both CNP peptides in plasma and CSF were increased by dexamethasone. Tissue concentration of CNP and NTproCNP was higher in dexamethasone-treated sheep in 6 and 11 of the 14 regions examined, respectively. Highest CNP responses (delta %) were observed in occipital cortex (370%), olfactory bulb (320%), and hippocampus (300%). Relative to controls, CNP gene expression (*NPPC*) in dexamethasone-treated animals was 3-fold higher in hypothalamus and hippocampus. Patterns of responses differed in pituitary tissue. Whereas peptide abundance greatly exceeded that of brain tissues, neither peptide nor gene expression in posterior pituitary was increased by dexamethasone. In anterior pituitary, despite a 5-fold increase in *NPPC* expression after dexamethasone, CNP concentration did not change and the increase in NTproCNP was not significant.

This is the first report of enhanced production and secretion of CNP by dexamethasone in brain tissues. The surprisingly diverse activation of CNP secretion within CNS tissues by dexamethasone suggests an important role for CNP in settings of acute stress. Differential responses within pituitary tissues may be related to functions of the stored hormone, in addition to specific regulation of CNP by enzymic hydrolysis or clearance receptors.

2B.4: Characterizing the effects of general anaesthesia on circadian rhythm and clock gene expression in Drosophila

Li, D.[1], Warman, G.R.[1], Cheeseman, J.F.[1]

[1]Department of Anaesthesiology, University of Auckland, Auckland, NZ.

General anaesthesia (GA) is an essential component for surgical practices; however, the long-term effects on both patients and animal subjects' post-treatment remain relatively unclear. Research conducted in the honeybee suggests GA causes a three hours phase delay in the circadian clock after a six hour 2% Isoflurane treatment 1. In this study, *Drosophila* are used to investigate the impact of GA on the circadian clock. The overall aim is to explore the mechanisms of GA on the clock through study of *Drosophila* locomotor activity and the clock gene expression. Here we present results of the effects of GA on the *Drosophila* activity rhythms. First a durational dose response curve was constructed by using different durations of 2% Isoflurane, which indicates six hours GA can produce a significant phase shifts in the circadian rhythm. In a second experiment we constructed a preliminary phase response curve (PRC) using 6h GA treatment at different circadian times. This PRC was characterised by phase advances in the morning from circadian time 0 (CT 0) to circadian time 10 (CT 10) and a phase delays in the evening between CT 10 and CT 22. In a third experiment we combine light and anaesthesia to test whether we can mitigate the phase shifting effect of the anaesthesia. These results will be presented at the meeting. We expect our research results will contribute to theoretical support for mechanism of general anaesthesia in clinical trials by light treatment for GA affection.

1. Cheeseman, J. F., Winnebeck, E. C., Millar, C. D., Kirkland, L. S., Sleigh, J., Goodwin, M., Warman, G. R. (2012*). General anesthesia alters time perception by phase shifting the circadian clock*. Proc Natl Acad Sci U S A, *109*(18), 7061-7066. 10.1073/pnas.1201734109

2B.5: Automatic cardiac auscultation decision support system for improved screening and teaching

Meintjes, A.[1], Lowe, A.[1], Legget, M.[2]

[1]Institute of Biomedical Technologies, Auckland University of Technology, Auckland, NZ, [2]School of Medicine, University of Auckland, Auckland, NZ.

Cardiac auscultation provides a low-cost, effective method of cardiovascular disease screening. Unfortunately auscultation skills are not well taught in medical schools and it is left up to the medical students to listen to different heart sounds and acquire the necessary skills as they go through their in-ward training. As can be attested to by a number of recent studies most clinicians are not able to accurately distinguish between pathological and physiological murmurs. This leads to unnecessary referrals, expensive tests, unwarranted anxiety for patients and their families, as well as potentially life-threatening misdiagnoses.

A possible solution to this problem has been proposed in the form of computer aided heart sound analysis. Recent work in this field has focused on the use of machine learning algorithms to classify the pathology present in a heart sound, based on features extracted from a recorded heart sound. Overall these methods have presented high sensitivities and specificities, although the testing and training sets are small and not well described. The digital processing techniques described in the literature provide powerful methods of analysing and identifying features of the heart sound, but classification schemes suffer due to a lack of external knowledge and the limited information available in an isolated recording.

The aim of this research will firstly be to construct a heart sound analysis algorithm that is able to extract clinically useful information about the timing, quality, and intensity of any murmurs or added sounds present in a heart sound recording. The second aim will be to create a multimedia training tool that is able to use the developed heart sound analysis algorithm to assist medical students and residents in obtaining and training the necessary cardiac auscultation skills and knowledge.

2B.6: The vasculoprotective effects of community-based, self-regulated aerobic interval training

Sethi, S.[1], Kilding, A.[2], Lowe, A.[3], Hastings, B.[4]

[1]Sports Performance Research Institute New Zealand, Auckland University of Technology, Auckland, NZ, [2]Sports Performance Research Institute New Zealand, Auckland University of Technology, Auckland, NZ, [3]Institute of Biomedical Technologies, Auckland University of Technology, Auckland, NZ, [4]Les Mills International Limited, Auckland, NZ.

Traditional laboratory-based studies have demonstrated that aerobic exercise (AE) and interval training can confer vasculoprotection, thereby combating early vascular ageing (EVA) and reducing cardiovascular risk. The current study was undertaken to determine the external validity of laboratory-based findings by investigating the vascular effects of 'real-world' community-based, self-paced, mixed-intensity cycling.

An eight-week repeated-measures intervention design was adopted during which fifteen healthy, sedentary adult males (31.8±6.1 years) were split into intervention and control groups. The intervention group undertook 45 minutes of self-paced concurrent aerobic interval exercise thrice weekly for eight weeks. The gymnasium-based indoor cycling intervention was based on principles of AE interspersed with both high-intensity interval and sprint interval exercise within a single session. Physiological assessments were carried out at baseline (PRE), after four weeks (MID), and post-intervention (POST). Resting arterial health indices assessed pertained to target-organ-damage-related tissue biomarkers of EVA and included operative arterial stiffness (carotid-femoral pulse wave velocity, cfPWV), wave reflections (augmentation index, AIx@75), central pulse pressure (cPP), wall thickness (common carotid and femoral intima-media thickness, cIMT and fIMT respectively), and arterial geometry (common carotid end-diastolic diameter, cEDD, and wall:lumen ratio, cWLR).

The average heart rate during the self-regulated sessions was 81±7%HR_{peak} (indicating vigorous exercise). Improvements in VO_{2peak}, anthropometric, clinical and arterial health measures from PRE to POST were observed in the intervention group only *($p<0.05$)*. At POST, there were significant between-group differences in VO_{2peak}, cfPWV, cPP, fIMT, cEDD, and cWLR *($p<0.05$)*.

In healthy, untrained adults, self-paced aerobic interval cycling significantly improves cardiorespiratory fitness and arteriosclerotic indices in addition to causing systemic outward arterial remodelling. The present results are consistent with those of controlled laboratory-based studies and demonstrate the feasibility and effectiveness of a community-based exercise approach to enhance arterial health. Further work into individual responsiveness and the resistance exercise component of this training is warranted.

2B.7: Feasibility of a novel extra-aortic balloon cuff with peristaltic motion and counterpulsation to assist heart function.

Wangdee Jones, P.N.[1], Lowe, A.[1], Kilby, J.[2]

[1]Instiute of Biomedical Technologies, Auckland University of Technology, NZ, [2]Department of Electrical and Electronics, School of Engineering, Auckland University of Technology, NZ.

The development of an extra-aortic balloon cuff with peristaltic motion and counterpulsation is explored to investigate the practicality for future treatments for chronic heart failure (CHF). This concept is an extension of existing heart assisting technology marketed as C-Pulse by Sunshine Heart[1] which is used to treat patients with New York Heart Association (NYHA) class III and ambulatory class IV heart failure.

This study incorporates experiments of both software simulation and hardware aspects. The software experiment simulated the aortic pressure and flow waveform under the influence of external peristaltic augmentation using a 1 dimensional wave propagation mode. The data was obtained from the simulation and a prototype device was constructed using the parameters from the simulation to test the overall feasibility of a novel extra-aortic balloon cuff. The hardware prototype was developed using Arduino base controller that drives multiple pneumatic pumps that inflate and deflate the cuff according to the rhythm of the heartbeat. A devised left ventricle mechanism with an attached phantom aorta was used as a testing platform for the functionality of the prototype.

Preliminary results from both simulation and experiment show that the system can augment the pressure waves in the descending aorta. Further testing is planned and will be compared with the C-Pulse system and other CHF devices in the efficacy of modulating coronary flow and cardiac afterload. This research has the potential to not only provide knowledge of modelling hemodynamic with peristaltic augmentation, but to also introduce a novel medical device that could assist heart function for patients with CHF in the near future.

1. *"C-Pulse Heart Assist System | Heart Failure Products," Sunshine Heart. [Online]. Available: http://www.sunshineheart.com/c-pulse-technology/. [Accessed: 01-Jun-2016].*

2B.8: Composite films consisting of regenerated cellulose/polypyrrole/silver nanoparticles/ ionic liquid are potential alternative to wound healing

Chowdhury, N.A.[1], Al-Jumaily, A.M.[1]

[1]Institute of Biomedical Technologies, Auckland University of Technology, Auckland, New Zealand

In this study, we synthesized films consisting of regenerated cellulose/polypyrrole/silver nanoparticles/ionic liquid (RC/PPy/Ag/IL) for wound healing applications. Silver nanoparticles (AgNPs) were incorporated in PPy and deposited on RC film during polymerization. To prepare conducting RC/PPy/Ag composite films, silver nitrate ($AgNO_3$) was used as an oxidant. It is a one step process where strong oxidizing agents were not used. Later, the films were coated with ionic liquid. When IL was in contact with AgNPs, positive charge appeared on the AgNPs surface. Such charged Ag atoms inhibit the growth of gram-positive and gram negative bacteria. In addition, ionic liquids effectively disrupt biofilms and neutralize pathogens. Moreover, free ion pairs in ionic liquid enhance polymer chain mobility which results in higher electrical conductivity and diffusion of oxygen gas through the membrane. Oxygen permeability through the films is an important factor in the wound healing process. Electrical conductivity and strong antimicrobial activity of the composite films make that a suitable candidate in wound healing applications. RC/PPy-Ag/IL composite films were characterized using scanning electron microscopy (SEM), and FTIR spectroscopy.

3A.1: Viral-mediated gene transfer prevents stereotypical disease development in ovine Batten disease

Mitchell, N.L., Barrell, G.K.[1,2], Russell, K.N.[1,2], Wellby, M.[1,2], Melzer, T.R.[2,3], Wicky, H.E.[2,4], Hughes, S.M.[2,4], Assis, A.B.[2,5], Cooper, J.D.[2,5], Gray, S.J.[6,2], Palmer, D.N.[1,2]

[1]Faculty of Agriculture and Life Sciences, Lincoln University, NZ, [2]Batten Animal Research Network (BARN), [3]Department of Medicine, University of Otago and New Zealand Brain Research Institute, Christchurch, NZ, [4]Department of Biochemistry, Brain Health Research Centre, University of Otago, NZ, [5]Department of Basic and Clinical Neuroscience, Institute of Psychiatry, Psychology and Neuroscience, King's College London, UK, [6]Gene Therapy Center and Department of Ophthalmology, University of North Carolina, USA.

Gene therapy represents a promising treatment strategy for the monogenic NCLs. With their large complex human-like gyrencephalic brain and recapitulation of the key molecular, pathological and clinical features of the human NCL phenotype, sheep with naturally occurring NCLs are ideal translational subjects for such studies.

Successful treatment of six CLN5 affected sheep via combinatorial intracerebroventricular and intraparenchymal injections of either lentiviral or AAV9 vectors expressing ovine *CLN5* has been achieved providing sustained protection from stereotypical disease onset and progression. *In vivo* monitoring was extended beyond the intended endpoint to 27 months because cognitive and neurological functions were preserved, as determined by maze testing and neurological examinations whilst longitudinal neuroimaging by CT and MRI scanning revealed normalisation of intracranial volumes and structural brain integrity. Quality of life was profoundly improved and one AAV9 treated sheep is still grazing peacefully. The onset of visual deficits was delayed, from 11 months in untreated affected sheep to 21-24 months in the treated cohorts.

Collection of supporting neuropathological data detailing CLN5 transgene expression and the impact upon the lysosomal storage pathology, glial activation and neuronal loss is underway. In a more clinically relevant paradigm, four affected sheep with established disease have been injected with self-complimentary AAV9 vectors to determine if they can be rescued by intraventricular gene therapy. Similar results were obtained for one out of six CLN6 affected sheep and a study of another cohort with self-complimentary AAV9 vectors is promising.

3A.2: Does rate of rewarming after hypothermia affect seizure activity and white matter integrity after global cerebral ischaemia in term-equivalent fetal sheep?

Draghi, V.[1], Davidson, J.O.[1], Dhillon, S.[1], Wassink G. [1], Bennet, L.[1], Gunn, A.J.[1]

[1]Department of Physiology, University of Auckland, Auckland, NZ.

Hypothermia is the first effective treatment for infants with hypoxic-ischaemic encephalopathy (HIE) but is partially effective. Limited evidence suggests that slower rewarming after hypothermia may improve neuroprotection. In these preliminary studies, we tested the hypothesis that very slow rewarming from post-ischaemic hypothermia would attenuate seizure activity, reduce white matter inflammation or improve myelination.

Term-equivalent fetal sheep (0.85 gestation) were randomised to sham-control (n=8), ischaemia with normothermia (n=8), or ischaemia plus starting 3 h later, by 72 h hypothermia (n=8), or 48 h hypothermia (n=8), or 48 h hypothermia plus slow rewarming over 24 h (n=3). Seizures were counted on EEG recordings. Sheep were killed after 7 days for immunohistochemistry to assess numbers of microglia and myelin basic protein (MBP) density in white matter.

Cerebral ischaemia was associated with intense seizure activity from 12–72 h, increased microglia and loss of MBP expression compared to sham controls ($P<0.05$). Hypothermia for 72 h was associated with reduced seizure burden from 24–27 hours, reduced numbers of microglia and increased MBP ($P<0.05$). Hypothermia for 48 h was associated with increased seizures after rewarming, and less attenuation of microglia and reduced MBP density compared to hypothermia for 72 h ($P<0.05$). Slow rewarming after 48 h hypothermia reduced microglial activation compared to hypothermia for 48 h alone but did not prevent rebound seizure activity or improve density of MBP at day 7.

These preliminary data suggest that although slow rewarming over 24 h after 48 h of cerebral hypothermia may help attenuate post-ischaemic inflammation, it did not prevent rebound seizure activity and was associated with less protection of myelination than simply continuing cooling for 72 h. Further studies are needed to confirm these findings.

3A.3: Pleurodesis with Picibanil during fetal life is associated with neuroinflammation and white matter injury in the preterm brain

Dhillon, S.[1], Davidson, J.O.[1], Galinsky, R.[1], Gunn, A.J.[1], Bennet, L.[1]

[1]Department of Physiology, The University of Auckland, Auckland, NZ.

Picibanil (killed streptococcus pyogenes) causes significant inflammation and fusion of pleural membranes and is thus used clinically to fetal hydrothorax in preterm fetuses. Of concern, however, is the fact that inflammation is strongly associated with preterm brain injury. We previously reported, in preterm fetal sheep, that a single intrapleural injection of Picibanil caused a hippocampal infarct in one fetus, and moderate white matter injury in others. However, the dose used in this study was lower than that now routinely used clinically. The purpose of the current study was to examine the neural effects of a higher clinical dose. Fetal sheep at 0.7ga (~28-30 weeks human brain maturation) were instrumented for continuous measurement of fetal heart rate, blood pressure (BP), cerebral blood flow (CBF), body movements, and electroencephalographic (EEG) activity. Fetuses were given an intra-pleural injection of 1mg Picibanil (n=5) or saline (n=8). Brains were collected at day 7 for histology.

Picibanil caused transient tachycardia, no change in BP and a progressive increase in CBF. Body movements and EEG activity were suppressed between 2-6hrs ($p < 0.05$) and seizure-like activity was observed between 24-48hrs post-Picibanil exposure. Picibanil was associated with significant microgliosis ($p<0.05$) and astrogliosis ($p<0.05$) in the periventricular white matter, loss of mature and immature oligodendrocytes ($p < 0.05$) and reduced cortical area in the parasagittal cortex ($p<0.05$). Significant neuronal loss was observed in one fetus in the cortical, hippocampal, striatal and thalamic regions. Despite normotension and increased cerebral perfusion, high dose Picibanil was associated with seizures and significantly greater white matter injury than seen with the low dose. Reduced cortical volume suggests decreased synaptic density. These patterns of injury are associated with neurodevelopmental impairment. Our data suggest that the clinical fetal use of Picibanil requires further consideration and post-natal neurological assessment of patients.

3A.4: Head cooling for 48 hours is suboptimal for neuroprotection after global cerebral ischemia in term-equivalent fetal sheep

Davidson, J.O.[1], Draghi, V.[1], Whitham, S.[1], Dillon, S.[1], Wassink, G.[1], Bennet, L.[1], Gunn, A.J.[1]

[1]Department of Physiology, University of Auckland, Auckland, NZ.

Therapeutic hypothermia for 72 hours reduces death and disability in neonates with hypoxic-ischemic encephalopathy. However, it is unclear that this duration is optimal. If a shorter period of cooling was effective, then it would help reduce the impact of treatment on affected families. Indeed, in adult rodents cooling for 48 h is highly protective. Thus, in this study we contrasted neuroprotection with head cooling for 48 h compared to 72 h.

Term-equivalent fetal sheep (0.85 gestation) received 30 min of sham ischemia (n = 8) or ischemia induced by bilateral carotid artery occlusion followed by normothermia (n = 8) or head cooling started 3 h after ischemia, and continued for either 48 h (n = 8) or 72 h (n = 8). Fetuses were killed 7 days after ischemia for histology.

Cerebral Ischemia was associated with profound loss of EEG power after 7 days recovery, with severe loss of neurons in the cortex and hippocampus, loss of oligodendrocytes in the intragyral and periventricular white matter tracts and induction of Iba-1-positive microglia. Head cooling for 72 h markedly improved recovery of EEG power and overall neuronal survival, partially restored numbers of oligodendrocytes and suppressed microglial induction ($P < 0.05$). In contrast, although head cooling for 48 h was associated with improved outcomes compared to normothermia, compared to cooling for 72 h, it was associated with less recovery of EEG power ($P < 0.05$), less improvement in neuronal survival in the parasagittal cortex and the CA4 region of the hippocampus ($P < 0.05$), less attenuation of microglial induction ($P < 0.05$), but a similar partial improvement in numbers of oligodendrocytes ($P < 0.05$).

Conclusion: Head cooling for 48 h is partially neuroprotective, but is suboptimal compared to cooling for 72 h after global cerebral ischemia in fetal sheep.

3A.5: Reward sensitivity of cue responses of single dorsal raphe nucleus neurons may critically depend on background uncertainty

Hyland, B.I.[1], Lindemann, C.[1]

[1]Department of Physiology, Otago School of Medical Sciences & Brain Health Research Centre, University of Otago, NZ.

The dorsal raphe nucleus (DRN) is the origin of serotonergic projections to the rest the brain, implicated in stress & reward, and to depressive disorders. We previously found in a contextual conditioned approach task that single DRN neurons were more responsive to conditioned auditory cues that predicted no reward, than to cues that predicted reward delivery[1]. In that contextual task, there was a consistent relationship of cues with outcomes across each block of trials. We have now completed another study of DRN neurons, in which reward and non-reward trials were intermingled in pseudorandom sequence. Of 220 neurons included in the data set, 133/(60.5%) showed a response to one or other of the cues. However, significantly more neurons showed a preference for the reward cue, with 68/133 (51%) responding solely to the rewarded cue, 60 (45%) responding to both stimuli and only 5 (4%) showing the reverse selectivity ($P < 0.0001$, Chi-square test). Quantitative analysis of the responses in cells that had detectable excitatory peaks in firing rate following both reward and no-reward predictive cues revealed a significantly larger area under the curve for the peak in rewarded trials ($t(59) = 3.8$, $P = 0.0004$). This was due to a longer peak duration ($t(59) = 3.2$, $P = 0.0025$), with no difference in peak amplitude ($t(59) = 1.6$, $P = 0.12$), suggesting that the difference may specifically relate to later components of the response. Together, these data indicate that, in contrast to results using a block-design, in an intermingled trial design DRN neurons show enhanced responsiveness to reward cues compared to non-reward. A key difference between the tasks is the likely relative levels of uncertainly from trial to trial in the intermingled task, which could alter the relative salience of the cue.

1 Li, Y., Dalphin, N. & Hyland, B. I. *Association with reward negatively modulates short latency phasic conditioned responses of dorsal raphe nucleus neurons in freely moving rats*. *J. Neurosci.* 33, 5065-5078, (2013).

3A.6: Feeding-induced regulation of Wnt/beta catenin signaling in the mouse hypothalamus

Carter, K.[1,2], Rizwan, M.[1,2,3], Ladyman, S.R.[1,2,3], Grattan, D.R.[1,2,3]

[1]Centre for Neuroendocrinology, University of Otago, Dunedin, NZ, [2] Department of Anatomy, University of Otago, Dunedin, NZ, [3]Maurice Wilkins Centre for Molecular Biodiscovery, NZ.

Recent findings from Genome Wide Association Studies and meta-analysis of human studies have identified molecular mechanisms that may underlie an individual's susceptibility to development of Type 2 diabetes (T2D) and other metabolic disorders. Specific polymorphisms in a transcriptional co-factor, Transcription Factor 7-Like 2 (TCF7L2) have been associated with increased risk of T2D[1]. TCF7L2 is a transcription factor activated as part of the Wnt/Beta-Catenin signaling pathway, suggesting that this pathway is involved in the regulation of glucose homeostasis. Malfunction of this pathway may lead to pathophysiological features seen in T2D and other metabolic disorders. Recent data suggests that this pathway regulated by the metabolic hormone leptin in nuclei of the hypothalamus that are associated with the integration of endocrine signals and subsequent metabolic regulation[2]. Our lab have also recently shown this this pathway is physiologically responsive to natural fasting and non-fasting states whereby the pathway's activity increases after feeding in male rats[3]. The aim of this study is to determine whether activation of this pathway by feeding can also be detected in a mouse model, thereby facilitating future use of transgenic animals to determine the physiological significance of this pathway in the regulation of glucose homeostasis.

We will use Western blot analysis to determine whether beta-catenin protein is stabilized in the mouse hypothalamus under fasted/re-fed conditions. In addition, we will use quantitative RT-PCR to determine whether feeding results in increased expression of TCF/beta catenin-responsive genes in the hypothalamus. It is hypothesized that mice in the re-fed condition will show time-dependent increases in beta-catenin in the hypothalamus and consequent increases in beta-catenin responsive gene expression.

1. Grant, S. F., et al., *Variants of transcription factor 7-like 2 (TCF7L2) gene confers risk of type 2 diabetes.* Nature Genetics, 2006. **38**(3), 320-3.
2. Benzler, J., Andrews, Z. B., Pracht, C., Stöhr, S., Shepherd, P. R., Grattan, D. R. & Tups, A, *Hypothalamic WNT signaling is impaired during obesity and reinstated by leptin treatment in male mice.* Endocrinology, 2013. **154**(12), 4737-45.
3. McEwen HJ, Cognard E, Ladyman SR, Khant-Aung Z, Shepherd PR and Grattan DR. (2016). *Feeding and GLP-1 receptor activation stabilizes beta-catenin in hypothalamic neurons and regulates neuropeptide secretion: beta-catenin involvement in hypothalamic nutrient sensing.* Submitted
4. Helfer, G. and Tups, A, *Hypothalamic Wnt Signalling and its Role in Energy Balance Regulation.* J Neuroendocrinol, 2016. **28**(3).

3A.7: The role of the prolactin receptor in the developing brain

Boyes, K.[1,2], Kokay, I.C.[1,2], Wyatt, A.[3], Boehm, U.[3], Grattan, D.R.[1,2,4]

[1]Centre for Neuroendocrinology, University of Otago, Dunedin, NZ, [2]Department of Anatomy, University of Otago, NZ, [3]Department of Pharmacology and Therapeutics, University of Saarland, Homburg, Germany, [4]Maurice Wilkins Centre for Molecular Biodiscovery, NZ.

Prolactin signalling through the prolactin receptor plays a significant role in many physiological processes[1]. The diverse biological functions attributed to prolactin are largely dependent on the distribution of it receptor. In particular, the distribution of the prolactin receptor has been well characterised in the adult brain of rodents[2], but has yet to be fully documented in the developing brain of neonates. Activation of this receptor is known to stimulate neurogenesis in the maternal brain of an adult rodent[3]. In addition to this action, development of at least one population of neurons appear to be dependent on prolactin during fetal and/or early postnatal life[4]. As such, the prolactin receptor may contribute to neurogenesis in the developing brain.

To determine the role of the prolactin receptor in the developing brain of neonates, we have developed a transgenic mouse in which cre-recombinase is expressed under the control of an internal ribosomal entry site (IRES) in the prolactin receptor gene (Prlr-IRES-Cre). The Prlr-IRES-Cre mouse has been crossed with a cre-dependent tau-GFP reporter line. In this study tau-GFP will be expressed wherever the prolactin receptor gene has been transcribed. This is important, because it enables us to study the projections of prolactin-responsive neurons for the first time, which has not been possible in earlier methods. Therefore, we will be able to visualise the anatomical distribution of prolactin receptor expressing cells.

1. Grattan, D.R. and I.C. Kokay, *Prolactin: a pleiotropic neuroendocrine hormone.* J Neuroendocrinol, 2008. **20**(6): p. 752-63.
2. Brown, R.S., et al., *Distribution of prolactin-responsive neurons in the mouse forebrain.* Journal of Comparative Neurology, 2010. **518**(1): p. 92-102.
3. Larsen, C. and D. Grattan, *Prolactin, neurogenesis, and maternal behaviors.* Brain, behavior, and immunity, 2012. **26**(2): p. 201-209.
4. Romero, M.I. and C.J. Phelps, *Prolactin replacement during development prevents the dopaminergic deficit in hypothalamic arcuate nucleus in prolactin-deficient Ames dwarf mice.* Endocrinology, 1993. **133**(4): p. 1860-1870.

3A.8: Effect of diabetes on pro-apoptotic microRNA-532 in heart

Chandrasekera, D.[1], Fomison-Nurse, I.[1], Rawal, S.[1], Bunton, R.[2], Galvin, I.[2], Katare, R.[1]

[1]Department of Physiology, University of Otago School of Medical Sciences, Dunedin, NZ, [2]Department of Cardiothoracic Surgery, Dunedin Hospital, Dunedin, NZ.

Hyperglycaemia in diabetes promotes cell death among cardiomyocytes either by apoptosis and/or necrosis. Early molecualr alterations have been shown to be accelearting this cell death process in response to the hyperglycemic conditions. MicroRNA-532 (miR-532), originally demonstrated to have oncogenic properties. Recent studies show that miR-532 could regulate apoptotic cell death. Therefore, aim of this study is to determine the differential expression of miR-532 in diabetic heart to understand its role in diabetes induced cardiomyocytes cell death.

The RNA and protein were extracted from human right atrial appendage (RAA) samples collected from patients undergoing coronary artery bypass graft surgery at Dunedin Hospital through Heart-Otago. In order to determine the changes in miR-532 during the evolution of diabetes, RNA and protein was also extracted from heart tissue of type-2 diabetic (db/db) and lean mice in age groups ranging from 8 to 32 weeks.

Quantitative RT-PCR analysis showed significant increase in the expression of miR-532 in human RAA. Interestingly, the onset of changes in miR-532 were observed at 16 weeks of age in diabetic mice when cardiac dysfunction is fully evolved. Further western blotting will be carried out to analyse changes in expression of apoptosis repressor with caspase recruitment domain (ARC), target protein for miR-532.

To determine if therapeutic modulation of miR-532 would influence the death of cardiomyocytes, adult moue cardiomyocytes (HL-1 cells) will be transfected with antagomir for miR-532 to knockdown the expression of miR-532 and a scramble sequence as a control. The transfected cells will then be cultured in either normal (5mM) or high (30mM) glucose concentrations, followed by caspase assay to determine the effect of miR-532 on apoptosis.

Positive results from this study will not only identify a novel mechanism for increased apoptosis in diabetes, but also a novel therapeutic modality to treat diabetes-induced cardiovascular disease.

3A.9: The effect of prolactin on AgRP neurons in the arcuate nucleus

MacLeod, M.A.[1,2], Ladyman, S.R. [1,2,3], Grattan, D.R.[1,2,3]

[1]Centre for Neuroendocrinology, University of Otago, Dunedin, NZ, [2]Department of Anatomy, University of Otago, Dunedin, NZ, [3]Maurice Wilkins Centre for Molecular Biodiscovery, NZ.

One adaptive response that occurs during pregnancy is the development of a positive energy balance to support the demands of growth of fetal and maternal tissues as well as to increase energy stores in preparation for the metabolic demands of lactation. Leptin levels increase as pregnancy advances, along with fat deposition and increased appetite. This is somewhat unusual, as the role of leptin in the non-pregnant state is to decrease food intake and increase energy mobilization. Therefore, it has been concluded that leptin is not being recognized during pregnancy ("leptin resistance"). Additionally, there is increased plasma prolactin observed during pregnancy. It is known that there are prolactin receptors in the same regions of the brain that control food intake. It is also known that prolactin has an orexigenic effect and acts via the same intracellular signaling pathways as leptin, so we hypothesise that the pregnancy hormone, prolactin, may be a mediator of this resistance to leptin.

It is clear that leptin responsive neurons, such as AgRP and POMC neurons in the arcuate nucleus of the hypothalamus, do not respond normally to leptin during pregnancy. The aim of this study is to examine whether prolactin directly targets these leptin responsive neurons. We are using an AgRP-cre-tdTomato transgenic mice model to identify AgRP neurons within the mouse brain, and investigating whether prolactin-induced phosphorylation of STAT5 can be detected in these neurons.

3A.10: The effect of pregnancy-induced adaptations on glucagon like-peptide-1 receptor activation-induced stabilisation of beta-catenin in hypothalamic neurons in female rats.

Kaplish, M.[1,2], Ladyman, S.R.[1,2,3], Grattan, D.R.[1,2,3]

[1]Centre for Neuroendocrinology, University of Otago, Dunedin, NZ, [2]Department of Anatomy, University of Otago, Dunedin, NZ, [3]Maurice Wilkins Centre for Molecular Biodiscovery, NZ.

Glucagon-like peptide-1 (GLP-1) acts in the brain where it regulates food intake and glucose homeostasis[1,2]. Recently our laboratory has shown that GLP-1 receptor activation is involved in a metabolic sensing mechanism via beta-catenin stabilisation in specific hypothalamic neurons of male rats[3]. Beta-catenin is a key partner with TCF7L2, a transcription factor that has strongly associated with diabetes type II[4], suggesting that this pathway might play an important role in the central regulation of glucose homeostasis. In female rats, physiological demands during pregnancy induce a well-orchestrated range of adaptations to metabolic homeostasis to cope with the immediate and potential competing needs. Hyper-phagia and adiposity are the strategies to feed the growing foetus and prepare for the metabolic demands of lactation[5], and there are also significant changes in glucose homeostasis with the development of insulin resistance and increased glucose-stimulated insulin secretion. The aim of the present study is to determine firstly, whether the GLP-1-induced stabilisation of beta catenin in the hypothalamus also occurs in females, and if so, whether this response is altered during pregnancy. We will use immunohistochemistry to determine the levels of beta-catenin protein in the paraventricular, arcuate, and dorsomedial hypothalamic nuclei. In additional groups of animals, these nuclei will be microdissected and expression of TCF/beta-catenin responsive genes will be assessed using quantitative real time Polymerase Chain Reaction. These studies will further our understanding about the role of TCF/beta-catenin signalling in the brain in metabolic homeostasis.

1. Turton M.D., O'Shea D., Gunn I., Beak S.A., Edwards CMB, Meeran K., Choi SJ, Taylor GM, Heath M.M. *A role for glucagon-like peptide-1 in the central regulation of feeding*. Nature. 1996. 379: 69-72
2. Sandoval D.A., Bagnol D., Woods S.C., D'Alessio D.A. and Seeley R. *Arcuate glucagon-like peptide 1 receptors regulate glucose homeostasis but not food intake*. Diabetes.2008.Vol. 57:2046-2054.
3. Clever H. Wnt/beta-catenin signaling in development and disease.Cell. 127(3):439-480.
4. McEwen HJ, Cognard E, Ladyman SR, Khant-Aung Z, Shepherd PR and Grattan DR. (2016). *Feeding and GLP-1 receptor activation stabilizes beta-catenin in hypothalamic neurons and regulates neuropeptide secretion: beta-catenin involvement in hypothalamic nutrient sensing*. Unpublished manuscript.
5. Augustine RA, Ladyman SR and Grattan DR. *From feeding one to feeding many: hormone-induced changes in bodyweight homeostasis during pregnancy*. J.Physiol.2008. 387-397.

3A.11: Examining the role of endogenous ghrelin in vascular homeostasis using a murine model of hind-limb ischaemia

Neale, J.P.H.[1], Katare, R.[1], Schwenke, D.[1]

[1]Department of Physiology, HeartOtago, University of Otago, Dunedin, NZ.

Ghrelin is a 28-amino acid peptide cleaved from the precursor preproghrelin. Ghrelin has potent orexigenic actions and largely documented cardiovascular benefits. Recently, we have shown that exogenous ghrelin has angiogenic potential in a murine model of CLI, through activation of anigomiRs. Despite this, research investigating the vascular homeostatic role of endogenous ghrelin is limited. Therefore, it is of great interest to elucidate the role of endogenous ghrelin in vascular homoeostasis and to identify the mechanistic pathway(s) for this. We hypothesise that endogenous ghrelin is essential for vascular homoeostasis through regulation of angiogenic miRNA's especially under the conditions of peripheral artery disease (PAD). In this study, hind-limb ischemia will be induced in ghrelin-deficient mice (KO; ghr-/-; 30-34 wk old; B.W. ~28-34 g; n = 14) and controls (Ghr +/+; 30-34 wk old; B.W. ~25-33 g; n = 14) by femoral artery ligation to simulate PAD. Micro-computed tomography will be used to assess collateral artery growth. Angiogenesis will be identified by IHC staining using isolectin-B4 (endothelial marker) and α–smooth muscle actin for capillary and arteriole density, respectively. Superficial foot perfusion will be measured using an infrared thermal sensitive camera postoperatively and at days 3, 7, 10 and 14. A functional assessment of limb damage will also be conducted on these days. Adductor and gastrocnemius muscles will be collected for molecular and histological analysis. Finally, quantification of angiogenic miR's will be carried out to identify potential mechanistic pathway(s) underpinning ghrelin's role in vascular homoeostasis. This work will broaden our knowledge of vascular homoeostasis and its regulators and, furthermore, advocate the use of ghrelin as a potential new therapy in the treatment of ischemic conditions including PAD and CLI.

3A.12: Preventing changes in coronary blood flow associated with type 2 diabetic heart disease through exercise - assessed using Synchrotron Radiation Microangiography

Wei M.Y.[1], Lew J.K.S.[1], Pearson J.T.[2], Katare R.[1], Schwenke D.O.[1]

[1]Department of Physiology, Otago School of Medical Sciences, University of Otago, Dunedin, NZ, [2]Department of Cardiac Physiology National Cerebral and Cardiovascular Center, Suita, Japan.

Type 2 diabetes has reached epidemic proportions worldwide and is associated with numerous long-term health complications. In particular, cardiovascular diseases, or diabetic heart diseases, account for 50-80% of deaths in diabetic patients. Unfortunately the onset of heart disease in type 2 diabetes begins at a very early stage with impairment of coronary blood flow being a precursor for cardiac functional and structural deterioration. This is due to the functional capacity of the heart being highly dependent of adequate blood flow. As diabetic heart disease covers a wide spectrum of heart diseases, there is limited success in treating it.

Exercise is generally viewed as an excellent prophylactic strategy for ameliorating or preventing the onset of type 2 diabetes due to its benefits on weight management, blood glucose control and insulin sensitivity. Moderate exercise effectively reverses endothelial dysfunction in 'pre-diabetic' subjects, whilst high intensity exercise has shown to be effective in reversing the progression of diabetic heart disease. However, once diabetic heart disease has become well established, the level of exercise intensity to impede the progression of cardiac dysfunction is often unsustainable for most patients. Therefore, this study proposes that initiation of moderate intensity exercise in the early stages of diabetes, prior to the onset of cardiac dysfunction, will prevent coronary artery dysfunction and hence prevent diabetic heart disease.

The experimental protocol involves db/db mice that are divided into pre-diabetic heart disease and post-diabetic heart disease groups, with non-diabetic mice used as controls. Mice are then subjected to one hour of either high intensity or moderate intensity exercise, with a sub-group subjected to no exercise. After 8 weeks of exercise, the functional capacity of the coronary vessels will be directly visualised and assessed based on vasoactive mediators using synchrotron radiation microangiography.

3A.13: CaMKII activation in endothelial dysfunction

Worthington, LP.[1], Erickson, J.R.[1], Heather, A.K.[1]

[1]Department of Physiology, University of Otago, Dunedin, NZ.

Atherosclerosis is the leading cardiovascular disease affecting the developed world. Atherosclerosis is the development of plaques within the artery wall, which is driven by the net accumulation of cholesterol in the artery. Over time plaques grow and disturb blood flow, which can manifest in ischaemic attacks, including myocardial infarctions and strokes. An early event preceding the development of atherosclerotic plaques is endothelial dysfunction. Endothelial dysfunction is characterized by increased inflammation and a reduction in nitric oxide (NO) bioavailability, governed by endothelial nitric oxide synthase (eNOS). eNOS represents a double-edged sword, as, during elevated oxidative stress, eNOS switches from a NO to a superoxide ($O_2^{\cdot-}$) producing enzyme. eNOS activity is regulated by local calcium transients and by phosphorylation of the enzyme. In a healthy artery, calcium /calmodulin dependent protein kinase II (CaMKII) interacts and phosphorylates eNOS at Ser^{1177} to stimulate NO production. CaMKII is of particular interest due to its well-described role in driving cardiac disease when it undergoes post-translational modifications. Under increased conditions of oxidative stress, CaMKII is oxidized and becomes chronically active. Whether oxidized CaMKII influences eNOS derived $O_2^{\cdot-}$ production remains to be identified. Apolipoprotein E null (Apo $E^{-/-}$) mice will be culled at 13 or 20 weeks. Another group of Apo $E^{-/-}$ mice will undergo treatment with the selective CaMKII inhibitor KN-93 from 16 to 20 weeks of age. The aortic sinus and aortic arch will be dissected and subject to serial sectioning for plaque analysis and immunohistochemistry targeting total eNOS/ P-Ser^{1177} eNOS, CaMKII/ oxidized-CaMKII, CD31/VCAM-1. We hypothesise that high levels of ROS within the atherosclerotic prone regions will lead to the oxidized modification of CaMKII. Furthermore, oxidized CaMKII will be associated with elevated levels of P-Ser^{1177} and VCAM-1, an effect that will be reduced with KN-93 treatment. Results from this study may unravel a new mechanism by which chronically active CaMKII sustains oxidative stress in endothelial dysfunction and ultimately drives early plaque formation.

3A.14: Development of RyR2-based redox sensor for H2O2 quantification in cardiac dyad microdomain

McLachlan, J.[1], Jones, P.[1]

[1]Department of Physiology, University of Otago, NZ.

Protein oxidation, driven by reactive oxygen species (ROS) is a fundamental event in cardiomyocytes that involves the covalent, post-translational modification of proteins. In contrast to cell-wide events, ROS-mediated effects are differentially regulated in distinct regions of the cell, termed ROS microdomains. However, the lack of tools to spatiotemporally resolve ROS microdomains prevents us from further understanding the magnitude of ROS involved in signal transduction. Previous research has concluded that ROS generation via NADPH-oxidase modulates contraction, but in excess can result in heart failure. These alterations have been attributed to oxidation of the cardiac ryanodine receptor (RyR2), responsible for the calcium release required for excitation-contraction of the myocardium. Expressed within the cardiac dyad, RyR2 remains inaccessible to the cytosol. This narrow space between the transverse tubule and sarcoplasmic reticulum restricts diffusion, thus creating a unique but yet unquantified ROS microdomain imperative to cardiac function. Recently, the development of genetically encoded redox sensors has provided a novel mechanism for ROS measurement. Two of the latest generation, HyPer3 and roGFP2-Orp1 provide a non-invasive, cell-wide mechanism of hydrogen peroxide measurement *in vivo*. Based on fluorescent proteins conjugated to redox-sensitive proteins derived from bacteria, oxidation of these probes results in a conformational change that can be visualised by an alteration in the fluorescence excitation spectrum. As these probes have been shown to successfully be tethered to specific proteins with a neutral effect on structure and function, we are developing a RyR2-tethered sensor that will provide an invaluable mechanism to quantify the cardiac dyad ROS microdomain. Our research aims to develop a novel mechanism to measure ROS signalling within the cardiac dyad microdomain to determine how alterations in the magnitude of ROS regulate physiological and pathological calcium release.

3B.1: Responses to vesiculin identify the existence of a signaling pathway that can bypass insulin resistance

Lee, K.L.[1], Aitken, J.F.[1], Williams, G.M.[2], Brimble, M.A.[2], Cooper, G.J.S.[1,3,4]

[1]School of Biological Sciences, [2]School of Chemical Sciences, The University of Auckland, NZ, [3]Maurice Wilkins Centre for Molecular BioDiscovery, The University of Auckland, NZ, [4]Centre for Advanced Discovery and Experimental Therapeutics, Manchester Biomedical Research Centre, Central Manchester University Hospitals NHS Foundation Trust, and the School of Biomedicine, University of Manchester, UK.

Pancreatic islet-derived peptide hormones play key roles in the maintenance of systemic energy homeostasis and glucose balance, and defects in their regulation are strongly implicated in the pathogenesis of obesity and diabetes, both of which have emerged as global pandemics in recent times. It is therefore important to understand the biological roles of islet hormones in both their target tissues and the whole organism. Insulin-like growth factor II (IGF-II) is an insulin homolog secreted by the islet β-cells. Vesiculin is a newly discovered peptide hormone, processed from IGF-II and secreted from islet β-cells in response to glucose, whose biological role is poorly understood [1-3]. Like insulin, vesiculin is a two-chain hormone and so has structural similarities to insulin although it has the amino acid sequence of IGF-II. Based on these observations, we postulated that vesiculin might act to regulate systemic glucose metabolism.

Here we report our original investigations of vesiculin's activity in glucoregulation. Insulin tolerance tests (ITTs) in mice were used to compare the capacity of vesiculin and IGF-II for lowering blood glucose. ITTs were also performed in two different mouse models of inslin resistance.

Vesiculin and IGF-II displayed similar dose-response relationships for lowering blood glucose in insulin-responsive mice. By contrast, the ability of IGF-II to lower blood glucose was blunted in insulin-resistant triprolyl human-amylin transgenic mice, whereas vesiculin's ability to lower blood glucose remained largely unaffected. Analysis of signaling by vesiculin and IGF-II in islet β-cells indicated that vesiculin does not signal through the type-1 IGF receptor (IGF1R), the main receptor for IGF-II, indicating that removal of only four amino acids has generated a new peptide hormone with distinct bioactivity relevant to blood-glucose regulation.
Investigating the differences among vesiculin, IGF-II and insulin signaling may provide new insights into the development of insulin resistance, a usual feature of progression to type-2 diabetes.

1. Buchanan, C.M., A.R. Phillips, and G.J. Cooper, *A novel two-chain IGF-II-derived peptide from purified beta-cell granules.* Growth hormone & IGF research, 2010. **20**(5): p. 360-6.
2. Lee, K.L., M.J. Middleditch, G.M. Williams, M.A. Brimble, and G.J. Cooper, *Using mass spectrometry to detect, differentiate, and semiquantitate closely related peptide hormones in complex milieu: measurement of IGF-II and vesiculin.* Endocrinology, 2015. **156**(3): p. 1194-9.
3. Williams, G.M., G.J. Cooper, K. Lee, L. Whiting, and M.A. Brimble, *Synthesis of the IGF-II-like hormone vesiculin using regioselective formation of disulfide bonds.* Org Biomol Chem, 2013. **11**(19): p. 3145-50.

3B.2: Basis function modelling of respiratory patients with high or low auto-PEEP

Langdon, R.[1], Docherty, P.D.[1], Blane, G.[1]

[1]Department of Mechanical Engineering, University of Canterbury, NZ.

For patients with acute respiratory distress syndrome (ARDS), mechanical ventilation (MV) is an essential therapy in the intensive care unit (ICU). Suboptimal ventilator settings may cause ventilator induced lung injury (VILI), which is associated with and increased mortality. Mathematical models that capture patient-specific information can enable individualised MV and reduce the incidence of VILI.

Data from ten fully sedated adult ARDS patients was investigated. The patients began at a positive end expiratory pressure (PEEP) of zero, and PEEP was increased by 5cmH_2O three to six times. Four patients had a high auto-PEEP (>=8cmH_2O), and were diagnosed with COPD. Auto-PEEP can result from the limitation of expiratory flow, and is thus common in COPD patients. Of the six patients with low auto-PEEP, one had a COPD diagnosis. A basis function model of pulmonary mechanics was fit to each patient data set. The model consisted of basis functions to capture a pressure-dependent elastance curve, and a linear pressure-dependent resistance relationship. The model fit was compared with patients' diagnoses and auto-PEEP. Mean residuals were comparatively low and unbiased for low auto-PEEP patients, across the entire recruitment manoeuvre (mean RMS residuals 0.93 (range 0.80-1.18) vs. 2.1 (range 1.42-2.91), $p<0.01$). For high auto-PEEP patients, the model yielded consistently poor fits at low PEEP due to a higher than expected peak pressure. The model was unable to fit this non-linear behaviour, and the true lung elastance at low PEEP was much higher than accounted for by the model. Additionally, it was likely that COPD patient airways changed during the recruitment manoeuvre as blockages in the bronchial pathway were altered with increased PEEP. The consistency of the results validates our modelling strategy and highlights the physiological differences of patients with high auto-PEEP and COPD.

3B.3: Magnocellular neuronal activation in response to acute myocardial infarction

Roy R.K.,[1] Brown, C.H.[1], Schwenke, D.O.[1]

[1]Department of Physiology, University of Otago, Dunedin, NZ.

Acute myocardial infarction (MI) is a global health problem, which is associated with the alteration of the neuro-hormonal homeostasis. Hormones that are elevated following acute MI are also produced by the hypothalamic magnocellular neurons. However, the activation level of these magnocellular neurons is yet to be explored.

In this study we aimed to assess the activation of magnocellular neurons in response to acute MI. Magnocellular neurons were located in two hypothalamic nuclei; supraoptic nucleus (SON) and paraventricular nucleus (PVN). In order to investigate their activation, rats were transcardially perfused under anesthesia 90 min following acute MI or sham operation. Immunohistochemistry for Fos protein was performed on brain sections as a marker of neuronal activation. MI rats had a significantly higher number of Fos-positive cells in the SON and PVN than sham operated rats (p=0.0002, unpaired t-test and p<0.0001, unpaired t-test respectively).

We next determined the phenotype of the activated magnocellular neurons using double label immunohistochemistry. In SON, significantly higher number of Fos-positive oxytocin (OT) neurons was identified compared to sham (p<0.0001, unpaired t-test). In PVN, acute MI was associated with significantly higher number of Fos-positive vasopressin (VP) and oxytocin (OT) neuron to sham (p=0.0022, unpaired t-test and p<0.0001, unpaired t-test respectively). Taken together these results suggest that the activation of magnocellular VP neurons may co-relate to the increased expression of circulating VP hormone, which has been previously reported in chronic heart failure.

3B.4: An ovine model of renovascular hypertension: role of the carotid body chemoreceptors

Mahesh, D.[1], McBryde, F.D.[1], George, B.[1], Paton, J.F.[2], Ramchandra, R.[1]

[1]Department of Physiology, The University of Auckland, Auckland, NZ, [2]School of Physiology and Pharmacology, University of Bristol, Bristol, UK.

Hypertension remains one of the strongest predictors of premature death and an increase in sympathetic nerve activity has been implicated in the pathogenesis of hypertension. Recent studies have suggested that the peripheral chemoreceptors may play an important role in mediating hypertension. We hypothesised that a) hypertension would be associated with greater sympathetic drive to the heart and b) that carotid body chemoreceptors contribute to this hypertension.

Renovascular hypertension was induced by surgical clipping of one renal artery. Following three weeks post-clip, electrodes were surgically implanted into cardiac sympathetic nerve fascicles of adult sheep. Following recovery from surgery, resting levels of mean arterial pressure, heart rate and cardiac sympathetic nerve activity were recorded. In conscious sheep, the renal clipping procedure induced hypertension relative to sham operated controls (106 ± 4 vs. 86 ± 6 mmHg, n=5 per group). However, no significant change in heart rate was observed between the two groups. Direct cardiac sympathetic nerve activity recording in conscious sheep showed that burst frequency of cardiac sympathetic nerves was significantly higher in renovascular hypertensive sheep (n=5) compared to sham control ewes (39 ± 2.6 vs 30 ± 1.8 bursts per minute, $p < 0.05$).

Pharmacologic stimulation of the peripheral chemoreceptor reflex produced a larger transient blood pressure response in hypertensive sheep than in control animals, demonstrating chemoreceptor hyper-reflexia (17 ± 3 vs 5 ± 2 mmHg; $P<0.05$). Additionally, preliminary data indicate that bilateral denervation of the carotid body chemoreceptors significantly decreased blood pressure in the hypertensive animals (n=4) but not in the normotensive animals (n=3). Our data includes the first ever recordings of cardiac sympathetic nerve activity in hypertension and suggest that carotid body chemoreceptors contribute to mediating renovascular hypertension in conscious sheep.

3B.5L Shift of dominant pacemaker site during reflex vagal stimulation is the result of propagation failure not rate entrainment

Ashton, J.L.[1,2], LeGrice, I.J.[1,2], Paterson, D.J.[3], Paton, J.F.R.[4], Trew, M.L.[1], Gillis, A.M.[5], Smaill, B.H.[1,2]

[1]Auckland Bioengineering Institute, University of Auckland, NZ, [2]Department of Physiology, University of Auckland, NZ, [3]Department of Physiology, University of Oxford, UK, [4]School of Physiology & Pharmacology, Bristol Heart Institute, University of Bristol, UK, [5]Libin Cardiovascular Institute of Alberta, University of Calgary, CA.

Impaired reflex vagal function is an established risk factor in heart disease. Reflex vagal activity can cause rapid and profound heart rate slowing and a concomitant caudal shift of the impulse origin within the sino-atrial node. While there is general consensus on how factors at cell and tissue levels contribute to stable pace-setting by the sino-atrial node at rest, the mechanisms which give rise to dominant pacemaker shift during reflex vagal activity are largely unknown. To address this issue we acquired optical maps of right atrial activation from a rat working heart-brainstem preparation. Impulse propagation was analysed during baroreflex pressure stimuli and compared to responses recorded during peripheral chemoreflex stimulation and perfusion of carbachol, before (n=10) and after (n=5) I_f channel inhibition with ivabradine.

Baroreflex-induced caudal pacemaker shifts were synchronous with substantial increases in cycle length (ΔCL=73.4±102.0 ms, 95% CI [42.0, 104.8]) and were associated with significant slowing of conduction through the rostral SA node. Chemoreflex also triggered pacemaker shifts with large increases in CL (ΔCL=117.3±68.9 ms, 95% CI [73.57, 161.1]). In contrast, carbachol produced caudal shifts that occurred with small changes in CL (ΔCL=15.3±45.3 ms, 95% CI [-17.12, 47.68]). Post-ivabradine, CL increased significantly faster during reflex and carbachol responses.

There is a wide-spread notion that pacemaker shift occurs when cells in the rostral sino-atrial node slow, allowing caudal cells less sensitive to vagal stimulation to assume control at a higher rate. Our findings from reflex stimulation are not consistent with this view, but instead indicate that caudal shift can occur due to reduced safety of propagation from the rostral sino-atrial node. The speed with which this effect develops is dependent on I_f. We conclude that the dominant pacemaking region in the sino-atrial node is defined by both the highest rate and the capacity to drive activation in the surrounding myocardium.

3B.6: Quantifying myocardial stiffness uncertainty in heart failure patients using personalised ventricular mechanics

Wang, Z.J.[1], Wang, V.Y.[1], Bradley, C.P.[1], Young, A.A.[1,2], Cao, J.J.[3], Nash, M.P.[1,4]

[1]Auckland Bioengineering Institute, University of Auckland, NZ, [2]Department of Anatomy and Medical Imaging, University of Auckland, NZ, [3] The Heart Centre, St Francis Hospital, Roslyn, NY, USA; [4]Department of Engineering Science, University of Auckland, NZ.

Heart failure (HF) poses one of the greatest challenges to the healthcare system worldwide with an alarming rate of increase in prevalence, especially in the ageing population [1]. Heart failure (HF) patients are clinically categorised into those with reduced ejection fraction (HFrEF) or preserved ejection fraction (HFpEF). Clinical understanding of the underlying mechanisms of HF is lacking [2], and investigations into the mechanical properties of myocardial tissue could provide better insight.

Conventional methods, using the gradient of the pressure-volume curves during diastole, have been used widely as measures of chamber stiffness [3]. However, these measures are not tissue-specific and so has limited contributions to understanding the mechanisms of HF. Finite element models of the left ventricle (LV) were used in this study to integrate magnetic resonance imaging (MRI) data and catheter LV pressure data to provide patient-specific estimates of myocardial tissue stiffness.

The parameter estimation framework was applied to data from 28 patients, which were recruited at the St. Francis Hospital (New York). We found that the tissue stiffness of HF patients was significantly higher than that of control subjects and that the HFrEF group had greater tissue stiffness than the HFpEF group [4].

We also analysed the sensitivity of the myocardial stiffness parameter estimation to beat-to-beat variability in LV pressure measurements. This provides a measure of the uncertainty in the stiffness estimation for each subject and better informs group comparisons.

1 Hosenpud, J.D. and B.H. Greenberg, *Congestive Heart Failure*. 2007: Lippincott Williams & Wilkins.

2 Owan, T.E., et al., *Trends in prevalence and outcome of heart failure with preserved ejection fraction.* New Eng.l J. Med., 2006. **355**: p. 251-259.

3 Pasipoularides, A., *Right and left ventricular diastolic pressure-volume relations: a comprehensive review.* J. Cardiovas. Trans. Res., 2013. **6**: p. 239-252.

4 Wang, Z.J., et al., *Quantifying passive myocardial stiffness and wall stress in heart failure patients using personalised ventricular mechanics.* Journal of Cardiovascular Magnetic Resonance 2016. **18**(1): p. O17.

P1: Role of kisspeptin in the prolactin-induced suppression of the pulsatile secretion of luteinizing hormone

Lien, R.[1,2], Brown, R.S.E.[1,2], Kokay I.C. [1,2], Grattan, D.R.[1,2,3]

[1]Centre for Neuroendocrinology, University of Otago, Dunedin, NZ, [2] Department of Anatomy, University of Otago, Dunedin, NZ, [3]Maurice Wilkins Centre for Molecular Biodiscovery, NZ.

Elevated prolactin in the blood is a known cause of infertility in both sexes, however, the mechanism by which prolactin inhibits the reproductive axis remains to be elucidated. Recent studies showing the lack of prolactin receptor (PRLR) expression in the gonadotropin-releasing hormone (GnRH) neurons suggests an indirect inhibitory effect of prolactin in the regulation of GnRH secretion. Kisspeptin neurons in the anteroventral-periventricular nucleus (AVPV) and arcuate nucleus (ARC) are known to regulate GnRH neurons and are prolactin-responsive. The aim of this study was to determine whether these neurons mediate the prolactin-induced suppression of gonadotropin secretion, using mice in which the PRLR gene was deleted from kisspeptin neurons in both AVPV and ARC regions. Mice in which the PRLR gene is flanked by LoxP sites ($PRLR^{flox}$) line were crossed with mice expressing Cre-recombinase under the kisspeptin-specific promoter (Kiss1-Cre) to generate kisspeptin-speicifc PRLR knockout mice (Kiss1-PRLR-KO). The pattern of luteinizing hormone (LH) secretion was measured in intact female animals during the diestrous stage of the estrous cycle, using rapid sampling (every 6 minutes for 3 hours) from the tail vein. LH secretion could be observed in a pulsatile pattern, with a frequency of approximately 1 pulse per hour. After prolactin treatment (0.2 mg s.c., 45 minutes prior to blood sample collection), both the frequency and amplitude of LH pulses was significantly suppressed ($P < 0.05$). In contrast, in Kiss1-PRLR-KO mice, prolactin failed to alter the pattern of LH secretion. These data suggest that kisspeptin neurons mediate the inhibitory actions of prolactin on fertility.

P2: Impaired pregnancy-induced changes to glucose homeostasis in mice lacking prolactin receptors in the pancreas

Aung, Z.K.[1,2], Grattan, D.R.[1,2,3], Ladyman, S.R.[1,2,3]

[1]Centre for Neuroendocrinology, University of Otago, Dunedin, NZ, [2]Department of Anatomy, University of Otago, NZ, [3]Maurice Wilkins Centre for Molecular Biodiscovery, NZ

During pregnancy, the mother develops a state of relative insulin insensitivity to facilitate partitioning of glucose to meet the needs of the developing fetus. To ensure adequate uptake of glucose by maternal tissues despite decreased insulin insensitivity, a number of metabolic adaptations occur during pregnancy including a lower threshold for glucose-stimulated insulin secretion and expansion of pancreatic □-cells. Dysfunction of glucose regulation during pregnancy, particularly when □-cells fail to compensate for the insulin resistance of late pregnancy, leads to gestational diabetes mellitus which can have long term adverse consequences on the offspring. Pregnancy is associated with high levels of prolactin signaling, both due to prolactin itself and also to high levels of placental lactogen, a pregnancy-specific hormone that acts on the prolactin receptor (Prlr). □-cells express Prlr, and there is a dramatic increase in Prlr levels during pregnancy[1]. The aim of this study was to determine if there is a critical role for prolactin/placental lactogen in pregnancy-induced changes in glucose homeostasis. Mice with a deletion of the Prlr in the pancreatic □-cells, generated by crossing Pdx-Cre mice with Prlr flox mice, underwent a glucose tolerance test before and during late pregnancy (day 16-17). Deletion of the Prlr was confirmed by in situ hybridization for Prlr mRNA, and by loss of prolactin-induced phosphorylation of STAT5, an intracellular signaling molecule activated by prolactin, in the pancreatic □-cells. There was no significant difference in glucose tolerance in virgin female KO or WT mice, however during pregnancy KO mice had impaired glucose tolerance compared to pregnant WT mice. These results indicate dysfunction of glucose homeostasis during pregnancy in mice with a conditional deletion of Prlr in the pancreas and emphasis the key role of prolactin/placental lactogen in the adaptation of glucose homeostasis, particularly □-cell function, during pregnancy.

1. Sorenson RL & Stout LE. Prolactin receptors and JAK2 in islets of langerhans: *An immunohistochemical analysis.* Endocrinology **136**, 4092-4098, (1995).

P3: Morphological characterization of tyrosine hydroxylase immunoreactive neurons in the rat hypothalamus

York, J.[1], Yip, S.H.[1], Hyland, B.[2], Grattan, D.R.[1], Bunn, S.J.[1]

[1]Centre for Neuroendocrinology, Department of Anatomy, University of Otago, Dunedin School of Medicine, NZ, [2]Department of Physiology, University of Otago, Dunedin School of Medicine, NZ.

Prolactin secretion from the anterior pituitary is regulated by dopaminergic inhibition arising from the tuberoinfundibular dopaminergic (TIDA) neurons located in the arcuate nucleus of the hypothalamus. As expected the TIDA neurons express the enzymes required for catecholamine biosynthesis including tyrosine hydroxylase (TH) and DOPA decarboxylase (DDC). Previous studies have identified an additional population of TH-expressing cells within the hypothalamus, which lack the latter enzyme and are thus unable to synthesize dopamine. Our initial examination of the rat arcuate nucleus indicated the presence of two, apparently distinct, sub-populations of TH-immunoreactive neurons expressing either a round or fusiform morphology. We have tested the hypothesis that these two distinct morphologies correlate with the TH sub-populations noted above. Adult female rats were perfused with paraformaldehyde (4%), hypothalamic coronal sections prepared and processed for TH and DDC dual-label immunohistochemistry. Cell morphologies were distinguished by the ratio of longest to shortest diameter and number of stained cells counted in the dorsomedial and ventrolateral region of the arcuate nucleus. (n=5 animals). Immunohistochemical analysis showed similar numbers of TH or DDC stained cells were recorded in each region. The relative proportion of round or fusiform cells was also similar in each region, with between 40-60% of each morphology. Dual-labeling revealed that approximately 50% of TH immunoreactive cells in each region also expressed DDC and were thus capable of dopamine synthesis. Contrary to the original hypothesis a similar proportion of round or fusiform cells expressed both catecholamine-synthesizing enzymes. In summary these data support the proposal that the rat acurate nucleus contains dopaminergic neurons, expressing TH and DDC, and the so-called monoenzymatic cells, expressing only DDC. These populations were not however aligned to particular cell morphology nor confined to a subdivision of this nucleus.

P4: Female mutant mice with selective disruption of lactotrope D2Rs have chronic hyperprolactinemia and altered liver and adipocyte genes related to glucose and lipid balance

Lopez-Vicchi, F.[1], Luque, G.M.[1], De Winne, C.[1], Rubinstein, M.[2], Ornstein, A.[1], Becu-Villalobos, D.[1]

[1]Laboratory of Pituitary Regulation, IByME-CONICET, Buenos Aires, Argentina, [2]INGEBI-CONICET, Buenos Aires, Argentina.

Mice that selectively lack D2Rs from pituitary lactotropes (lacDrd2KO) have hyperprolactinemia, increased body weight beginning at 6 months of age, and a phenotype of fatty liver and adiposity accretion which intensifies with age (measured at 12 months) (1). We found glucose metabolism imbalance at both ages: glucose intolerance, hyperinsulinemia, increased pancreatic insulin content and impaired insulin response to glucose or feeding in lacDrd2KO mice compared to controls (*Drd2*$^{loxP/loxP}$). The aim of this study was to characterize changes in tissues (liver and adipose) that might underlie this metabolic imbalance.

Liver and not adipose tissue *Prlr* mRNA levels were higher in lacDrd2KO at both ages, and we found tissue and age-specific failure in transcription factors related to lipogenesis, *Srebp-1c* and *Chrebp* and in glucokinase expression in hyperprolactinemic mice. Before morbid adiposity onset, i.e. at 5 months, liver *Chrebp* mRNA expression was increased in lacDrd2KO mice compared to *Drd2*$^{loxP/loxP}$; furthermore, there was a marked loss of response of liver *Srebp-1c* to refeeding in lacDrd2KO. On the other hand, glucokinase and glycogen synthase 2 expression as well as glycogen content were similar in both genotypes, indicating a preferential alteration of transcription factors involved in *de novo* lipogenesis in the liver already at 5 months of age.

In adipose tissue *Chrebp* expression was consistently decreased in *ad libitum*, fasted and refed conditions, in obese 10 month-old; and *Srebp-1c* mRNA was also lower in 10 but not in 5 month-old lacDrd2KO mice.

We conclude that over production of prolactin may profoundly affect lipid synthesis in liver and white adipose tissue, by targeting lipogenic transcription factors, and in relation to alterations evoked in insulin and glucose metabolism.

1 Perez Millan MI, Luque GM, Ramirez MC, Noain D, Ornstein AM, Rubinstein M, Becu-Villalobos D. *Selective disruption of dopamine D2 receptors in pituitary lactotropes increases body weight and adiposity in female mice.* Endocrinology. 2014 Mar;155(3):829-39

P5: Quantifying skin stretch induced motion artifact from an electrocardiogram signal - A pilot study

Kalra, A.[1], Lowe, A.[1], Al-Jumaily, A.[1]

[1]Institute of Biomedical Technologies, Auckland University of Technology, NZ.

This work presents a 2D quantification of strain field caused due to the motion artifact in an Electrocardiogram (ECG) measurement. The objective of this work is to estimate the skin stretch induced motion artifact in an ECG signal. An ECG measurement was obtained from a subject for 10 seconds using standard Ag/AgCl electrodes by continuously moving the arm back and forth during the measurement. A Poly dimethyl siloxane (PDMS) patch of dimensions 40mm x 45mm x 0.254mm was adhered to the arm during motion. The movement of the PDMS patch during the ECG measurement was recorded in a video and motion artifact was quantified in terms of normal and shear strain components. These values were derived using feature detection and Euclidean distance feature mapping. The motion artifact was eliminated from the ECG signal using Principal Component Analysis (PCA) and Independent Component Analysis (ICA).

A novel approach to simulate the strain values reflecting skin stretch is accomplished by acquiring a video recording of a moving PDMS patch during the ECG measurement.

P6: Parametric electrical modelling of human forearm simulation response using multi-frequency electrical bioimpedance

Anand, G.[1], Lowe, A.[1], Al-Jumaily, A.M.[1]

[1]Institute of Biomedical Technologies, AUT University, Auckland, NZ.

This work focusses on modelling the electrical response of human forearm tissues through a simulation of multi-frequency Electrical Bioimpedance analysis (MF-EBIA). The objective is to estimate an electrical equivalent representation for tissue response in terms of resistance and capacitance values for three tissue layers in the forearm - the fat, muscle and artery, using parametric fitting. Following up from a simulation study of the human forearm model using Ansys® High Frequency Structure Simulator (HFSS), this work assumes an electrical model of the human forearm section for every tissue and calculates the electrical parameters. The tissue model was considered to be isotropic with regards to the dielectric properties and the consideration of blood flow was realised by taking three instances of radial artery diameter. The proposed model was validated by using the obtained values of model components to reproduce the overall response. The obtained values of resistance and capacitance for every tissue domain provide an insight into their significant contribution to the overall electrical response, which can be important while analysing their individual electrical behaviour and also helpful in various pre-experimental studies related to dielectric characterization of living tissues.

P7: Functionalised lipid nanoparticles loaded with paclitaxel for targeted release to ovarian cancer tissue

Adil, A.A.[1,4], Lasham, A.[2], Shelling, A.N.[3], Al-Kassas, R.[4]

[1]Institute of Biomedical Technologies, Auckland University of Technology, Auckland, NZ, [2]Department of Molecular Medicine and Pathology, Faculty of Medical and Health Sciences, University of Auckland, Auckland, NZ, [3]Department of Obstetrics and Gynaecology, Faculty of Medical and Health Sciences, University of Auckland, Auckland, NZ, [4]Department of Pharmacy, Faculty of Medical and Health Sciences, University of Auckland, Auckland, NZ.

Ovarian cancer (OVCA) is the fifth leading cause of cancer-related deaths in New Zealand women. The heterogeneity of OVCA, associated with late diagnosis, is regarded as responsible for the higher mortality in OVCA patients. Current treatments have been shown to have low efficacy due to poor specificity and selectivity. Novel nanostructured-lipid carriers (mNLCs) were developed to address these drawbacks, through functionalising them with hyaluronic acid (HA) to achieve active delivery of Paclitaxel to the OVCA. HA was suggested as it is able to bind the overexpressed antigen (CD44) on OVCA cells. mNLCs were developed by adding silica to the lipid matrix. Optimisation studies were carried out using the homogenisation-ultrasonication technique. The optimised mNLCs formulation was loaded with Paclitaxel and functionalised with HA, following the Electrical-attraction method. Characterisation of the mNLCs was performed using various techniques such as TEM, PCS, DSC, In vitro, and in vivo cytotoxicity studies. The resulting nanoparticles were spherical in shape, and have a size of (298.1± 11.3 nm), making them suitable for IV administration. In terms of EE% and DL%, the mNLCs has given 95%, and 4.8%, respectively. Thermal studies have confirmed the solid status of the mNLCs lipid core, suggesting that incorporation of silica has improved the physical stability, without compromising the EE and DL percentages. Functionalising the mNLCs with HA led to an increase in particle size (575.2 ± 15 nm), and altered the drug release percentage (from 85% to 70 %), acting as a physical barrier. However, in vivo cytotoxicity results, have shown an improvement in the antitumor efficacy, suggesting that HA was efficient in binding the CD44, and the mNLCs formulation was able to deliver the antitumor dose. The novel mNLCs formulation showed promising performance, and was able to target the ovarian cancer cells, delivering the drug with an improved antitumor efficacy.

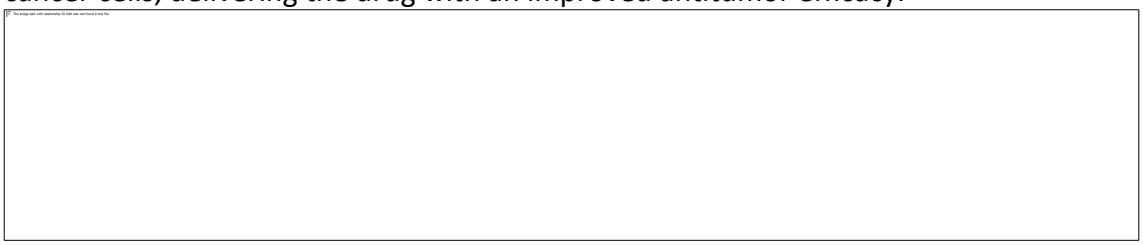

Figure 1. Cell viability % for treated formulations

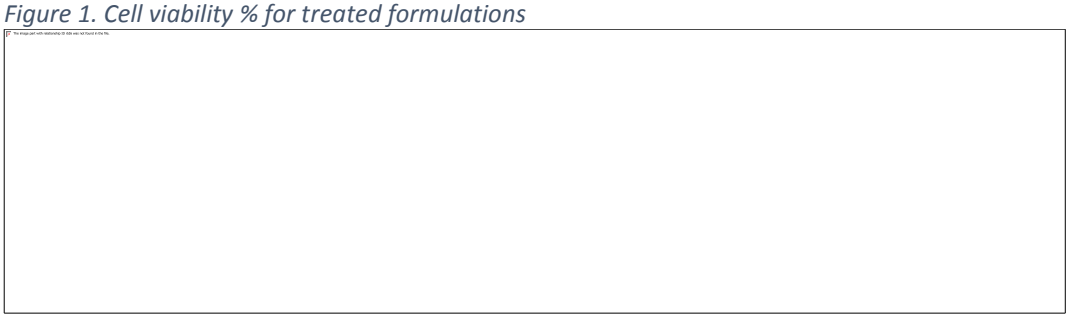

Figure 2. In vitro release profile of PTX from developed formulations (n=3, mean±SD)

P8: Murine models for acute and chronic asthma respiratory outcomes

Roos, K.L.T.[1], Jo-Avila, M.[1], Al-Jumaily, A.M.[1]

[1]Institute of Biomedical Technology, Auckland University of Technology, Auckland, NZ.

Acute and chronic asthma are respiratory diseases characterized by inflammation, airway hyperresponsiveness (AHR) and obstruction of the airways. During an asthma attack, the contraction of airway smooth muscle (ASM) in combination with increased mucus production reduces the bronchial diameter, increasing the resistance to airflow into the lungs. New Zealand has one of the highest prevalence rates for asthma in the world, with a total estimated cost of NZ$825 million per year. The intrinsic causes of asthma are currently not well understood. Several treatments have been developed, but none of them present a cure for this disease. Most of these treatments are pharmaceutical, and side effects are sometimes fatal.

ASM contraction is believed to be the primary mechanism of action in asthmatic attacks. The response of ASM in healthy and asthmatic airways seems to be influenced by breathing patterns such as tidal breathing and deep inspiration, with strong differences between healthy and asthmatic airways. Additionally, the ASM response in acute and chronic asthmatic models further differentiates the broad spectrum of the disease. Therefore understanding airway mechanics and the dynamic response of ASM *in vivo* is likely an essential component in the search for new alternatives in the treatment of asthma.

The proposed research investigates the response of ASM in sensitized (acute and chronic) models in the presence of imposed oscillations *in vivo* and *in vitro*. The results from these studies, in combination with the previous work done in this area, help to increase the understanding of how length oscillations affect the response of ASM in healthy subjects, and acute and chronic asthmatic subjects.

P9: Finite element modeling of the carotid artery for simulation of the pulse wave velocity measurement

Parittotokkaporn, T.[1], Ali, A.A.[1], Al-Jumaily, A.M.[1], Lu, J.[2]

[1]Institute of Biomedical Technologies, [2]Faculty of Health and Environmental Sciences, Auckland University of Technology, Auckland, NZ.

Stroke is the third major cause of mortality in New Zealand. Early detection and effective management of stroke risk can reduce the burden of stroke. The new stroke predictor has been largely focused on the detection of carotid artery stiffness responsible for several stroke risk factors[1]. Valuable information on arterial stiffness can be obtained from pulse wave velocity (PWV) assessment[2]. The carotid PWV can be measured the time delay of the pulse wave between two locations along the common carotid artery covered by the skin of the neck. There is a need for quantitative study for the carotid PWV measurement using computer modeling and simulation. This simulation-based study aims to use a finite element model of pressure propagation in an elastic artery to describe the transmission of the pressure waves from the arterial wall to the skin of the neck. The model of the neck consists of three separate parts: soft tissue, bone and carotid artery. We are able to simulate the pulse pressure waves in the model at different values of elastic moduli of the arterial wall regarding the effects of arterial stiffness and illustrate how these pulse waveforms transmit to the skin. The model shows the behaviour of the soft tissue and the skin displacement as a consequence of pulse wave propagation and also demonstrates that: (i) the distance between the two points along the carotid artery correlates to the pulse transit time, and (ii) the variation of the carotid artery stiffness has a significant effect on PWV measurement. Hence, the model can be used to develop the two-point pulse sensor for the PWV measurement. Further research is necessary to be validated by experiments as well as clinical data to confirm that more accurate carotid artery and neck model will improve the measure of carotid PWV.

1. Mattace-Raso, F. U. S. et al. *Arterial stiffness and risk of coronary heart disease and stroke: The Rotterdam Study.* Circulation 113, 657–663 (2006).
2. Mookerjee, A., Al-Jumaily, A. M. & Lowe, A. *Arterial pulse wave velocity measurement: Different techniques, similar results-implications for medical devices.* Biomech. Model. Mechanobiol. 9, 773–781 (2010).

P10: The effect of retinal microstructure on retinal prosthesis performance

Shalbaf, F.[1], Lovell, H.N.[2], Dokos, S.[2], Trew, M.[1], Vaghefi, E.[1,3]

[1]Auckland Bioengineering Institute, the University of Auckland, Auckland, NZ, [2]Graduate School of Biomedical Engineering, University of New South Wales, Sydney, Australia, [3]Department of Optometry and Vision Sciences, Faculty of Health and Medical Sciences, University of Auckland, Auckland, NZ.

Retinal prosthesis aims to restore vision for those suffering from retinal degenerative diseases, such as retinitis pigmentosa and age-related macular degeneration, by electrically stimulating the surviving retinal ganglion cells (RGCs). Developing a computational model of the retina that can reflect the microstructure of the retinal cells would give an insight into the pattern of electric charge distribution and thus, an accurate prediction of the device performance.

A 3D anatomically based model of the human retina was generated from healthy optical coherence tomography images and the retinal structure was modeled by employing Poisson and bidomain equations based on earlier works [1]–[3]. However, here, for the first time, the microstructure of the retinal cells was incorporated within the bidomain equations using fiber coordinates. The fibre coordinate system in the retina represented how far the neural bodies were aligned with the overall retinal structure.

The fibre angle was increased from 45◦ to 90◦ and the pattern and the threshold of activation were compared. When the cells were aligned to the overall retinal structure the electric charge received by the active region was increases which decreased the threshold of activation. The effect of anisotropy of the extracellular space was investigated by keeping the fibre angle constant and increasing the extracellular conductivity 2, 4 and 8 times higher along the fibre orientation. Increasing anisotropy in the extracellular space prevented charge distribution along the surface of the retina and helped to deliver more electric charges to the RGC layer. This decreased the threshold of activation and displaced the origin of activation towards the fibre orientation.

These results indicate that the microstructure of the retina is an important factor in determining the pattern, the origin and the threshold of activation which ultimately can affect the performance of the retinal prostheses.

[1] F. Shalbaf, J. Turuwhenua, E. Vaghefi, and S. Dokos, “An image processing pipeline for segmenting the retinal layers from optical coherence tomography images,” in *Image and Vision Computing New Zealand (IVCNZ), 2013 28th International Conference of*, 2013, pp. 70–75.

[2] F. Shalbaf, S. Dokos, N. H. Lovell, J. Turuwhenua, and E. Vaghefi, “Generating 3D anatomically detailed models of the retina from OCT data sets: implications for computational modelling,” *J. Mod. Opt.*, vol. 62, no. 21, pp. 1789–1800, 2014.

[3] F. Shalbaf, P. Du, N. H. Lovell, S. Dokos, and E. Vaghefi, “A 3D - continuum bidomain model of retinal electrical stimulation using an anatomically detailed mesh,” in *Engineering in Medicine and Biology Society (EMBC), 2015 37th Annual International Conference of the IEEE. IEEE, 2015.*, 2015, pp. 2291–2294.

[4] J. Chen, Q. Wang, S. Chen, S. A. Wickline, and S. K. Song, “In vivo diffusion tensor MRI of the mouse retina: A noninvasive visualization of tissue organization,” *NMR Biomed.*, vol. 24, no. 5, pp. 447–451, 2011.

P11: Carvedilol and its non-ß-blocking analog VK-II-86 prevent digitalis-induced Ca++ waves in cardiac myocytes

Gonano, L.A.[1,2], Sepúlveda, M.[1], Morell, M.[1], Tottef, T.[1], Jones, P.P.[2], Back, T.G.[3], Wayne Chen, S.R.[4], Mattiazzi, A.[1], Petroff, M.V.[1]

[1]Centro de Investigaciones Cardiovasculares, Conicet-Universidad Nacional de La Plata, Argentina, [2]Department of Physiology. University of Otago, Dunedin, NZ, [3]Department of Chemistry, University of Calgary, Calgary, Alberta, Canada, [4]Libin Cardiovascular Institute of Alberta, Department of Physiology and Pharmacology, University of Calgary, Calgary, Alberta T2N 4N1, Canada.

Cardiotonic glycosides inhibit the sarcolemmal Na^+/K^+-ATPase and cause an increase in intracellular Na^+, which reduces Ca^{++} extrusion through the Na^+/Ca^{++} exchanger. The result is an increase in sarcoplasmic reticulum (SR) Ca^{++} load and cardiac contractility. However, these compounds have associated arrhythmic effects due to the occurrence of spontaneous SR Ca^{++} waves as a result of SR Ca^{++} overload and CaMKII-dependent phosphorylation of RyR2.
Taking into account that Carvedilol and its non-β-blocking analog VK-II-86 are able to prevent spontaneous SR Ca^{++} waves, we hypothesize that Carvedilol and VK-II-86 would be able to prevent digitalis-induced SR Ca^{++} waves/spontaneous contractile activity without affecting inotropic response.

In rat cardiac myocytes, paced at 0.5 Hz and perfused in the presence of 50 µM Ouabain for 20 minutes, we observed an increase in cell shortening of 60±5% (n=15). We also observed spontaneous contractile activity as an index of SR Ca^{++} waves after stopping electrical stimulation. On average, Ouabain-treated cells presents a significantly higher number of non-stimulated events (NSE) compared with control cells (69±10 NSE/10min vs 11±4 NSE/10 min respectively)

In similar experiments performed in the presence of 1 µM Carvedilol, the frequency of NSE was significantly reduced to 24±4 events/10min (n=13). To confirm that the effect of Carvedilol was dependent on its capacity to reduce RyR2-mediated spontaneous Ca^{++} release instead of its β-blocking effect, we used Atenolol (a β-blocker without effects on RyR2 function) and VK-II-86. The presence of Atenolol did not significantly alter the frequency of NSE promoted by Ouabain. In contrast, VK-II-86 significantly reduced the frequency of NSE promoted by Ouabain (39±9 events/10min; n=14).

Additionally, VK-II-86 did not affect the development of the positive inotropic response and the increase in SR Ca^{++} load induced by Ouabain treatment.

We conclude that the combination of cardiac glycosides with VK-II-86 would improve cardiac contractility without increasing the risk of triggered-arrhythmias.

P12: Development of a specific immunoassay to measure BNP1-32 in plasma without the confounding influences of precursor peptides and peptide metabolites: could this improve heart failure diagnosis?

Lewis, L.K.[1], Raudsepp, S.D.[1], Yandle, T.G.[1], Richards, A.M.[1]

[1]Christchurch Heart Institute, University of Otago, Christchurch, NZ.

Objectives: Heart failure is a leading cause of death worldwide. Plasma concentrations of B-type natriuretic peptides (BNP) reflect elevations in cardiac dysfunction and are used in the diagnosis of heart failure and in prediction of adverse outcomes[1]. Current BNP assays provide useful diagnostic data, but as well as measuring the bioactive BNP1-32 form, they also detect BNP metabolites and the precursor peptide proBNP, which all have reduced bioactivity. A more specific assay that measures only the BNP1-32 peptide will better reflect the actual circulating level of bioactive BNP1-32 and may provide more clinical benefit than the current assays.

Design and Methods: We have developed and partially validated a specific BNP1-32 luminex based immunoassay using antibodies specific for the C-terminal and N-terminal ends of BNP1-32.

Results and discussion: The BNP1-32 assay did not cross react with known BNP metabolites and had negligible cross reactivity with glycosylated or non-glycosylated proBNP standards. Recovery of BNP1-32 from samples ranged from 44-68%, CVs were <10%, and samples diluted in parallel with a BNP1-32 standard curve. As expected concentrations reported by our specific BNP1-32 assay were much lower than levels reported by other less specific BNP assays and were raised in heart failure patients (24.9±7.1 pmol/L n=42) compared to controls (0.1±0.01 pmol/L, n=22). The step up between heart failed and normal individuals exceeded that seen with other BNP assays, which may increase the predictive or prognostic power of results.

Conclusions: We have developed the first assay specific for BNP 1-32. This assay has minimal cross reactivity with either proBNP or BNP metabolites. Using this assay we showed that full length BNP1-32 concentrations increased between normal and heart failed individuals. This assay will now be used to measure full length BNP1-32 levels in larger patient groups to determine its clinical utility compared to current less specific methods.

1. Yancy, C. W., et.al. (2013). *2013 ACCF/AHA guideline for the management of heart failure: a report of the American College of Cardiology Foundation/American Heart Association Task Force on Practice Guidelines.* J Am Coll Cardiol, 62(16), e147-239.
2. Luckenbill, K. N., et.al. (2008). *Cross-reactivity of BNP, NT-proBNP, and proBNP in commercial BNP and NT-proBNP assays: preliminary observations from the IFCC Committee for Standardization of Markers of Cardiac Damage*. Clinical chemistry, 54(3), 619-621.

P13: Analysis of pressure dependent resistance and elastance in high auto-PEEP versus low auto-PEEP patients

Langdon, R.[1], Docherty, P.D.[1], Blane, G.[1]

[1]Department of Mechanical Engineering, University of Canterbury, NZ.

Patient-specific respiratory models can optimise mechanical ventilation for patients suffering from acute respiratory distress syndrome (ARDS). The selection of positive end expiratory pressure (PEEP) is particularly important for ventilation of ARDS lungs.

A model of pulmonary mechanics was fit to retrospective data from ten fully sedated ARDS patients. The model contained basis functions that enabled both a convex pressure dependent elastance, and a linear pressure dependant resistance to be captured. The patients underwent a recruitment manoeuvre, where PEEP began at zero and was increased by 5cmH_2O three to six times. Four patients had a high auto-PEEP (>=8cmH_2O) and were diagnosed with COPD. High auto-PEEP is common in COPD patients who have blockages in the bronchial pathway that obstruct the flow during expiration. The modelled resistance and elastance parameters were compared with patient diagnoses and auto-PEEP.

Modelled elastance was similar for both high and low auto-PEEP patients. However the high auto-PEEP patients had a significantly higher modelled resistance at low pressure compared with low auto-PEEP patients ($p<0.01$). For all patients, resistance decreased with pressure. The resistance gradient was generally much steeper in the high auto-PEEP patients ($p<0.01$), leading to similar resistance values at high pressure across both groups.

These results were in accordance with expectations. COPD is associated with higher resistance to air flow due to blockages and narrowing of the bronchi and bronchioles. Furthermore, the increased pressure due to increasing PEEP causes recruitment and widens bronchial passages, and causes decreased resistance.

While high residuals often existed between the measured pressure and model when a high auto-PEEP was present, modelled elastance and resistance displayed expected behaviour for these ten patients. The clinically important differences between high and low auto-PEEP patients were consistently observed by the model.

P14: Oxidised CaMKII – A novel mechanism in the pathophysiology of FSHD

Denny, A.[1], Jones, P.P.[1], Erickson, J.R.[1], Heather, A.K.[1]

[1]Department of Physiology, University of Otago, Dunedin, NZ.

Facioscapulohumeral muscular dystrophy (FSHD) is an inherited myopathy and is characterised by skeletal muscle wasting and weakness. These characteristics stem from the increased oxidative stress and inflammation as a result of the expression of DUX4, along with disturbed calcium (Ca^{2+}) handling and impaired skeletal muscle contraction. This research area is still in its infancy, with only a small part of the disease state being understood. Using a C2C12 cell culture model, our laboratory has investigated a novel mechanism of FSHD induction via the multifunctional calcium/calmodulin dependent kinase II (CaMKII), which may be activated due to the pro-oxidant state and can potentially feedback and further increase the oxidative stress and inflammation. Ca^{2+} signalling is altered in FSHD, along with an impaired contraction of the skeletal muscle. CaMKII is a key Ca^{2+} signalling protein involved in muscle contraction, and phosphorylation and oxidation of CaMKII in cardiac myocytes distorts Ca^{2+} signalling and contraction leading to arrhythmias. We hypothesised that, due to the pro-oxidant state during FSHD, CaMKII is oxidised and plays a crucial role in altered Ca^{2+} signalling and impaired skeletal muscle contraction. To test this hypothesis, we transfected C2C12 cells with DUX4 for 48 hours and performed immunoblot analysis to measure total CaMKII expression along with the ratio of phosphorylated (Thr287) and oxidised (Met281/282) CaMKII. No significant differences were present between control and DUX4 transfected C2C12 cells in both total CaMKII and phosphorylated CaMKII; however, oxidised CaMKII was significantly increased ($p<0.05$) in DUX4 transfected C2C12 cells. These novel findings are central to further understanding the mechanisms and model of FSHD and provides a base on knowledge to conduct further experiments into the mechanisms which underlie the disease.

P15: Regulation of RyR2 by Protein Kinase CK2

Chakraborty, A.D.[1], McLay, J.[1], Jones, P.[1]

[1]Department of Physiology, University of Otago, NZ.

Under normal conditions, depolarization of cardiac myocytes activates the L-type Ca^{2+} channels, leading to a small Ca^{2+} influx which then activates RyR2, resulting in a large Ca^{2+} release from the sarcoplasmic reticulum (SR) and subsequent muscle contraction. This process is known as Ca^{2+}-induced Ca^{2+} release (CICR). Spontaneous SR Ca^{2+} release via RyR2 can occur under the conditions of SR Ca^{2+} overload, a process also termed store-overload–induced Ca^{2+} release (SOICR), an onset mechanism for arrhythmia. Phosphorylation of RyR2 by kinases (PKA, CaMKII, etc) have been shown to increase the propensity for SOICR. Calsequestrin (CSQ2), which is a Ca^{2+} buffering protein is an important regulator of RyR2, is closely linked to Protein Kinase CK2. CSQ2 has 3 phosphorylation sites known to be phosphorylated by the kinase. CK2 knockdown has been found to lower CSQ2 phosphorylation, altering the open probability (Po) of RyR2 and changing its function. However, a direct role for CK2 regulation of RyR2 has not yet been identified.

We have used Ca^{2+} imaging to show an increase in the activity of RyR2 (propensity of SOICR) when CK2 is inhibited. CK2 inhibition was achieved using an inhibitor (CX-4945) and CK2 specific siRNA. We have subsequently identified several new CK2 phosphorylation sites within RyR2 using mass spectrometry following *in-vitro* phosphorylation of RyR2. Mutants to specific sites have been generated to study the effects of phosphorylation and dephosphorylation of RyR2 by CK2. Our data indicate a novel role for CK2 in regulating the function of RyR2.

P16: A high resolution reconstruction of 3D atrial tissue architecture following tachypacing-induced heart failure in the sheep

Thomas, B.[1], Sands, G.B.[1], LeGrice, I.J.[1,2], Smaill, B.H.[1], Zhao, J.[1]

[1]Auckland Bioengineering Institute, University of Auckland, Auckland, NZ, [2] Department of Physiology, University of Auckland, Auckland, NZ.

Atrial fibrillation is the most common heart rhythm disturbance and its prevalence increases with age and in heart disease. We are developing computer models to investigate how changes in atrial structure that occur in heart failure (HF) contribute to atrial electrical dysfunction. A first step towards this is to establish appropriate 3D representations of atrial tissue architecture in an established animal HF model. Crossbred sheep were subjected to 6 weeks of high rate ventricular pacing (200 per minute) followed by 4 weeks without pacing. The atria were then fixed at realistic volumes, embedded in paraffin wax and serial surface images (1225 planes at 6.25 x 6.25 x 25 μm^3) were acquired after topical application of May Grunwald stain to identify myocytes, collagen and fat. A novel purpose-developed multi-scale image processing pipeline was developed to (i) register serial images (ii) remove artifact, (iii) identify inner and outer atrial surfaces, and (iv)segment myocytes, connective tissue and fat. Myofibre orientation was then determined throughout the atria using structure-tensor analysis. The integrity of the semi-automatic segmentation algorithm across this very large dataset over multiple scales indicates the applicability of this approach to any large-scale dataset of noisy images with discontinuous edges where reasonable gradients separate the foreground from background. The general observations from this study are (i) atrial dilatation observed in 3D reconstruction of MRI images, which in this case is more pronounced in left than right atrium, (ii) evidence of regions of necrosis and replacement fibrosis. In conclusion, the accurate geometry and associated fibre structure of the resulting 3D representation make it a suitable platform to study the effects of atrial structural remodelling.

P17: Is ferroptosis the driver for the onset of type-2 diabetes under hyperuricemic conditions?

Shin, B.[1], Bahn, A.[1]

[1]Department of Physiology, Otago School of Medical Sciences, University of Otago, Dunedin, NZ.

Pancreatic β-cell death and dysfunction are hallmarks of type 1 and 2 diabetes mellitus. Studies show diabetics exhibit hyperuricemia, especially in the early stages of impaired glucose tolerance. In human pancreatic β-cells, hyperuricemia has been shown to induce significant cell death. This cell death has generally been linked to apoptosis, yet full extent of cell death pathways involved is unknown. Therefore, our project aimed to observe if the novel cell death pathway ferroptosis is implicated in hyperuricemia-induced human pancreatic β-cell death while also investigating the implication of another novel cell death pathway - necroptosis.

Immortalized human pancreatic β-cells (1.1B4) were exposed to varying uric acid conditions and cell viability was tested using a dimethylthiazol (MTT) assay. 1.1B4 cells were exposed to Ferroptosis inhibitor (Ferrostatin-1/Fer-1) and necroptosis inhibitor (Necrostatin-1/Nec-1) in conjunction with the hyperuricemic condition (500µM urate) to observe if inhibitors independently or in combination prevented hyperuricemia induced pancreatic β-cell death. Hyperuricemia (72 hours, 500µM urate) induced 22% decrease in cell viability ($P < 0.0001$, one-way ANOVA) compared to normal physiological urate (72 hours, 300µM urate). Known ferroptosis inducer erastin (72 hours, 1 mM) induced 75% decrease in cell viability ($P < 0.0001$, one-way ANOVA) compared to control (72 hours, 1% DMSO), indicating 1.1B4 cells exhibit the capacity to facilitate ferroptosis. However, Fer-1 (10µM) and Nec-1 (10µM) independently or in combination did not prevent the decrease in cell viability of 1.1B4 cells under hyperuricemic conditions ($P > 0.05$, one-way ANOVA). Therefore, ferroptosis and necroptosis may not be directly implicated in hyperuricemia-induced human pancreatic β-cell death.

However, Fer-1 and Nec-1 are known only inhibit a significant, yet partial portion of their respective cell death pathway, indicating the complete exclusion of their involvement in hyperuricemia induced β-cell death entirely is premature, and more studies are still necessary, using a wider range of inhibitors.

P18: O-GlcNAcylation regulates RyR2 function directly

Okolo, C.A.[1], McLachlan, J.J.[1], McLay, J.C.[1], Erickson, J.R.[1], Jones, P.P.[1]

[1]Department of Physiology and HeartOtago, University of Otago, Dunedin, NZ.

O-GlcNAcylation is the enzymatic addition of a sugar, O-linked ß-N-Acetylglucosamine, to the serine and threonine residues of proteins, and it is abundant in diabetic conditions due to hyperglycaemia. We have recently shown that O-GlcNAcylation can indirectly increase pathological Ca^{2+} leak through the cardiac ryanodine receptor (RyR2) due to activation of Ca^{2+}/calmodulin-dependent kinase II (CaMKII). However, as RyR2 is well known to be directly regulated by other forms of serine and threonine modification (phosphorylation) this study aimed to determine whether RyR2 is directly modified by O-GlcNAcylation and if this also alters the function of RyR2. We found that RyR2 is O-GlcNAcylated and that this modification is increased in diabetic patients. O-GlcNAcylation of RyR2 was also observed in HEK293 cells expressing RyR2 and was increased by the addition of thiamet-G (an O-GlcNAc promotor). Using the same HEK293 cells we found that high glucose increases the level of Ca^{2+} leak through RyR2 and that this effect was enhanced by thiamet-G and blunted by the O-GlcNAc inhibitor, diazo-6-oxornoleucine (DON). Intriguingly, the application of the CaMKII inhibitor, KN93, in HEK293 cells, could not completely reverse the effect of thiamet-G. Combined, these data suggest that the function of RyR2 can be directly regulated by O-GlcNAcylation, in addition to indirect regulation by CaMKII.

P19: Role of uric acid in cardiac stem cell function

Cheakhun, C.[1], Dixit, P.[1], Katare, R.[1], Bahn, A.[1]

[1]Department of Physiology, University of Otago, Dunedin, NZ.

In New Zealand, 1 in 20 adults have been diagnosed with cardiovascular disease (CVD)[4]. Cardiac pathophysiology along with diabetes mellitus has always been associated with glucose metabolism, but recently it has been suggested that elevated serum uric acid (SUA) could be a major driver of these complications[1-3]. Cardiac stem cells (CSCs) are a new therapy approach for CVD, however, the therapeutic effects are usually mixed. A major contributing factor could be the necrotic environment, where stem cells are being isolated from or transplanted back into. Elevated SUA could contribute significantly to the necrotic environment. Hence, our goal is to characterise the effects of elevated SUA, reflected by changes in extracellular uric acid, or changes of intracellular uric acid, a new concept we are suggesting, on CSC function in order to improve stem cell therapy.

We characterised the uric acid transporter expression profile in human CSCs including known renal transporters, namely ABCG2, MRP4, GLUT9, URAT1, OAT1, OAT2, OAT4 and NPT4, using qPCR. Human CSCs as well as mRNA from human heart tissue express uric acid efflux transporters ABCG2 and MRP4 to a greater extent than uric acid influx transporter GLUT9, irrespective of diabetic status. This transporter profile in human CSCs support our new concept of a 'cellular uric acid homeostasis' (CUAH), and the fact that a disturbance of CUAH, as in diabetes mellitus, may be detrimental to the function of CSCs and ultimately affect stem cell therapy. Experiments are underway to confirm expression of the detected transporters on the protein level, to evaluate intracellular uric acid levels under changing SUA, and to determine pluripotency by measuring proliferation, apoptosis and differentiation potential of CSCs under hyperuricemic conditions. In addition, known inhibitors or a knock-down of the detected transporters will be used to determine contribution of these transporters to CSC pluripotency and function.

1. Fang, J., & Alderman, M. H. (2000). *Serum uric acid and cardiovascular mortality the NHANES I epidemiologic follow-up study*. 1971–1992. National Health and Nutrition Examination Survey. JAMA*, 283*.
2. Feig, D. I., Kang, D. H., & Johnson, R. J. (2008). *Uric acid and cardiovascular risk*. The New England journal of medicine*, 359*.
3. Hoieggen, A., Alderman, M. H., Kjeldsen, S. E., Julius, S., Devereux, R. B., De Faire, U., Lederballe-Pedersen, O. (2004). *The impact of serum uric acid on cardiovascular outcomes in the LIFE study.* Kidney Int, *65*.
4. Ministry of Health. (2015). *Annual Update of Key Results 2014/15: New Zealand Health Survey*. Retrieved from https://http://www.health.govt.nz/publication/annual-update-key-results-2014-15-new-zealand-health-survey

P20: Sexually differentiated co-expression of neuronal nitric oxide synthase (nNOS) in arcuate nucleus GABA neurons

Desroziers, W.[1], Marshall, C.J.[1], Prescott, M.[1], Campbell, R.E.[1]

[1]Department of Physiology and Center for Neuroendocrinology, Otago School of Medical Sciences, University of Otago, Dunedin, NZ.

GABA neurons (GABA-N) in the arcuate nucleus (ARN) are implicated in mediating impaired gonadal steroid hormone feedback to gonadotropin-releasing hormone neurons (GnRH-N) in the common infertility disorder polycystic ovary syndrome (PCOS) (1). To begin to address the functional relevance of ARN GABA-N in regulating fertility and infertility it is essential to define co-expressed neurotransmitters. This study focuses on nitric oxide (NO), a gaseous neurotransmitters demonstrated as an important player in the neural control of puberty onset and ovulation (2). The co-immunolabeling of neuronal nitric oxide synthase (nNOS) with transgenic tdTomato reporter expression of vesicular GABA transporter (VGAT, to identify GABA-N) was investigated in males, females and prenatally androgenised PCOS-like mice. Confocal images were used to quantify co-expression. We found ~10% of ARN GABA-N co-express nNOS and inversely ~50% of ARN nNOS-N coexpress GABA. This is the first evidence of GABA/nNOS co-expression in the ARN. nNOS populations in other hypothalamic regions demonstrated much lower co-expression (~5%) sugesting nNOS/GABA co-expression is specific to the ARN. Females were found to have a significantly greater proportion of ARN GABA-N co-expressing nNOS than males (i.e. in the medial ARN female 12.49 ± 1.4 vs male 6.43 ± 1.76, p=0.02), demonstrating that this is a sexually dimorphic population. The absence of a significant difference between male and PCOS-like females suggests that this population may be partially masculinised in the PCOSlike state and may contribute to disrupted reproductive function. These data suggest a potential role for this previously unappreciated population of ARN GABA/nNOS-N in fertiltiy regulation and future studies will invetigate that steroid hormone sensitivity of this population in fertilte and PCOS-like mice.

1. Aleisha M. Moore and Rebecca E. Campbell, *The neuroendocrine genesis of polycystic ovary syndrome : a role for arcuate nucleus GAB neurons.* Journal of Sterois Biochemistry and molecular biology. 2015
2. Bellefontaine N, Hanchate NK, Parkash J, Campagne C, de Seranno S, Clasadonte J, d'Anglemont de Tassigny X, Prevot V. *Nitric oxide as key mediator of neuron---to---neuron and endothelia---to---glia communication involved in the neuroendocrine control of reproduction.* Neuroendocrinology. 2011;93(2):74---89.

P21: Non-rigid lung image registration using finite element methods

Minaeizaeim, H.[1], Kumar, H.[1], Hoffman, E.A.[2], Tawhai M. H. [1], Clark A.R.[1]

[1]Auckland Bioengineering institute, University of Auckland, Auckland, NZ, [2]Department of Radiology, University of Iowa, University of Iowa, USA.

Lung image registration allows tracking of tissue movement between image sets. This enables evaluation of changes in lung tissue over time and through breaching and tracking tumours for surgical purposes. Over the past few decades, several methodsbased on image pixel intensity or landmarks (mapping known anatomical points between images) have been proposed for lung image registration [1]. However, these methods do not consider for the physical deformation of lung tissue under gravity lung. This deformation is significant and makes tracking abnormalities between the normal imaged posture (supine) and normal functional posture (upright) difficult. Also, clinical imaging sometimes captures only part of the lung and, particularly in children, does not provide a full volumetric set of images. Based on the nature of current methods, we hypothesize that most existing registration algorithms would possibly fail in this case

Here we use a finite element model lung tissue deformation [2] to guide registration of computed tomography (CT) lung images between functional residual capacity (FRC) and total lung capacity (TLC) images for three healthy young subjects. The lung shape was segmented from images and a finite element model of the lung was first constructed. Tissue deformation between FRC and TLC was then modelled as a quasi-static process under a gravitational load to obtain transformation model for warping the TLC image to the FRC image. The accuracy of the method is computed and compared with conventional lung image registration. The obtained results our preliminary results show that finite element method is a promising method for the lung image registration especially in clinical setup in early prediction and diagnosis of lung diseases.

1. Werner, René. " Biophysical Modeling of Respiratory Organ Motion." *4D Modeling and Estimation of Respiratory Motion for Radiation Therapy*. Springer Berlin Heidelberg, 2013. 61-84.
2. Tawhai, Merryn H., et al. "Supine and prone differences in regional lung density and pleural pressure gradients in the human lung with constant shape." *Journal of Applied Physiology* 107.3 (2009): 912-920.

P22: Shear force activation of the epithelial sodium channel (ENaC): role of the β and γ subunits

Baldin, J-P.[1], Fronius, M.[1]

[1]Department of Physiology, University of Otago, Dunedin, NZ.

The epithelial sodium channel (ENaC) is involved in physiological processes such as salt/water homeostasis and blood pressure regulation. Common ENaC is built of three homologous subunits: α, β, γ and its activity is regulated by shear force (SF). However, little is known about the role of the individual ENaC subunits for SF regulation. Previous studies have shown that SF sensation of αβγ-ENaC in oocytes is due to an interaction between the extracellular matrix (ECM) and N-glycosylated asparagines of α-ENaC. Glycosylated asparagines are also present in the β and γ-ENaC subunit, suggesting they could be also important for SF sensation. To clarify the role of the β and γ for SF sensation two different approaches were implemented. Firstly, the investigation of homomeric (α, β, γ) and dimeric ENaCs (αβ, αγ, βγ), to determine whether they are responding to SF. Secondly, glycosylated asparagine deficient β-ENaC mutants were investigated. Channels were expressed in Xenopus oocytes and ENaC currents were measured by two electrode voltage clamp (TEVC) electrophysiology. Homomeric α-ENaC was activated by SF, whereas β or γ-ENaC did not respond to SF. Dimeric αβ-ENaC is less activated and αγ-ENaC gets more activated by SF compared with αβγ, whereas βγ did not respond to SF. The examination of glycosylated asparagine deficient β-ENaC mutants (co-expressed with α and γ-ENaC) showed no significant differences in SF activation compared with αβγ-ENaC. These experiments show that the SF response of ENaC is modulated by the composition of its subunits. These findings, suggest a modulatory purpose of the β- and γ-ENaC in the response to SF.

Support or Funding information
The work was supported by an University of Otago Scholarship and the Royal Society of New Zealand (Marsden Fund).

P23: How the heart grows - from multiscale data to multiscale computational model

Ebrahimi, N.[1], Bogle, G.[1], Cooling, M.T.[1], Hunter, P.J.[1]

[1]Auckland Bioengineering Institute, University of Auckland, Auckland, NZ.

Heart development consists of sequential events including the formation of the cardiac crescent followed by linear heart tube formation. The heart tube then undergoes ventral bending prior to a helical torsion to form a looped heart, leading to proper alignment of the future cardiac chambers and tracts. Different stages of heart development have been studied by various disciplines. Many groups have studied the biology and genetics of heart development, and quite a few have examined the mechanical processes during growth. Despite the significant volume of existing data, the underlying mechanisms controlling heart development are unclear. Indeed, it is not known how molecular and cellular processes are regulated to achieve coordinated morphological and functional properties during heart development.

In this study we aim to take a multi-scale approach to integrate time course experimental data into a computational model of the bending stage of the looping phase.

We use open source platforms, CellML and FieldML, for computational modeling. We have developed CellML models of signaling pathways that control the virtual expression of specific cardiac genes in response to spatial signals. These cardiac genes represented in the model directly or indirectly control myocardial cell proliferation and growth. Cellular growth will then be linked to tissue remodeling through a growth function. Due to the lack of data in literature, we are currently obtaining our own data at tissue, cellular, and subcellular level using micro-CT, confocal microscopy, and mass spectrometry, respectively. Time course data obtained during early heart development will then be used to integrate into the computational models and to validate these models.

This study will address the question of how gene regulatory pathways control proliferation and growth of myocardial cells to contribute to the bending component of the looping process.

P24: 17β-Estradiol induced calcification and alters CaMKII expression in a mouse model of atherosclerosis

Ebenebe, O.V.[1], Heather, A.K.[1], Erickson, J.R.[1]

[1]Department of Physiology, Otago School of Medical Sciences, University of Otago, Dunedin, NZ.

Vascular calcification, a complication of vascular diseases, underlies a number of major adverse cardiovascular events. The calcification of atherosclerotic plaques, an indication of disease severity, results in instability and increased risk of plaque rupture. Epidemiological studies have shown an increased prevalence of adverse cardiovascular events in older postmenopausal women, exacerbated by long-term hormone replacement therapies (HRTs). The mechanisms through which HRTs contribute to adverse cardiovascular events remain unknown. We have evidence that 17β-Estradiol (E2) promotes calcification of vascular smooth muscle cells; the signaling pathways are yet to be elucidated. It is now widely accepted that some key signaling factors of bone mineralization also play a role in vascular calcification. The nodal signaling molecule calcium/calmodulin kinase II (CaMKII) has been shown to regulate these calcification pathways. This project examined the effects of E2 on plaque calcification and CaMKII expression in a murine model of atherosclerosis. Female ApoE-deficient mice with intermediate (25 weeks) or advanced (45 weeks) stage atherosclerosis were treated with E2 bi-weekly for 8 weeks. Alizarin Red staining for calcium in the innominate artery showed that E2 altered the composition of intermediate plaques by promoting calcification compared to vehicle-treated mice (mean calcified volume: 0.365 ± 0.1 μm^3 and 0.164 ± 0.04 μm^3, respectively; $p<0.05$). As arteries of mice with advanced plaques already showed significant calcification, no additional morphological effects were observed in those treated with E2. Western blot data comparing CaMKII expression and activity in WT and ApoE null mice suggest increased activation of CaMKII in this model of atherosclerosis. Our results offer initial evidence that CaMKII is associated with atherosclerosis and may play a role in E2-induced plaque calcification.

P25: Increase in kisspeptin fibre projection to the oxytocin system in late pregnancy in the mouse

Augustine, R.A.[1,2,3], Bouwer, G.T.[1,2,3], Seymour, A.J.[1,2,3], Brown, C.H.[1,2,3]

[1]Brain Health Research Centre, [2]Centre for Neuroendocrinology, and [3]Department of Physiology, Otago School of Medical Sciences, University of Otago, Dunedin, NZ.

The hormone, oxytocin, promotes uterine contractions during parturition. Oxytocin is synthesized by magnocellular neurones in the hypothalamic supraoptic (SON) and paraventricular (PVN) nuclei and is released into the circulation from the posterior pituitary gland in response to action potential firing. In rats, central kisspeptin administration increases oxytocin neuron activity in anaesthetized late-pregnant rats (days 18 – 21 of gestation) but not in non-pregnant rats. Immunohistochemistry also revealed that rats on the expected day of parturition had a higher density of kisspeptin-positive fibres in the perinuclear zone surrounding the supraoptic nucleus than in non-pregnant rats. Here, we addressed whether mice have kisspeptin projections to the PVN and SON, if the fibre density increases in late pregnancy and whether central kisspeptin can activate oxytocin neurons using Fos as a marker.

We found dense kisspeptin fibres in the PVN and SON, which increased in late pregnancy (day 19 gestation). However, central administration of kisspeptin on day 18 of pregnancy did not induce Fos in PVN or SON oxytocin neurons. To investigate whether kisspeptin might act indirectly on oxytocin neurons via interneurons, we used immunohistochemistry to examine whether kisspeptin fibres make close appositions to excitatory glutamatergic neurons in the PVN and SON and found no evidence for this. The PVN and SON are also innervated by excitatory noradrenergic inputs (NA) from the nucleus tractus solitarius (NTS). We examined whether kisspeptin fibres innervated the NTS and area prostrema (AP), followed by Fos expression in tyrosine hydroxylase (TH)-expressing cells in these areas in pregnant mice after central kisspeptin administration. Again, Fos was not activated in NTS or AP TH-expressing cells after central kisspeptin. Taken together, these results show increased kisspeptin fibre innervation in the PVN and SON at the end of pregnancy in the mouse but as yet the functional significance of this increase in kisspeptin fibres during pregnancy is unknown.

P26: Ventricular specific cardiomyocyte differentiation of mouse embryonic stem cells through modulation of molecular pathways.

Satthenapalli, R.[1], Hore, T.A.[2], Lamberts, R.R.[1], Katare, R[1].

[1]Department of Physiology, University of Otago, Dunedin, NZ. [2]Department of Anatomy, University of Otago, NZ.

Acute myocardial infarction diminishes blood flow to the heart leading to loss of large number of cardiomyocytes and causing tissue damage mainly in the left ventricle. In an effort to regenerate the lost cardiomyocytes, stem cells are gaining tremendous interest. Among the stem cells, pluripotent stem cells (PSC) are becoming popular due to their capability to proliferate and differentiate into any lineage, including cardiac lineage. Various protocols have been established to differentiate PSC into cardiomyocytes, however, all these protocols resulted in the development of a heterogeneous population of cardiomyocytes (atrial, nodal and ventricular). This is a major drawback because once transplanted to the left ventricle these nodal cells will generate unwanted cardiac arrhythmias.

In the current study, we designed a protocol with the aim to differentiate mouse embryonic stem cells (mESC) specifically to ventricular cardiomyocytes. By inhibiting Wnt signalling in the early stage, mESC should develop to cardiomyocyte lineage while inhibition of Retinoic acid signaling in the later stages should provide them a ventricular phenotype. To enhance the differentiation, ascorbic acid was added throughout the process. Gene expression of stage specific cardiomyocyte markers was validated by qPCR and protein expression was validated by flow cytometry and immunofluorescence analysis. The preliminary results show that the expression of all the cardiac markers, including the ventricular specific IRX4 and MLC-2V, are expressed at 14 days after treatments. The next step is to validate the function of the cells to understand the efficacy of the differentiated cells. The development of a specific differentiation protocol of PSC to ventricular cardiomyocytes will significantly contribute to the cardiac regeneration field.

P27: Predicting the impact of trophoblast plugs on the utero-placental circulation in early pregnancy

Saghian, R.[1], James, J.L.[2], Tawhai, M.H.[1], Clark, A.R.[1]

[1]Auckland Bioengineering Institute, [2]Department of Obstetrics & Gynaecology, University of Auckland, NZ.

Background: The placenta is responsible for nutrient exchange between mother and baby. For most of gestation, maternal blood flows out of uterine spiral arteries (SAs) and percolates between placental structures called villi, ensuring maximal exchange. Before 12wks of gestation the SAs are occluded by plugs of placental cells (trophoblasts) and most uterine blood flow is redirected to uterine arterio-venous shunts. Trophoblast plugs (TPs) affect SA haemodynamics by lowering wall shear stress (WSS) which may promote a trophoblast-induced remodelling of SAs into wide bore conduits. Loose trophoblast plugging is associated with complicated pregnancies. As early human implantation sites are extremely difficult to study in vivo, a computational model of a plugged SA including shunts was used to predict blood flow and WSS in and around the TPs.

Methods: Our model was parameterised with previously published colour Doppler ultrasonography data of blood flow velocity in the uterine vasculature and intervillous space between 6-15wks of gestation[1], and published measurements of uterine vessel dimensions.

Results and Conclusions: Over a physiological range of TP porosities (0.25−0.6) and lengths (0.5-2mm), blood flow from the SA remains <0.4ml/min (consistent with observed ultrasound rates of 0.15-0.34ml/min[1]) confirming that TPs limit blood flow to the placenta in early pregnancy. Small changes in plug porosity were predicted to result in rapid increases in 1) blood flow into the intervillous space, and 2) the WSS experienced by trophoblasts within the plug and vascular cells/migratory trophoblast upstream of the plug. Increases in the flow of oxygenated maternal blood in the intervillous space in early pregnancy may negatively impact success by damaging delicate villous tissue and exposing the developing placenta to oxidative stress. Increases in WSS in the SA during early pregnancy may affect the ability of trophoblasts to adequately remodel the SAs, predisposing the pregnancy to pathological complications such as pre-eclampsia.

1. Merce L. T., Barco M. J. and Bau S. , 1996, *Color Doppler sonographic assessment of placental circulation in the first trimester of normal pregnancy*, Journal of ultrasound in medicine, Vol. 15, pp. 135--142.

P28: Characterising ENaC expression in vasculature

Mugloo, S., Leader, C.[1,2], Sammut, I.A.[1], Walker, R.[2], McDonald, F.J., Fronius, M.

Department of Physiology, Department of Pharmacology and Toxicology[1], School of Medicine[2] ,University of Otago, Dunedin, NZ.

The epithelial sodium channels (ENaC) located in epithelial cells of the distal kidney and colon are crucial for salt and water homeostasis. Recently, a role for ENaC in blood vessels has been revealed suggesting that ENaC regulates vascular tone. Since vessel response to increased blood pressure is compromised in vascular diseases, changes in ENaC expression or function in vessels may contribute to these disease processes. However, there is limited information about expression of ENaC in different vessels particularly under pathological conditions such as hypertension. Therefore, the aim of this study is to characterise expression of the α-, β-, and γENaC subunits in different types of artery from normo- and hypertensive rats. Male Cyp1a1-Ren2 transgenic rats were euthanised and mesenteric and carotid arteries were isolated from each animal. Real-time qRT-PCR and Western blotting techniques were used to quantify the expression levels of α-, β-, and γ-ENaC subunits in mesenteric and carotid arteries. qRT-PCR analysis confirmed presence of α-, β-, and γENaC transcripts in mesenteric and carotid arteries. In mesenteric arteries γENaC expression level was higher than that of α- and βENaC subunits. In contrast, in carotid arteries, the expression of βENaC was higher than that of α- and γENaC. In addition, western blotting revealed expression of α-, β-, and γENaC proteins.

In conclusion, ENaC subunits are expressed in mesenteric and carotid arteries and this places ENaC in a key position to influence vascular physiology and to be implicated in vascular changes during hypertension. However, the function and regulation of each ENaC subunit in vessels needs to be defined. Future studies will address whether ENaC expression is changed in the Cyp1a1-Ren2 hypertension model. This project will improve understanding of ENaC as a new determinant, and therapeutic target in vascular pathophysiology and hypertension.

P29: microRNA-126 and microRNA-132 are the early modulators of diabetic microangiopathy in heart

Rawal, S.[1], Munasinghe, P.E.[1], Cameron, V.[2], Manning, P.[3], Williams, M.J.A.[4], Jones, G.T.[5], Bunton, R.[6], Galvin, I.[6], Katare, R.[1]

[1]Department of Physiology-HeartOtago, Otago School of Medical Sciences, [2]Christchurch Heart Institute, University of Otago, Departments of [3]Medicine, [4]Medicine-HeartOtago, [5]Surgery and [6]Cardiothoracic Surgery, Dunedin School of Medicine, University of Otago. NZ.

Background: Diabetes-induced microvascular abnormalities are implicated in altering cardiac function and structure, a condition referred as diabetic microangiopathy in heart (DMAH). Endothelial-enriched microRNAs (angiomiRs) have been recently demonstrated to play a major role in regulating angiogenesis. However, their pathophysiological role in development of DMAH is elusive.

Objective: To investigate the modulation of angiomiRs (miR-126, miR-132) with evolution of DMAH and demonstrate if restoration of angiomiRs can improve functional properties of high glucose treated endothelial cells.

Methods & Results: Cardiac tissues were collected from type-2 diabetic mice (BKS.Cg-m+/+Leprdb/J) every 4Wks, from 8 to 32Wks of age. qPCR revealed significant downregulation of miR-126 and -132 starting at 12Wks and continued till 32 Wks (miR-126: 0.30±0.03; miR-132: 0.22±0.05,$p<0.001$ vs. age matched non-diabetic). Downregulation of angiomiRs preceded alterations in cardiac microvasculature, evident by reduced capillaries and arterioles and increased endothelial cells apoptosis, the hallmark of microangiopathy. This was associated with concomitant dysfunction of cardiac functions (assessed through echocardiography). Western blotting analysis confirmed marked dysregulation of VEGF and p120RasGap ($P<0.05$ vs. non-diabetic), the target proteins for miR-126 and -132, respectively. Further, to determine if restoration of miR-126 and -132 could reduce the development of DMAH, high glucose (HG)-treated Human Umbilical Vein Endothelial Cells (HUVECs) were transfected with miR-126 or -132 mimics. Results showed that restoration of both the miRs markedly improved the cell proliferation, migration and angiogenesis properties along with reduced cell death, $p<0.05$ for all the parameters. Of note, overexpression of miR-126 alone tends to restore the expression of miR-132 and vice versa in HG-treated HUVECs, suggesting an orchestrated role of miRs in regulating angiogenesis.

Conclusion: These novel findings demonstrate that downregulation of angiomiRs is a major underlying mechanism for the development of microangiopathy in diabetic heart. Therefore, therapeutic restoration of angiomiRs could become a potential approach to combat the cardiovascular complications of diabetes.

P30: New insights on cardiac activation heat

Pham, T.[1,2], Han, J.C.[2], Tran, K.[2], Mellor, K.[1,2], Hickey, A.[4], Taberner, A.J.[2,3], Loiselle, D.S.[1,2]

[1]Department of Physiology, University of Auckland, Auckland, NZ, [2]Auckland Bioengineering Institute, University of Auckland, Auckland, NZ, [3]Department of Engineering Science, University of Auckland, Auckland, NZ, [4]School of Biological Sciences, University of Auckland, Auckland, NZ.

Cardiac activation heat arises from two major sources during the contraction of muscle. It reflects the metabolic expenditure associated with Ca^{2+} pumping by the sarcoplasmic reticular Ca^{2+} ATPase and Ca^{2+} translocation by the $Na^{+}Ca^{2+}$ exchanger coupled to the $Na^{+}K^{+}$ ATPase. Investigators commonly estimate its magnitude by progressively reducing muscle length to the point where twitch force is zero. But at zero macroscopic active force, the observed heat risks being contaminated by microscopic residual crossbridge activity. To eliminate this putative thermal contribution, crossbridge cycling activity must be abolished. To achieve this, we have used blebbistatin since it is a selective inhibitor of myosin II ATPase. Using a microcalorimeter, we measured the force production and heat output, as functions of muscle length, of isolated rat trabeculae from both ventricles contracting isometrically at 5 Hz and at 37 °C. Experiments were performed in both the absence and in the presence of blebbistatin (15 μM). In the presence of blebbistatin, active force was zero but heat output remained constant, independent of muscle length. Furthermore, heat measured in the presence of blebbistatin was not different from that estimated at zero active force in its absence. Our study allows us to reach two conclusions. First, activation heat is independent of muscle length. Finally, and more importantly, the residual crossbridge heat is negligible at zero active force. That is, the intercept of the cardiac heatforce relation provides an uncontaminated estimate of activation heat. This result settles a longstanding dispute in the literature.

P31: Effects of diet composition on development of high fat diet-induced obesity and insulin resistance in rodents.

Benson, V.L.[1], Liu, J.Y.[1], Li, X.[1], Delbridge, L.M.[2], Mellor, K.M.[1,2,3]

[1]Department of Physiology, University of Auckland, Auckland, NZ, [2]Department of Physiology, University of Melbourne, Melbourne, Australia, [3]Auckland Bioengineering Institute, University of Auckland, Auckland, NZ.

The reported obesogenic effects of high fat diets (HFDs) in rodents vary widely, with inconsistent findings between different diets and species. Our aim was to determine the optimal diet composition of the HFD and reference diet for induction of dietary-induced insulin resistance. Male Sprague Dawley rats and C57Bl/6 mice were fed custom-made standard diet, AIN93G, (Specialty Feeds) or regular chow (#2018, Harlan) from weaning for 12-20 weeks. Body weight, blood glucose levels, food intake, energy consumption and glucose tolerance were measured. The effect of 24%-HFD vs 60%-HFD (w/w) was determined in rats at 13-14 weeks diet duration.

Rats fed AIN93G had 15% higher body weight and 29% higher blood glucose levels compared with regular chow ($p<0.05$), with a trend towards slower glucose disappearance in response to an i.p. glucose challenge. In mice, body weights and blood glucose levels were similar with the two control diets, but a trend towards glucose intolerance was evident in the AIN93G-fed mice. Rats fed 24% HFD had 26% higher body weight ($p<0.05$) and 23% higher blood glucose levels ($p<0.05$) vs. regular chow but not AIN93G. Conversely, rats fed the 60% HFD exhibited no differences in body weight or blood glucose level relative to either control diet.

These findings demonstrate that the AIN93G control diet may provide an elevated body weight and glycemic baseline, thus confounding the comparison with high fat diets in rodents. An extreme high fat diet (60% w/w) does not induce an obese, insulin resistant phenotype, regardless of control diet. This study suggests that diet interventions using the 24% HFD relative to regular chow provides an optimal differential for characterising an obese, insulin resistant phenotype in rats. Differences in systemic response to the two control and HFD diets may be explained by contrasting carbohydrate content and source in each diet.

P32: Automatic principal component based lung lobe segmentation from computed tomography scans

Zhang, Y.[1], Osanlouy, M.[1], Clark, A.R.[1], Hoffman, E.A.[2], Tawhai, M.H[1]

[1]Auckland Bioengineering Institute, University of Auckland, Auckland, NZ, [2]Department of Radiology and Biomedical Engineering, University of Iowa Carver College of Medicine, Iowa City, IA, USA.

Human lungs are divided into five distinct anatomical regions, the pulmonary lobes. Automatic identification of lobes from imaging is important in lung disease assessment and treatment planning. However, quick and effective automatic lobe segmentation is a challenging task. The fissures that separate the lobes can be incomplete, and areas of lung disease can make these fissures hard to distinguish. Currently, lobe segmentation methods rely heavily on anatomic knowledge and largely ignore individual variability. This results in regular segmentation failure in pathological lungs, and in expiratory CT (computed tomography) scans, where fissure locations are difficult to distinguish.

In this study, we use a statistical shape model (a principal component model) to guide lobar segmentation. By deforming an average lobar model onto an individual's lung shape, we predict fissure locations approximately, to refine our search region for lobar structures. Then, we use an eigenvalue of Hessian matrix analysis and a connected component eigenvector based analysis to determine a set of fissure-like candidate points. A smooth multi-level B-spline curve is fitted to the most fissure-like points (those with high "fissureness") and the fitted fissure plane is extrapolated to the lung boundaries. The method was tested on 20 inspiratory and expiratory CT scans in healthy young subjects and older subjects with idiopathic pulmonary fibrosis. Slice thickness was 0.5-3.0mm, with the higher end of this scale representing normal clinical imaging. A quantitative evaluation showed that the algorithm has accuracy of 72.5% to 92.6% for healthy cases and an accuracy of 53.8% to 85.7% for pathological cases with strict 3mm evaluation criteria. The algorithm was able to detect fissures in all subjects, whereas existing segmentation tools failed in several subjects. Our new procedure does not depend on prior segmentation of anatomical structures (airways/vessels) and has promising potential as a clinically useful automatic lobe segmentation procedure.

P33: Computational modelling of glucose uptake in enterocytes using CellML

Afshar, M.[1], Hunter, P.[1], Suresh, V.[1,2], Nickerson, D.[1]

[1]Auckland Bioengineering Institute, [2]Department of Engineering Science, University of Auckland, NZ.

Nutrients, electrolytes and water are absorbed into blood through the mucosa of the small intestine. The primary route of absorption is via enterocytes that are epithelial cells lining the lumen. The uptake, transport, and metabolism of nutrients activate signaling pathways and feedback mechanisms that regulate effects over a range of time and length scales (e.g. expression of glucose transporter proteins, insulin secretion, appetite regulation, and growth). Mathematical modelling of nutrient uptake can improve understanding of the complex feedback mechanisms and how they are disrupted in disease. Here we present a validated computational model of glucose uptake in enterocytes driven by sodium gradients implemented in the open source, modular CellML modelling environment. The transport pathway consists of an apical (lumen-facing) sodium-glucose linked transporter (SGLT1) and a basolateral sodium-potassium ATPase. We use previously published kinetic models for the transporters in order to calculate the transient glucose flux and glucose concentration in the enterocyte in response to an exogenous stimulus. We determine model parameters (kinetic rate constants and transporter densities) by fitting to published measurements in a human intestinal epithelial cell line IEC-6 and validate the model by predicting data not used in the fitting process. This represents an initial step towards the development of an integrated model of nutrient uptake.

P34: Photo-curable thiol-ene gelatin based hydrogels as bioinks for bioprinting

Soliman, B.G.[1], Brown, G.C.J.[1], Lim, K.S.[1], Woodfield, T.[1]

[1]Christchurch Regenerative Medicine and Tissue Engineering (CReaTE) group, Department of Orthopaedic Surgery, University of Otago, Christchurch, NZ.

3D Bioprinting is a rapidly advancing technique often employed within tissue engineering. This technique requires development of specialised biomaterials (bioinks) with specific rheological properties to allow fabrication of constructs of high shape fidelity. Gelatin has been commonly used as bioink for Bioprinting as it possess unique thermosensitive rheological behaviour. Moreover, gelatin is often modified with photo-polymerisable functional groups such as methacryloyl to allow direct spatial control over the shape, size and composition of fabricated constructs. However, a major limitation using gelatin-methacryloyl (Gel-MA) in Bioprinting is oxygen inhibition during photo-polymerisation1, whereby oxygen scavenges radicals resulting in incomplete cross-linking, negatively influencing construct shape fidelity. In the present research, we aim to utilise thiol-ene photo-click chemistry, speculated to resist oxygen-mediated radical quenching, as an alternative to methacryloyl chemistry.2

We applied two gelatin-based systems, gelatin-allyl (GelAGE) and gelatin-norbornene (GelNOR). Hydrogels were fabricated (Ig2959 photoinitiator, 365nm, 5.4 J/cm2) using thiolated crosslinker molecules (dithiothreitol and thiolated 8-arm poly ethylene glycol). Hydrogel physico-chemical properties were characterized as a function of cross-linker concentrations, using gel-MA as control samples.

The physico-chemical properties of gelAGE and gelNOR hydrogels were highly tailorable (GelAGE: 5-30% sol fraction, 8-15% swelling ratio, gelNOR: 7-20% sol fraction, 15-25% swelling ratio). Furthermore, we demonstrated that gelAGE and gelNOR bioinks could be successfully Bioprinted, yielding porous constructs with high shape fidelity. After swelling, the shape fidelity of plotted fibres was noticeably improved in gelAGE and gelNOR-based constructs as compared to more commonly used Gel-MA, which may be attributed to the absence of oxygen inhibition.

In conclusion, we have developed a gelatin-based hydrogel system with highly tailorable physico-chemical properties. We have shown that these formulations can easily be adopted to biofabrication where high fidelity may be achieved as compared to currently used gelatin-based bioinks.

1. Lin, C.-C., Ki, C. S. & Shih, H. Thiol-norbornene photo-click hydrogels for tissue engineering applications. *J. Appl. Polym. Sci.* **132,** (2015).
2. Kharkar, P. M., Rehmann, M. S., Skeens, K. M., Maverakis, E. & Kloxin, A. M. Thiol–ene Click Hydrogels for Therapeutic Delivery. *ACS Biomater. Sci. Eng.* acsbiomaterials.5b00420 (2016). doi:10.1021/acsbiomaterials.5b00420

P35: Role of wall shear stress in placental pathology

Tun, W.[1, 2], James, J.[2], Clark, A.[1]

[1]Auckland Bioengineering Institute, University of Auckland, NZ, [2]Department of Obstetrics and Gynaecology, University of Auckland, NZ.

Introduction: The placenta nourishes the fetus throughout pregnancy. Optimal development of its vasculature, especially the placental capillaries where most gas exchange occurs, is important. Capillary formation (capillarisation) is poor in Fetal Growth Restriction (FGR) and is excessive in chronic maternal hypoxia. Abnormal capillarisation alters placental blood flow and wall shear stress (WSS) which influences vascular cell proliferation and new vessel formation (angiogenesis). However, little is known about *in vivo* WSS, due to limited accessibility of the placenta during pregnancy. We use computational modelling to assess the range of WSS for placental capillarisation representative of normal and pathological pregnancies.

Methods: Poor and excessive capillarisation was assumed to result in a 50% decrease and 66.67% increase in capillary connections respectively, based on morphological studies. A computational model of the feto-placental circulation was used to predict normal and pathological WSS. Elevated umbilical blood pressure (UBP) (100mmHg, compared with normal values of 50mmHg) has been shown experimentally to increase capillarisation. WSS at 100mmHg UBP was simulated with and without changes in capillarisation to assess if a pressure-induced increase in capillarisation could counterbalance increased WSS.

Results: WSS was predicted to be increased (82%) and decreased (34%) in poor and excessive capillarisation respectively. WSS increased 2.7-fold as UBP was increased to 100mmHg. Pressure-induced capillarisation lowered the WSS but it remained 2.3-fold higher than normal.

Discussion: High WSS was predicted as a result of poor capillarisation, as seen in FGR. This could impair angiogenesis, resulting in diminished fetal nutrient supply. In case of high UBP (placental outflow obstruction), high WSS could damage vascular structure as pressure-induced capillarisation is unlikely to reverse the WSS to normal levels.

P36: A statistical shape model of the lung to predict pulmonary fissures: Towards a fully automated lung lobe segmentation method

Osanlouy, M.[1], Zhang, Y.[1], Clark, A.R.[1], Kumar, H.[1], Hoffman, E.A.[2], Tawhai, M.H.[1]

[1]Auckland Bioengineering Institute, University of Auckland, Auckland, NZ, [2]Department of Radiology and Biomedical Engineering, University of Iowa Carver College of Medicine, Iowa City, IA, USA.

In recent years, statistical shape models (SSM) have become a prevalent trend in analysing human organ shapes from medical images. For example, Frangi et al. (2002) presented an automatic three-dimensional landmark generation method using cardiac statistical shape atlases [1].

Since the lobes are relatively independent anatomic compartments of the lungs, they play a major role in diagnosis and therapy of lung diseases. Correct segmentation of pulmonary X-ray computed tomography (CT) images is a crucial step for most pulmonary image analysis applications; however accurate and robust segmentation of the lobar fissures remains a challenge. In many clinical situations, current segmentation tools fail to correctly identify fissure location and appearance, and in some cases they even fail to identify a fissure at all due to the pathology causing poor contrast with surrounding structures, or image artefacts, basic individual (e.g. age-dependant) variations.

Statistical shape models (SSMs) have by now been firmly established as a robust tool for segmentation of medical images. Finite element models (FEMs), on the other hand, can accurately represent shape descriptors of medical images. In this study, we developed a technique that combines SSM and FEM for volumetric lung CT image segmentation. Here, we use this approach on human imaging at both end-expiratory and end-inspiratory volumes to describe individual pulmonary lobar shapes and to analyze variations. We show preliminary applications of our method to predict pulmonary fissure location and shape using only the lung surface shape data as input. The resulting prediction of fissure locations does not rely on segmentation of other structures (e.g. airway or vessel trees) and can provide a very good estimate for pulmonary segmentation algorithms to generate an automated and accurate lobe segmentation tool.

1. Frangi, Alejandro F., et al. "Automatic construction of multiple-object three-dimensional statistical shape models: Application to cardiac modeling. "*IEEE transactions on medical imaging* 21.9 (2002): 1151-1166

P37: Role of B-type natriuretic signal peptide on AKT and ERK1/2 activity in myocardial rat ischemia

Mbikou, P.[1], Byers, M.[1], Charles, C.J.[1], Rademaker, M.T.[1], Pemberton, C.J.[1]

[1]Christchurch Heart Institute, School of Medicine, University of Otago, Christchurch, NZ.

B-type natriuretic peptide (BNP) is a hormone secreted by the heart in response to left ventricular hypertrophy and pressure overload. Post-translational cleavage of the BNP precursor generates a signal peptide (BNPsp) which has recently been shown to circulate in the blood. In patients with acute myocardial infarction, plasma BNPsp levels rise very early after symptom onset, suggesting BNPsp has potential as a novel biomarker for cardiac ischaemia. In addition, BNPsp demonstrates cardioprotective effects post-ischaemia. The underlying mechanisms, however, are unclear. The current study investigated the effect of BNPsp on the activation of three key kinases: ERK1, ERK2 and AKT.

Methods: Using the Langendorff isolated heart system, rat hearts underwent five treatment protocols (n=5-6 rats/group): Sham (continuous perfusion with physiological buffer alone); Control (40min ischaemia followed by 20min reperfusion with buffer alone); BNPsp (40min ischaemia followed by 20min reperfusion with buffer containing 0.3, 1 or 3nM BNPsp). The left ventricles were subsequently removed for western blot analysis of phosphorylated AKT (pAKT) and ERK1/2 (pERK1, pERK2) levels. Values are expressed as mean±SEM.

Results: Ischaemia/reperfusion (I/R) injury alone had no effect on ventricular pERK1 or pERK2 concentrations (pERK1: Control 73.08±16.50% vs Sham 71.71±10.62%; pERK2: Control 111.78±18.27% vs Sham 97.40±10.26%). However, unlike pERK2 (0.3nM 114.58±14.55%; 1nM 117.77±13.30%; 3nM 90.93±19.46%) pERK1 was significantly increased following I/R in the presence of BNPsp doses 0.3nM (108.28±15.78%, $p<0.05$) and 1nM (106.74±12.08%, $p<0.05$). BNPsp at 3nM had no effect on either pERK1 (85.32±27.44%) or pERK2 (90.93±19.46%). Ischaemia/reperfusion alone doubled the level of the pAKT (Sham 43±4.09% vs Control 79.36±5.65%, $p<0.05$), which was then reversed following perfusion with the highest concentration of BNPsp (3nM: 40.72±3.32%). The lower concentrations of BNPsp did not affect pAKT levels (0.3nM 74.18±7.62%; 1nM 78.19±4.19%).

Conclusion: Following myocardial ischaemic injury, BNPsp at low concentration promotes ERK1 activity, whereas at high concentration it abolishes I/R-induced AKT activity.

Plenary 2: Synaptic and non-synaptic mechanisms regulate autonomic-neuroendocrine integration in the hypothalamus'

Stern, J.[1]

[1]Department of Physiology, Augusta University, Augusta, GA 30912, USA.

It is classically considered that the proper functioning of the central nervous system (CNS) depends on the highly precise transfer of information between pairs of neurons. This communication modality is mediated by fast-acting chemical neurotransmitters within spatially defined synapses. Over the last decades however, we have learnt that the portfolio of communication modalities within the CNS is much more multifaceted, and includes communication modalities that function at much slower and diffuse spatio-temporal scales, and that are not confined by synaptic wiring. An emerging model for the study of these non-conventional neurotransmission modalities is the hypothalamus, a brain region in which communication among functionally distinct neuronal populations is fundamental for the generation of multimodal bodily homeostatic responses. In this talk, I will present recent studies from our laboratory that highlight the importance of concerted interactions between synaptic and non-synaptic communication modalities in the regulation of hypothalamic neuronal activity. I will discuss the functional relevance of these diverse inter-neuronal communication modalities within the context of autonomic and neuroendocrine integration by the hypothalamus, and their implications in cardiovascular and fluid-electrolyte homeostasis in health and disease states.

S1A.1: Approaches for overcoming diabetes-induced cardiovascular nitric oxide resistance

Anthonisz, J.[1,2]*, Qin, C.X.[1]*, Kahlberg, K.[4], Leo C.H.[4], Jap, E.[1], Parry, L.J.[4], Horowitz, J.D.[5], Kemp-Harper, B.K.[3], Ritchie, R.H.[1,2]

[1]Baker IDI Heart & Diabetes Institute, Melbourne, VIC, Australia, Depts of [2]Medicine (CCS) and [3]Pharmacology, Monash University, Melbourne, VIC, Australia, [4]School of BioSciences, University of Melbourne, Parkville, VIC, Australia, [5]Dept of Cardiology, The Queen Elizabeth Hospital, Basil Hetzel Institute, The University of Adelaide, Woodville SA, Australia.

In patients with cardiovascular disease, impaired nitric oxide (NO•) signalling is an independent predictor of poor outcomes, including mortality. This loss of NO•-responsiveness (termed 'NO•-resistance') is particularly debilitating in diabetes, where cardiovascular emergencies (acute myocardial infarction [MI], transient ischaemia, cardiogenic shock) occur more frequently, but NO•-based pharmacotherapies are unable to effectively counteract platelet aggregation and vasoconstriction. Further, the extent of NO•-resistance appears critically dependent on concomitant circulating levels of blood glucose. We have now examined whether the myocardium, like platelets and vessels, is also susceptible to NO•-resistance such that NO• can no longer enhance left ventricular (LV) relaxation.

Hearts isolated from anaesthetised adult male streptozotocin (STZ) diabetic rats with severe (~30mM) or moderate hyperglycaemia(titrated to ~22mM with insulin), or non-diabetic shams were Langendorff-perfused. Following U46619 preconstriction of the coronary vasculature to 50%, dose-response curves to acute bolus doses of the NO• donor diethylamine NONOate (DEA-NO 10pmol-10µmol) were performed. Results were compared to those obtained in response to a donor of the NO• redox sibling nitroxyl, isopropylamine NONOate (IPA-NO). Using the selective inhibitor of soluble guanylyl cyclase, ODQ (10µM), the relative contribution of cGMP to these haemodynamic responses under normoglycaemia, moderate and severe hyperglycaemia were also elucidated. Our results demonstrated that diabetes impairs NO•-mediated coronary vasodilatation, LV relaxation and LV contractile function. The impaired NO vasodilatation persisted in hearts from moderately hyperglycaemic rats. In contrast, nitroxyl-mediated vasodilatation was preserved, and the positive inotropic and lusitropic effects were further enhanced, in diabetic myocardium. In conclusion, we have demonstrated for the first time that the haemodynamic responses to nitroxyl are preserved or enhanced in diabetes, whereas those of NO• are attenuated. We have hence identified in nitroxyl an exciting potential strategy for circumventing impaired NO• signalling.

S1A.2: Paradoxical cardiac response to metabolic stress

Delbridge, L.M.D.[1], Mellor, K.M.[2]

[1]Cardiac Phenomics Laboratory, Department of Physiology, University of Melbourne, Australia, [2]Cellular & Molecular Cardiology Laboratory, Department of Physiology, University of Auckland, NZ.

In a number of cardiac energy stress conditions, including diabetes, abnormal myocardial energy storage processes are evident. In particular when cardiomyocyte glucose uptake is limited there is paradoxical accumulation of glucose hexose monomers in the form of glycogen. In experimental settings, the cardiac glycogen content in fasted animals is increased despite reduced levels of plasma glucose induced by nutrient restriction. This cardiac glucose elevation occurs in parallel with skeletal muscle and hepatic glycogen depletion. In diabetic metabolic stress states where glucose transport is profoundly reduced, either due to insulin deficiency or insulin resistance, cardiac glycogen levels are also paradoxically elevated. Clinically, in severe diabetic states the extent of glycogen accumulation in cardiomyocytes is substantial. Our studies of a range of animal models of type 1 and type 2 diabetes, have revealed that glycogen accumulation is prominent and occurs in the context of deranged autophagic breakdown of glycogen through a glycophagy-specific pathway. We have identified specific molecular mediators of this process, which present as potential therapeutic targets.

S1A.3: Diabetes increases autophagy in the human heart through promotion of Beclin-1 mediated pathway

Katare, R.[1]

[1]Department of Physiology-HeartOtago, University of Otago, Dunedin, NZ.

Diabetes promotes the progressive loss of cardiac cells, which are replaced by a fibrotic matrix, resulting in the loss of cardiac function. In the current study we sought to identify if excessive autophagy plays a major role in inducing this progressive loss. Using the human right atrial appendages collected from diabetic and non-diabetic patients undergoing coronary artery bypass graft surgery, we showed marked increase in the level of autophagy in the diabetic heart. This was evidenced by increased expression of autophagy marker LC3B-II and its mediator Beclin-1 and decreased expression of p62, which incoroporates in to autophagosomes to be efficiently degraded. Moreover, we also observed a marked activation of pro-apoptotic caspase-3 in the diabetic heart. Electron microscopy showed increased autophagosomes in the diabetic heart. In vivo measurement of autophagic flux by choloroquine injection resulted in further enhancement of LC3B-II in the diabetic myocardium, confirming increased autophagic activity in the diabetic heart. Importantly, *in-vitro* genetic depletion of *beclin-1* in high glucose treated adult rat cardiomyocytes markedly inhibited the level of autophagy and subsequent apoptotic cell death. These findings demonstrate the pathological role of autophagy in the diabetic heart, opening up a potentially novel therapeutic avenue for the treatment of diabetic heart disease.

S1A.4: ROS and metabolic signalling in skeletal muscle

Merry, T.L.[1]

[1]Department of Molecular Medicine and Pathology, University of Auckland. NZ.

Reactive oxygen species (ROS) have traditionally been associated with the deleterious cellular function and the development of disease. Increasingly, however, discrete transient increases in ROS are becoming recognised as an important cellular signalling intermediate for the regulation of normal physiological processes as well as mediating long-term adaptations induced by cellular stress. Consistent with this, data will be presented that suggests insulin can stimulate the production of ROS in skeletal muscle, and that scavenging insulin-stimulated ROS with antioxidants can impair the regulation of blood glucose in a normal insulin sensitive state. Insulin-induced ROS appear to be derived from the NADPH oxidases and facilitate insulin signalling through oxidative-inhibition of protein tyrosine phosphatases. This suggests that there is contrasting dynamic to ROS, having the ability to both promote, and impair insulin sensitivity, and questions whether antioxidant supplementation is always beneficial to health. Indeed, there is building evidence that antioxidant supplementation may blunt the health promoting effects of regular exercise. Consistent with this we show that the oxidative stress sensitive transcription factor Nuclear Factor, Erythroid 2-Like 2 (NFE2L2/Nrf2) is responsive to exercise stress, and may be involved in regulating exercise-induced mitochondrial biogenesis. This suggests that ROS mediated activations of NFE2L2 is one of the mechanisms through which exercise improves oxidative metabolism.

S1B.1: Neurosecretion and novel mechanisms for its in vivo measurement

Le Tissier, P.R.[1], Murray, J.F.[1], Romano, N.[1], Mollard, P.[2], Ozawa, T.[3]

[1]Centre for Integrative Physiology, University of Edinburgh, Edinburgh, UK, [2]Institut de Génomique Fonctionnelle, Montpellier, France, [3]Department of Chemistry, The University of Tokyo, Japan.

Pulsatile secretion of hormones and dramatic differences in local concentrations of active peptides complicate studies of the mechanisms of action of different neuroendocrine hormones. Traditional methods of analysis, based on assays utilising antibody detection, generally only provide a snapshot of systemic concentrations of total hormone, which can be a poor reflection of that acting on cellular receptors within the target tissue. Ideally, quantification should allow monitoring of bioactive hormone at its site of action with a time resolution which can distinguish the pattern of stimualtion. Novel approaches for hormone quantification which require minimal animal handling and allow longitudinal studies would also have clear advantages.

Luciferase enzymes, producing light coincident with metabolism of substrate, have been utilised for non-invasive imaging and quantification in a number of biological systems in cells, tissues and *in vivo*. Systems based on luciferases have the advantage of very high signal to noise, fast temporal resolution and large dynamic ranges without any requirement for excitatory light. In addition, the enzyme can be split into enymatically inactive fragments, with are able to complement each other upon interaction, enabling detection of protein-protein interactions. We are developing bioimaging sensors based on split luciferase detection of hormone receptor activation by their endogenous ligands, principally to detect G-protein coupled receptor activation. Expression of these biosensors in cells allows sensitive detection of receptor activation, which is dependent on ligand concentration and has a very high dynamic range. These sensors can be used in simple, cell based assays, in *ex vivo* tissue and *in vivo*. Further development of these biosensors may allow dynamic, non-invasive monitoring of hormone action with high spatial and temporal resolution.

S1B.2: Control of insulin secretion in intact islets of Langerhans

Thorn, P.[1]

[1]Charles Perkins Centre, University of Sydney, Australia.

While significant progress has been made towards understanding the essential steps that link cell stimulation to insulin secretion, there remain fundamental questions as to how the beta cells actually regulate secretory output in the context of the native environment of the islets. In situ imaging is leading to a new understanding of beta cell structure and function in the islets of Langerhans. This seminar will present recent work that indicates that the spatial arrangement of beta cells within an islet and their interactions with islet vasculature are essential factors in secretory control.

S1B.3: Neurosecretion: a view from the adrenal chromaffin cell

Bunn, S.J.[1]

[1]Centre for Neuroendocrinology, Department of Anatomy, University of Otago, Dunedin, NZ.

This symposium presentation will highlight the major contribution that the adrenal medullary chromaffin cell has made to our understanding of the mechanism and consequences of neurosecretion. While in vivo the chromaffin cell is responsible for the stress-induced output of catecholamines in the classical “fight or flight” response, in vitro it has proved an invaluable experimental model. Most notably the chromaffin cell is a rare example of a post-mitotic, fully differentiated, neurosecretory cell that can be isolated and maintained in culture. It is thus probably of greater physiological relevance than similar preparations of cell-lines or tissue of embryonic origin. Studies on isolated chromaffin cells were among the first to reveal the complexities underlying stimulus-secretion coupling, including the temporal and spacial dynamics of the associated intracellular calcium signalling. Vesicle trafficking within the chromaffin cell has proved similarly complex, with the presence of functionally distinct and independently regulated vesicle pools. Recent work has provided a detailed, although arguably still incomplete, description of the molecular events responsible for both the exocytosis and subsequent endocytosis of secretory vesicles. While the majority of published studies have focused on nicotinic receptor mediated activation of the chromaffin cell it is now clear that in vivo co-transmitters, most notably PACAP, play a major role in maintaining the neurosecretory output. Similarly, findings from our own laboratory point to a potentially physiologically significant interaction between the chromaffin cells and a number of specific cytokines. While these latter stimuli do not appear to drive the neurosecretory event itself, they may profoundly influence its chemical composition by altering the neuropeptide content of the neurosecretory vesicles. In summary, these, and other studies, revealed both the molecular complexity responsible for neurosecretion and the way it is modulated in vivo to appropriately meet physiological demands.

S1B.4: Critical role for β-catenin in insulin secretion from β-cells by regulating insulin vesicle localization

Sorrenson, B.[1,2], Cognard, E.[1], Lee, K.L.[1,2], Hughes, W.E.[3], Shepherd, P.R.[1,2.]

[1]Department of Molecular Medicine and Pathology, Faculty of Medical and Health Sciences, The University of Auckland, NZ, [2]Maurice Wilkins Centre for Molecular Biodiscovery, The University of Auckland, NZ, [3]The Garvan Institute of Medical Research, Sydney, Australia.

The processes regulating glucose-stimulated insulin secretion (GSIS) and its modulation by incretins in pancreatic β-cells are only partly understood. Here we investigate the involvement of β-catenin in these processes. Reducing β-catenin levels using siRNA knockdown attenuated GSIS in a range of β-cell models and blocked the ability of GLP-1 to potentiate this. This could be mimicked in both β-cell models and isolated islets by short-term exposure to the β-catenin inhibitory drug pyrvinium. In addition, short-term treatment with a GSK3 inhibitor, which is known to increase β-catenin levels, results in an increase in insulin secretion. The timing of these effects suggests that β-catenin is required for the processes regulating trafficking and/or release of pre-existing insulin granules rather than for those regulated by gene expression. This was supported by the finding that overexpression of the transcriptional co-activator of β-catenin, TCF7L2, attenuated insulin secretion, consistent with the extra TCF7L2 translocating β-catenin from the plasma membrane pool to the nucleus. Using total internal reflectance fluorescence (TIRF) microscopy, we found that β-catenin is required for the glucose- and incretin-induced depletion of insulin vesicles from near the plasma membrane and that lack of β-catenin perturbs insulin vesicle release from the cell periphery. Overall these studies define a critical requirement for β-catenin in the mechanisms involved in modulating insulin secretory vesicle localization and/or fusion and suggest it acts as a rheostat to regulate the amount of insulin that can be secreted. These findings also provide insights as to how overexpression of TCF7L2 attenuates insulin secretion.

S1B.5: Sub-diffractional tracking of internalized molecules reveals heterogenous diffusive states of synaptic vesicles

Joensuu, M.[1], Papadopulos, A.[1], Durisic, N.[1], Padmanabhan, P.[1], Bademosi, A.T.D.[1], Cooper-Williams, L.[1], Morrow, I.C.[1], Harper, C.J.[1‡], Jung, W.[2,3], Parton, R.G.[2,3], Goodhill, G.J.[1,4], Meunier, F.A.[1]

[1]Clem Jones Centre for Ageing Dementia Research, Queensland Brain Institute, The University of Queensland, Brisbane, Australia, [2]Institute for Molecular Bioscience, The University of Queensland, Brisbane, Australia, [3]Centre for Microscopy and Microanalysis, The University of Queensland, Brisbane, Australia, [4]School of Mathematics and Physics, The University of Queensland, Brisbane, Australia, [‡]Current Address: Centre for Integrative Physiology, The University of Edinburgh, Edinburgh, Scotland.

Synaptic vesicles (SVs) are 45 nm structures found in presynapses that are able to release neurotransmitters upon exocytic fusion with the plasma membrane, thereby mediating neurotransmission. While fluorescence microscopy has played a key part in studying the endocytic pathway, our understanding of the SV recycling is severely restricted by the diffraction-limited systems, which restrict imaging to cellular structures larger than 200 nm in diameter. To address this, we developed a novel technique based on a pulse-chase of ligands destined to undergo endocytosis, which we have termed sub-diffractional tracking of internalised molecules (sdTIM). Specifically, we studied the activity-dependent internalization of VAMP2-pHluorin-bound anti-GFP Atto647N-tagged nanobodies into recycling SVs in live hippocampal presynapses. Using this technique, we have managed to image simultaneously a large number of SVs with unprecedented 50 nm localization precision. As a proof of concept, we compared the mobility of internalized VAMP2-pHluorin-bound Atto647-nanobodies to those transiting on the plasma membrane and showed that the mobility of SVs was significantly lower. In addition to classical mean square displacement and diffusion coefficient characterization of SV mobility, we also examined, for the first time, the heterogeneous mobility of SVs along individual trajectories using Bayesian model selection[1] applied to hidden Markov modeling[2]. By investigating the anomalous and sub-diffusive events, we were able to annotate heterogeneous mobility along each single SVs trajectory. Owing to the larger density of trajectories obtained, we discovered that in most nerve terminals, SVs constantly oscillate between an immobile and two transport states of opposite directions. Importantly, once a SV entered the immobile state it was less likely to switch back to the other transport states. These results highlight the potential of the sdTIM technique to provide new dynamic insights into endocytic pathways in various cellular settings.

1. Persson, F., M. Linden, C. Unoson, and J. Elf. (2013). *Extracting intracellular diffusive states and transition rates from single-molecule tracking data.* Nat Methods. 10:265-269.
2. Monnier, N., Z. Barry, H.Y. Park, K.C. Su, Z. Katz, B.P. English, A. Dey, K. Pan, I.M. Cheeseman, R.H. Singer, and M. Bathe. 2015. *Inferring transient particle transport dynamics in live cells*. Nat Methods. 12:838-840.

S2A.1 Renal denervation in diabetes

Yao, Y.[1], Harrison, J.C.[1], Davis, G.[2], Walker, R.J.[3], Sammut, I.A.[1]

[1]Department of Pharmacology and Toxicology, University of Otago School of Medical Sciences, NZ, [2]Department of Physiology, University of Otago School of Medical Sciences, NZ, [3]Department of Medicine, Dunedin School of Medicine, University of Otago, NZ.

Renal arteries are densely innervated with both efferent sympathetic nerves and afferent sensory nerves collectively serving to promote arteriolar vasoconstriction, plasma volume expansion and consequently increase blood pressure. Bilateral renal denervation (BRD) has been shown to reduce hypertension and improve renal function in both human and experimental studies. We hypothesized that chronic BRD intervention may also attenuate renal injury and fibrosis in diabetic nephropathy. This study was conducted in a female diabetic (mRen-2)27 rat (TGR) shown to capture the cardinal features of human diabetic nephropathy. Following diabetic induction with streptozotocin, BRD/sham surgeries were conducted repeatedly (at the 3rd, 6th and 9th week following induction) in both diabetic and normoglycemic animals.

Renal denervation produced a marked decrease in systolic blood pressure in both normoglycemic and diabetic hypertensive rats. Renal noradrenaline content was significantly raised following diabetic induction and ablated in denervated normoglycemic and diabetic groups. Diabetic kidney injury was associated with a significant increase in glomerular basement membrane thickening and mesangial expansion; this morphological appearance was markedly reduced by BRD. Immunohistochemistry and protein densitometric analysis of diabetic innervated kidneys confirmed the presence of significantly increased levels of collagens I and IV, α-smooth muscle actin, AT_1R and TGF-β. Renal denervation significantly reduced protein expression of these fibrotic markers. Furthermore, BRD attenuated albumin excretion in the diabetic animals (2.9±0.7 in the innervated *vs* 1.3±0.3mg/24hr in the denervated groups, $p<0.05$) and prevented the loss of glomerular podocin expression in this model of diabetic nephropathy. In conclusion, chronic renal denervation in the renin over-expressing rat decreased sympathetic over-activity and effectively reduced blood pressure. Denervation after diabetic onset curbed the development of renal fibrosis, glomerulosclerosis and albuminuria. The evidence presented strongly suggests that renal denervation may serve as a therapeutic intervention to attenuate the progression of kidney injury in diabetic nephropathy.

S2A.2: Heart failure: Are women less sympathetic than males

Pinkham, M.I.[1], Barrett, C.J.[1]

[1]Department of Physiology, University of Auckland. NZ.

Heart failure is a disease that affects men and women in equal numbers. However, men and women with heart failure display different symptoms and outcomes; women with heart failure live longer and display better heart function but concurrently have worse symptoms and lower quality of life. To date, heart failure research has been predominantly performed in males resulting in a bias in treatments that favour males. The sympathetic nervous system plays an important role in driving the development and progression of heart failure. Increases in sympathetic nerve activity (SNA), particularly to the heart and kidneys, are associated with worse outcome in heart failure patients. Beta-blockers, drugs that antagonize the actions of SNA, are effective in improving outcomes in heart failure but, once again, the knowledge underlying the use of beta-blockers has been developed in males. I will present findings in rats that suggest there are significant sex differences in the regulation of the sympathetic nervous system in heart failure and attempt to relate these to sex differences in outcomes seen in the lab and clinic.

S2A.3: Renal function in normotensive sheep in the first eight weeks after catheter-based renal denervation

Booth, L.C.[1], McArdle, Z.[1], Yao, S.T.[1], Hood, S.[1], Lankadeva, Y.[1], Kosaka, J.[1], Schlaich, M.[2], May, C.N.[1]

[1]Florey Institute of Neuroscience and Mental Health, Parkville, Melbourne, Victoria, Australia, [2]Baker IDI Heart & Diabetes Institute, Melbourne, Victoria, Australia.

Catheter-based renal denervation (RDN) has emerged as a novel treatment for resistant hypertension by targeting the afferent sensory and efferent sympathetic renal nerves to reduce blood pressure. Recent evidence suggests that there is partial functional and anatomical reinnervation at 5 months after catheter-based RDN and complete reinnervation after 11 months. The function of the reinnervated renal nerves has not been investigated in conscious animals. The aim of this study was to examine the effects of reinnervation of the renal nerves on renal function 1 and 8 weeks after renal denervation using the Symplicity Flex catheter.

Normotensive merino ewes underwent a battery of physiological challenges, including salt load, salt depletion, periods of mild hypertension and mild hypotension, during which changes in renal blood flow, heart rate, mean arterial pressure and neurohormonal markers were measured. Ewes then underwent either sham or bilateral RDN using the Symplicity Flex catheter. Physiological challenges were repeated at 1 and 8 weeks' post-RDN or sham denervation. Renal sympathetic nerve activity was recorded 8 after sham or bilateral RDN. Eight weeks after RDN the cumulative sodium excretion was lower in the RDN group compared to pre-RDN (27 ± 2 mmol and 42 ± 2 mmol, respectively) at the end of a 135 mM i.v. saline load at 0.09 mL/kg/min for 4 hours. There were no changes with sham denervation. In addition, we made the first recordings in conscious animals of renal sympathetic nerve activity after bilateral catheter-based RDN. The preliminary data from the present study suggest that there are changes in renal function and control of RSNA after catheter-based RDN.

S2A.4: Renal endovascular denervation in end-stage kidney disease patients: Cardiovascular protection – proof of concept study

Jardine, D.[1]

[1]Christchurch Hospital, Christchurch, NZ.

Aims: Chronic kidney disease (CKD) is characterised by sympathetic neural activation, which increases in severity as condition progresses to end-stage kidney disease (ESKD). Catheter-based renal denervation (RDN) reduces sympathetic neural activation and blood pressure (BP). We aimed to investigate the effect of RDN on sympathetic neural activation, left ventricular mass (LV mass) and systemic (BP), in patients with ESKD.

Methods and Results: Nine patients with ESKD (six haemo- and three peritoneal dialysis) mean dialysis vintage of 3.3 ± 2.8 years were included and treated with RDN (EnligHTN™ system). Data were obtained at baseline, 1, 3 and 12 months post-RDN measured on a non-dialysis day. At baseline sympathetic neural activation as indicated by muscle sympathetic nervous activity (MSNA) and plasma norepinephrine level were markedly elevated, left ventricular hypertrophy (LVH) was evident in 8 of the 9 patients, and all patients were hypertensive (office BP > 140/90 and ambulatory BP > 130/80 mm Hg). Post-RDN, MSNA (-12.2 bursts·min^{-1}, 95% CI [-13.6, -10.7]) but not plasma norepinephrine (-2631 pmol·L^{-1}, 95% CI [-5400, 1347]) was reduced at 12 months, LV mass (-27 g·m^{-2}, 95% CI [-47, -8]) and mean ambulatory BP (systolic: -24 mm Hg, 95% CI [-42, -5] and diastolic: -13 mm Hg, 95% CI [-22, -4]) were reduced at 12 months. Office BP was reduced as early as 1M (systolic: -25 mm Hg, 95% CI [-45, -5] and diastolic: -13 mm Hg, 95% CI [-24, -1]) with clinically significant reductions in ~60% of patients out to 12 months.

Conclusion: Catheter-based RDN significantly reduced MSNA, LV mass and systemic BP in patients with ESKD.

S2B.1: Mechanical ventilation and acute lung injury

Bates, J.H.T[1]

[1]Deptartment Medicine, Department Molecular Physiology & Biophysics, University of Vermont College of Medicine, Burlington, Vermont, USA.

Acute respiratory distress syndrome (ARDS) is a non-cardiogenic form of pulmonary edema that has a variety of causes. ARDS is often fatal and so is typically managed in the intensive care unit, frequently with the involvement of mechanical ventilation. However, the stresses and strains wrought by mechanical ventilation on damaged lung tissue can exacerbate ARDS by causing ventilator-induced lung injury (VILI). Decreases in ARDS mortality have been achieved in recent decades by improved methods of mechanical ventilation that reduce VILI, particularly through use of a tidal volume (V_T) of 6 ml/kg ideal body weight. Nevertheless, while this may be best for the average patient, it is unlikely to be best for the individual patient given the heterogeneity of ARDS. To address this shortcoming, individual patient characteristics must be taken into account so that mechanical ventilation can be appropriately adjusted through feedback control. This involves the following three steps.

Step 1) An individual patient's characteristics are taken into account using appropriate sensors.

Step 2). A minimally injurious strategy for mechanical ventilation is devised based on these characteristics.

Step 3). This strategy is then implemented by a suitably responsive ventilator.

The third step is a purely technological issue that is readily addressed in principle, so we have been focusing our efforts on Steps 1 and 2. Assessing the characteristics of the lungs (i.e., Step 1), and thus determining if they are being adversely affected by injury, is most conveniently and rapidly achieved by determining lung mechanical function from ongoing measurements of airway pressure and flow. This allows the dynamics of recruitment and derecruitment of lung units, as well as the degree of over-distension of lung tissue, to be estimated. Deciding on the best ventilation strategy (i.e., Step 2), however, remains the greatest challenge, and requires the evaluation of a lung injury cost function. Recent experimental results in mice hint at the form of this injury cost function, which offers the possibility that its minimization might eventually lead to optimally safe patient-specific strategies for mechanical ventilation in ARDS.

S2B.2: Gas flow and lung injury in ventilated preterm babies

Bloomfield, F.H.[1], Oliver, M.H.[1], Kuschel, C.A.[2], Hooper, S.B.[3], Bach, K.P.[4]

[1]Liggins Institute, University of Auckland, Auckland, NZ, [2]Royal Women's Hospital, Melbourne, Victoria, Australia, [3]The Ritchie Centre, Hudson Institute for Medical Research, Monash, Victoria, Australia, [4]Newborn Services, National Women's Health, Auckland City Hospital, Auckland, NZ.

Survival following very and extremely preterm birth has been steadily increasing. Major advances in respiratory care, particularly antenatal glucocorticoids and postnatal surfactant have been instrumental in reducing mortality. However, the incidence of the major long-term respiratory complication, bronchopulmonary dysplasia (BPD), has not decreased. It now is clear that many factors contribute to the pathogenesis of BPD, in particular ventilator-induced lung injury (VILI). New approaches to ventilation have reduced ventilator days and short-term morbidity, but also have not reduced BPD.

We hypothesised that gas flow into the babies' lungs, which acts as a liquid, could contribute to VILI through rheotrauma analogous to the pathogenesis of vascular disease. Our investigations commenced with *in vitro* investigation into the relationship between gas flow and ventilator efficiency, before studies in newborn lambs demonstrated that gas flow impacts upon both ventilator efficiency and on acute lung injury. Reduced bias gas flows result in increased ventilator efficiency, decreased mRNA levels of early acute response genes in the lung and improved histological appearances.

We then translated these findings into a randomised controlled trial in extremely preterm babies, randomising babies to a standard bias gas flow of 10 $L.min^{-1}$ or a reduced bias gas flow of 4 $L.min^{-1}$. In this pilot trial, the primary outcome was cytokine concentration in tracheal aspirate, which are known to be elevated in babies at risk of BPD. Recruitment has just finished and we will present preliminary data from this trial.

1. Bach KP, Kuschel CA, Hooper SB, Bertram J, McKnight S, Peachey SE, Zahra VA, Flecknoe SJ, Oliver MH, Wallace MJ, Bloomfield FH. High bias gas flows increase lung injury in the ventilated preterm lamb. PLoS One. 2012;7(10):e47044. doi: 10.1371/journal.pone.0047044.

S2B.3: Innovative Devices And Therapies For Respiratory Diseases

Young, P.M

[1]Woolcock Institute of Medical Research, Glebe, Sydney, NSW, Australia, [2]Sydney Medical School, The University of Sydney, Sydney, NSW, Australia.

Respiratory diseases account for three of the top-five causes of death world-wide, with, respiratory infection (RTI) being the number one communicable cause of death globally. The reason for such poor outcomes in RTIs is, in-part due, to the lack of efficient treatment regiments and devices that target the site of infection likely to enhance health-care outcomes.

This presentation investigates a number of relatively inexpensive and effective targeted approaches to treating respiratory infection locally. Specifically, the effectiveness of: (1) super-hydrophobic thin film coatings for intubation tubes that can limit biofilm formation [1]; (2) the formulation of silver nano-particle therapies for ventilator associated pneumonia [2-4]; (3) high-dose lung targeted dry powder aerosol delivery systems for delivery of antibiotics to Tuberculosis patients [5-7]; and (3) inhaled controlled release therapies for controlling re-occurring infection in children with cystic fibrosis [8-9] will be presented.

1. Loo, Lee, Young, Cavaliere, Whitchurch Rohanizadeh (2015). "Implications and emerging control strategies for ventilator-associated infections." Expert Rev Anti Infect Ther 13(3): 379-393.
2. Loo, Young, Lee, Cavaliere, Whitchurch Rohanizadeh (2014). "Non-cytotoxic silver nanoparticle-polyvinyl alcohol hydrogels with anti-biofilm activity: designed as coatings for endotracheal tube materials." Biofouling 30(7): 773-788.
3. Loo, Young, Cavaliere, Whitchurch, Lee Rohanizadeh (2014). "Silver nanoparticles enhance Pseudomonas aeruginosa PAO1 biofilm detachment." Drug Dev Ind Pharm 40(6): 719-729.
4. Loo, Young, Lee, Cavaliere, Whitchurch Rohanizadeh (2012). "Superhydrophobic, nanotextured polyvinyl chloride films for delaying Pseudomonas aeruginosa attachment to intubation tubes and medical plastics." Acta Biomaterialia 8(5): 1881-1890.
5. Chan, Duke, Ong, Chan, Tyne, Chan, Britton, Young Traini (2014). "A Novel Inhalable Form of Rifapentine." Journal of Pharmaceutical Sciences 103(5): 1411-1421.Zhu, Young, Ong, Crapper, Flodin, Qiao, Phillips and D. Traini (2015). "Tuning Aerosol Performance Using the Multibreath Orbital (R) Dry Powder Inhaler Device: Controlling Delivery Parameters and Aerosol Performance via Modification of Puck Orifice Geometry." Journal of Pharmaceutical Sciences 104(7): 2169-2176.
6. Young, Salama, Zhu, Phillips, Crapper, Chan Traini (2015). "Multi-breath dry powder inhaler for delivery of cohesive powders in the treatment of bronchiectasis." Drug Dev Ind Pharm 41(5): 859-865.
7. Young, Crapper, Philips, Sharma, Chan Traini (2014). "Overcoming Dose Limitations Using the Orbital Multi-Breath Dry Powder Inhaler." J Aerosol Med Pulm Drug Deliv 27(2): 138-147.
8. Ong, Benaouda, D. Traini, Cipolla, Gonda, Bebawy, Forbes Young (2014). "In vitro and ex vivo methods predict the enhanced lung residence time of liposomal ciprofloxacin formulations for nebulisation." Eur J Pharm Biopharm 86(1): 83-89.
9. Ong, Traini, Cipolla, Gonda, Bebawy, Agus Young (2012). "Liposomal Nanoparticles Control the Uptake of Ciprofloxacin Across Respiratory Epithelia." Pharmaceutical Research 29(12): 3335-3346.

S2B.4: Respiratory therapy with nasal high flow

Tatkov, S.[1]

[1]Fisher & Paykel Healthcare, Auckland, NZ.

Recent studies report that an open nasal cannula system that generates nasal high flow (NHF) with or without supplemental oxygen can assist ventilation in patients with various respiratory disorders including acute and chronic respiratory failure. NHF therapy is well accepted both by clinicians and patients due to the ease of use and comfort. A number of clinically relevant benefits have been associated with NHF therapy: reduction in respiratory rate, change of minute ventilation and a reduction of work of breathing, although how NHF produces these effects is not yet understood.

The physiological mechanisms of NHF are complex but can be grouped into three major parts: respiratory support, airway hydration and delivered drugs such as oxygen. Respiratory support provided by NHF is very different from CPAP or NIV where a sealed mask is used. NHF is associated with a reduction of dead space due to a decreased rebreathing from anatomical dead space and positive airway pressure. Positive airway pressure dynamically changes according to breathing flow and at the end of expiration (PEEP) depends on flow from a device and leak around the prongs. The respiratory support changes a breathing pattern and can produce variable effects related to more efficient respiratory mechanics and an improvement of gas exchange. Airway hydration with NHF prevents epithelium from drying when the breathing pattern is abnormal and decreases viscosity of mucus in a presence of hypersecretion. Optimal humidity and temperature of gas are essential for NHF as unidirectional high flow of unconditioned gas would very quickly desiccate epithelium and make the therapy intolerable. Supplemental oxygen is used with NHF in patients with hypoxemia. Prevention of entrainment of ambient air makes oxygen delivery more consistent irrespective on respiration.

S3A.1: Measuring and modelling the ERK-MAPK signalling cascade in situ

Crampin, E.[1]

Systems Biology Laboratory, School of Mathematics and Statistics & Melbourne School of Engineering, University of Melbourne, Melbourne, Australia.

Phospho-protein signalling pathways have been intensively studied in vitro, yet their role in regulating tissue homeostasis is not fully understood. In the skin, interfollicular keratinocytes differentiate over approximately 2 weeks as they traverse the epidermis. The extracellular signal-regulated kinase (ERK) branch of the mitogen-activated protein kinase (MAPK) pathway has been implicated in this process. We examined ERK-MAPK activity within human epidermal keratinocytes in situ using a combination of confocal microscopy, image processing and mathematical modelling. Our results suggest that homeostasis is maintained via the MAPK signalling cascade operating at a steady state, with activity modulated by extracellular calcium gradients across the epidermis.

S3A.2 Vijay Rajagopal, University of Melbourne, Australia
Investigating sub-cellular structure-function relationships in cardiac cells

S3A.3: Capturing complexity in models of blood flow and oxygen exchange

Clark, A.R.[1]

[1]Auckland Bioengineering Institute, University of Auckland, Auckland, NZ

Efficient oxygen exchange from the environment to our blood is critical to maintain life. Before we are born we get oxygen from our mother's blood through the placenta, and after birth the lungs take over the placenta's role exchanging oxygen from the air. Both organs need to provide the maximum possible surface area for exchange, without taking up an excessive volume. The adult lung for example has approximately $100m^2$ of exchange surface contained in a 3L functional volume. Both the placenta and lung have evolved a complex branching structure to accommodate a large exchange surface. Perturbations to these structures are known to significantly influence gas exchange function, but can be very difficult to see clinically as they often occur at a smaller scale than can be observed in vivo with imaging.

Here I present our efforts to develop multi-scale computational models of gas exchange through life. This is achieved by developing whole organ models of blood flow and exchange functions that can be parameterised by models representing structure and function at the micro-scale. This includes anatomically accurate models of lung and placental tissue that span spatial scales, and the incorporation of knowledge obtained from these models into 'lumped-parameter' units in organ scale modelling. I will discuss some of the successes of this multi-scale approach in providing insight into pathology, and the challenges that we face in obtaining and interpreting data at the micro-scale from delicate and highly deformable tissue.

S3A.4: Real-time gait retraining to slow the progression of knee osteoarthritis

Besier, T.F.[1,2], Chen, D.[1], Haller, M.[1], Pizzolato, C.[3], Lloyd, D. G.[3]

[1]Auckland Bioengineering Institute, University of Auckland, Auckland, NZ, [2]Department of Engineering Science, University of Auckland, Auckland, NZ, [3]Griffith Health Institute, Griffith University, Gold Coast, Australia.

Our ageing and increasingly overweight population is creating an epidemic of osteoarthritis and the number of knee joint replacements is anticipated to rise by 700% in the next 15 years. Our health system will struggle to cope with this massive increase in demand, so we need alternative methods to alter the course of this debilitating disease. Gait retraining has the potential to alter the mechanical loads placed on skeletal tissue and restore normal function. The purpose of this research is to combine wearable sensors with computational models of the musculoskeletal system to provide gait retraining through precise, real-time haptic feedback to control the distribution of contact pressure across the tibiofemoral joint. To achieve this, we are developing surrogate contact models of the tibiofemoral joint that can be run in real-time, given muscle activity from electromyography, and joint kinematics (from motion capture or inertial sensors). To provide feedback to alter walking gait, we have explored the use of tactile apparent motion with small, vibrating motors that give an apparent feeling of stroking to the skin. Tactile feedback is intuitive to the user and enables subtle changes in joint posture during walking without the need to concentrate on a screen. Here we present the methods used to perform this real-time gait training, from generating accurate models of the musculoskeletal system to real-time muscle and joint contact force using surrogate models and tactile user experience studies.

Supported by The Royal Society of New Zealand MARSDEN Fund, Grant UOA1211.

S3B.1: Mechanisms of quality control in the female germ line

Hutt, K.J.[1]

[1]Development and Stem Cells Program, Monash Biomedicine Discovery Institute and Department of Anatomy and Developmental Biology, Monash University, Melbourne, Australia.

Within the ovary, immature oocytes are stored in structures called primordial follicles, collectively known as the ovarian reserve. All hormone producing follicles and mature ovulated oocytes are derived from primordial follicles, and because of this their number and quality are of paramount importance for female fertility and reproductive lifespan. Mounting evidence, primarily from the study of gene targeted mice, indicates a key role for the intrinsic apoptosis pathway in regulating primordial follicle number and quality. The intrinsic apoptosis pathway is controlled by the relative levels and activities of the members of the B-cell lymphoma-2 (BCL-2) family. Both pro and anti-apoptotic members of the BCL-2 family have been implicated in the control of the number primordial follicles initially established in the ovary at birth, as well as the number of primordial follicles maintained throughout reproductive life. In this talk, the relationship between the intrinsic apoptosis pathway, primordial follicle number, female fertility and reproductive longevity will discussed. In particular, our recent work using mice deficient in key cell death promoting BCL2 family members, p53 unregulated modulator of apoptosis (PUMA) and Bcl-2-modifying factor (BMF), suggests that there are two key periods of quality control within the ovary involving the apoptotic elimination of oocytes: the first occurs during embryonic life prior to the establishment of the initial reserve of primordial follicles, and the second coincides with the onset of puberty and early adulthood. Based on our data, we hypothesize that apoptosis is an important developmentally regulated mechanism to ensure that only the highest quality oocytes are available for ovulation and perpetuation of the next generation.

S3B.2: Transgenic overexpression of AMH reduces female fertility

Pankhurst, M.W.[1], Batchelor, N.J.[1], McLennan I.S.[1,2]

[1]Department of Anatomy, University of Otago, Dunedin, NZ, [2] Brain Health Research Centre, University of Otago, Dunedin, NZ.

Anti-Müllerian hormone (AMH) regulates ovarian function in a paracrine manner but it has not been determined if AMH acts as a hormone in females. In a transgenic mouse line generated in our lab, over-expression of AMH caused an infertility phenotype, but only in the females. The overexpression is in the brain but at sufficiently high levels that AMH is found at high concentrations in the blood. To determine how high AMH levels affect female fertility, wild-type and transgenic (Thy1.2-AMH) mice were mated with wild-type studs, with daily monitoring for copulatory plugs. The pregnancy of the dams was allowed to progress to birth or the dams were euthanised at various points after mating and the pups/concepti were quantified. The majority of wild-type dams gave birth to least one litter in the first two mating periods but only a single litter was observed from five Thy1.2-AMH dams. Foetuses were found to be present in Thy1.2-AMH dams at 10 days-post-coitus but ~40% showed signs of degeneration. Less than 5% of foetuses displayed signs of degeneration in wild-type dams. At 3.5 days-post-coitus, the majority of embryos had reached the blastocyst stage in the wild type dams but a lower percentage progressed to the blastocyst stage Thy1.2-AMH dams. These data suggest that overexpression of AMH causes miscarriage rather than failure of conception or anovulation. Early indications are that the defect occurs during oogenesis or early embryo development are affected but the exact site of action remains unclear.

S3B.3: Effects of obesity on offspring

Robker, R.L.[1]

[1]Robinson Research Institute, School of Medicine, University of Adelaide, Adelaide, Australia.

Obesity in women is associated with systemic insulin resistance and metabolic syndrome, as well as increased insulin and triglyceride in the ovarian follicular fluid surrounding the developing oocyte, and reduced conception rates. Obesity in females also alters fetal development during pregnancy and permanently programs the metabolism of offspring; however mechanisms responsible and whether they are preventable is not clear. Our studies in mice show that insulin resistance and hyperlipidemia lead to endoplasmic reticulum stress in the oocyte complex and altered mitochondrial activity in oocytes. In vitro fertilization of oocytes from obese mice demonstrates their impaired developmental potential and marked mtDNA loss by the blastocyst stage. Subsequently, fetuses from obese oocytes were heavier than controls and had reduced liver, heart and kidney mtDNA content. Treatment of the obese females with ER stress inhibitor salubrinal or the chaperone inducer BGP-15 immediately prior to IVF normalized oocyte mitochondrial activity as well as subsequent blastocyst development, fetal weight and fetal tissue mtDNA content. These results demonstrate that obesity in mothers imparts a legacy of mitochondrial loss in offspring, that is due to cellular stress during oocyte maturation but that is preventable prior to conception.

S3B.4: Reproductive characteristics of sheep with mutations in the leptin receptor

Juengel, J.L.[1] Quirke, L.D.[1], Kauff A.[1], Johnstone P.D.[1]

[1]Reproduction, Animal Sciences Group, AgResearch Limited, Invermay Agricultural Centre, Mosgiel, NZ.

We have recently identified three single nucleotide polymorphisms (SNPs) in the leptin receptor (*LEPR*) gene in sheep. The lowest frequency allele (the presumed mutation) for all three SNPs results in an amino acid change and these were often, but not exclusively, inherited together. One of the SNPs is located in the extracellular region of the protein, potentially affecting the ability of the receptor to bind leptin, while the other two are located in the intracellular region. Mutation in *LEPR* was associated with a delay in attainment of puberty, with over 30% of ewes homozygous for the mutation failing to attain puberty in the first year of life, compared to less than 10% for the wild-type contemporaries. Furthermore, ewe lambs homozygous for the mutations that did attain puberty during their first year of life did so, on average, 2 weeks later. Growth was not negatively affected by the mutation with homozygous ewes weighing 3 kg more than wild-type contemporaries at 18 months of age. The number of lambs born was reduced by approximately 10% in ewes homozygous for the mutation compared to wild-type contemporaries. This reduction was driven by lower ovulation rates, and lower embryo survival in ewes that maintained a high ovulation rate. In adult ewes, expression of oestrous was suppressed in ewes homozygous for the mutations, with 10-20% of the ewes failing to be bred during the first breeding cycle- ultimately doubling the number of ewes failing to become pregnant. To try to better understand how the mutations in *LEPR* might alter reproductive function, we examined expression of reproductive hormones during a reproductive cycle. Daily concentrations of FSH and progesterone were measured with RIA. However, no differences were observed between genotypes. Thus, mutations in the LEPR are associated with reduced reproductive potential however, the physiological mechanisms leading to the reduced reproductive performance are yet to be characterised.

NZSE Posters	
P1	**Hsin-Jui (Regina) Lien, University of Otago.** Role of kisspeptin in the prolactin-induced suppression of the pulsatile secretion of luteinizing hormone
P2	**Zin Khant Aung, University of Otago.** Impaired pregnancy-induced changes to glucose homeostasis in mice lacking prolactin receptors in the pancreas
P3	**Jade York, University of Otago.** Morphological characterization of tyrosine hydroxylase immunoreactive neurons in the rat hypothalamus
P4	**Maria Felicitas Lopez Vicchi, University of Otago.** Female mutant mice with selective disruption of lactotrope D2Rs have chronic hyperprolactinemia and altered liver and adipocyte genes related to glucose and lipid balance
IBTec Posters	
P5	**Anubha Kalra, Auckland University of Technology.** Quantifying skin stretch induced motion artifact from an electrocardiogram signal-A pilot study
P6	**Gautam Anand, Auckland University of Technology.** Parametric electrical modelling of human forearm simulation response using multi-frequency electrical bioimpedance
P7	**Ali Adil Ali, Auckland University Of Technology.** Functionalised lipid nanoparticles loaded with Paclitaxel for targeted release to ovarian cancer tissue
P8	**KLT Roos, Institute of Biomedical Technologies.** Murine models for acute and chronic asthma respiratory outcomes
P9	**Tassanai Parittotokkaporn, Institute of Biomedical Technologies**. Finite element modeling of the carotid artery for simulation of the pulse wave velocity measurement
MedSci Posters	
P10	**Farzaneh Shalbaf Hosseinabadi. The University of Auckland.** The effect of retinal microstructure on retinal prosthesis performance
P11	**Luis Gonano, University of Otago.** Carvedilol and its non-ß-blocking analog VK-II-86 prevent digitalis-induced Ca++ waves in cardiac myocytes
P12	**Lynley Lewis. University of Otago.** Development of a specific immunoassay to measure BNP1-32 in plasma without the confounding influences of precursor peptides and peptide metabolites: could this improve heart failure diagnosis?
P13	**Ruby Langdon, University of Canterbury.** Analysis of pressure dependent resistance and elastance in high auto-PEEP versus low auto-PEEP patients
Physiological Society of New Zealand Posters (*****PSNZ Student Poster Presentation Prize candidate)	
P14	**Adam Denny, University of Otago.** Oxidised CaMKII – A novel mechanism in the pathophysiology of FSHD
P15	***Akash Deep Chakraborty, University of Otago.** Regulation of RyR2 by Protein Kinase CK2
P16	***Belvin Thomas, Auckland Bioengineering Institute.** A high resolution reconstruction of 3D atrial tissue architecture following tachypacing-induced heart failure in the sheep
P17	***Brian Shin. University of Otago.** Is ferroptosis the driver for the onset of type-2 diabetes under hyperuricemic conditions?
P18	***Chidinma Okolo, University of Otago.** O-GlcNAcylation regulates RyR2 function directly
P19	**Cindy Cheakhun, University of Otago.** Role of uric acid in cardiac stem cell function
P20	**Elodie Desroziers, University of Otago.** Sexually differentiated co-expression of neuronal nitric oxide synthase (nNOS) in arcuate nucleus GABA neurons
P21	***Hamed Minaeizaeim, University of Auckland.** Non-rigid lung image registration using finite element methods
P22	***Jan-Peter Baldin, University of Otago.** Shear force activation of the epithelial sodium channel (ENaC): role of the β and γ subunits
P23	***Nazanin Ebrahimi, The University of Auckland.** How the heart grows - from multiscale data to multiscale computational model
P24	***Oby Ebenebe, University of Otago.** 17β-Estradiol induced calcification and alters CaMKII expression in a mouse model of atherosclerosis
P25	**Rachael Augustine, University of Otago.** Increase in kisspeptin fibre projections to the oxytocin system in late pregnancy in the mouse
P26	***Ramakanth Satthenapalli, University of Otago.** Ventricular specific cardiomyocyte differentiation of mouse embryonic stem cells through modulation of molecular pathways

P27	***Rojan Saghian, Auckland Bioengineering Institute.** Predicting the impact of trophoblast plugs on the utero-placental circulation in early pregnancy
P28	***Sama Mugloo, University of Otago.** Characterising ENaC expression in vasculature
P29	***Shruti Rawal, University of Otago.** microRNA-126 and microRNA-132 are the early modulators of diabetic microangiopathy in heart
P30	***Toan Pham, University of Auckland.** New insights on cardiac activation heat
P31	**Vicky Benson, University of Auckland.** Effects of diet composition on development of high fat diet-induced obesity and insulin resistance in rodents
P32	***Yuwen Zhang, Auckland Bioengineering Institute.** Automatic principal component based lung lobe segmentation from computed tomography scans
P33	***Nima Afshar, Auckland Bioengineering Institute.** Computational modelling of glucose uptake in enterocytes using CellML
P34	***Bram Soliman, University of Otago.** Photo-curable thiol-ene gelatin based hydrogels as bioinks for bioprinting
P35	***Win Tun, Auckland Bioengineering Institute.** Role of wall shear stress in placental pathology
P36	***Mahyar** Osanlouy**, University of Auckland.** A statistical shape model of the lung to predict pulmonary fissures: Towards a fully automated lung lobe segmentation method
P37	**Prisca Mbikou, University of Otago.** Role of B-type natriuretic signal peptide on AKT and ERK1/2 activity in myocardial rat ischemia